

**TiO<sub>2</sub> NANOPARTICLES COATED  
FORWARD OSMOSIS MEMBRANES  
FOR TREATMENT OF INDUSTRIAL TEXTILE EFFLUENT**



**Mr. Kaung Ko Ko Sint**

**จุฬาลงกรณ์มหาวิทยาลัย  
CHULALONGKORN UNIVERSITY**

**A Thesis Submitted in Partial Fulfillment of the Requirements  
for the Degree of Master of Engineering in Environmental Engineering  
Department of Environmental Engineering  
Faculty of Engineering  
Chulalongkorn University  
Academic Year 2018  
Copyright of Chulalongkorn University**

ฟอร์วัดออสโมซิสเมมเบรนที่เคลือบด้วยอนุภาคนาโนไททานเนียมไดออกไซด์สำหรับบำบัดน้ำ  
ทิ้งอุตสาหกรรมสิ่งทอ



วิทยานิพนธ์นี้เป็นส่วนหนึ่งของการศึกษาตามหลักสูตรปริญญาวิศวกรรมศาสตรมหาบัณฑิต  
สาขาวิชาวิศวกรรมสิ่งแวดล้อม ภาควิชาวิศวกรรมสิ่งแวดล้อม  
คณะวิศวกรรมศาสตร์ จุฬาลงกรณ์มหาวิทยาลัย  
ปีการศึกษา 2561  
ลิขสิทธิ์ของจุฬาลงกรณ์มหาวิทยาลัย

Thesis Title	TiO <sub>2</sub> NANOPARTICLES COATED FORWARD OSMOSIS MEMBRANES FOR TREATMENT OF INDUSTRIAL TEXTILE EFFLUENT
By	Mr. Kaung Ko Ko Sint
Field of Study	Environmental Engineering
Thesis Advisor	Associate Professor Chavalit Ratanatamskul, Ph.D.
Thesis Co Advisor	Dr. Wencho Xue

---

Accepted by the Faculty of Engineering, Chulalongkorn University in Partial Fulfillment of the Requirement for the Master of Engineering

..... Dean of the Faculty of Engineering  
(Professor Supot Teachavorasinskun, Ph.D.)

#### THESIS COMMITTEE

..... Chairman  
(Associate Professor Petchporn Chawakitchareon, Ph.D.)

..... Thesis Advisor  
(Associate Professor Chavalit Ratanatamskul, Ph.D.)

..... Thesis Co-Advisor  
(Dr. Wencho Xue)

..... Examiner  
(Associate Professor Patiparn Punyapalakul, Ph.D.)

..... Examiner  
(Associate Professor Wiboonluk Pungrasmi, Ph.D.)

..... External Examiner  
(Dr. Thanakorn Methatham)

จุฬาลงกรณ์มหาวิทยาลัย  
CHULALONGKORN UNIVERSITY

เกื่อง โก โก ชินต์ :

ฟอรัวคอสโมซิสเมมเบรนที่เคลือบด้วยอนุภาคนาโนไททาเนียมไดออกไซด์สำหรับบำบัดน้ำทิ้งอุตสาหกรรมสิ่งทอ . (  $TiO_2$  NANOPARTICLES COATED FORWARD OSMOSIS MEMBRANES FOR TREATMENT OF INDUSTRIAL TEXTILE EFFLUENT) อ.ที่ปรึกษาหลัก : ชวลิต รัตนธรรมสกุล,  
อ.ที่ปรึกษาร่วม : เวนชา ชู

น้ำเสียจากอุตสาหกรรมสิ่งทอเกิดขึ้นเนื่องจากความต้องการของน้ำของโรงงานอุตสาหกรรมสิ่งทอน้ำทิ้งที่ผ่านการแยกด้วยเมมเบรนเนื่องจากองค์ประกอบน้ำเสียที่ซับซ้อนและการมีองค์ประกอบของมลสารต่างๆ เช่น โลหะหนัก และเกลือคลอไรด์ สารอาหาร เช่น ไนโตรเจน , ซัลเฟต และ ฟอสเฟต ในกระบวนการบำบัดน้ำเสียและนำน้ำกลับมาใช้ใหม่ของน้ำเสียจากอุตสาหกรรมสิ่งทอ งานวิจัยนี้เป็นการศึกษาความเป็นไปได้ในการดำเนินงานโดยใช้กระบวนการโฟโตคะตะลิซิสแบบอนุภาคนาโนของ  $TiO_2$  เคลือบบนแผ่นเมมเบรน 2 ชนิดคือเยื่อแผ่นเซลลูโลสทริอะเทท (CTA) และเยื่อแผ่น Aquaporin (AqP) ผ่านทางเทคนิค 3-(trimethoxysilyl) propyl methacrylate-polymethyl methacrylate-bromide (MEMO-PMMA-Br) เป็นวิธีทางเลือกใหม่ในการบำบัดน้ำทิ้งโรงงานอุตสาหกรรมสิ่งทอ จากการศึกษาผลของความเข้มข้นของสีย้อมมลสารไอออนลบที่ละลายน้ำและ TOC ที่มีต่อการกำจัดสีรีแอกทีฟ พบว่าได้อัตราการกรองน้ำเริ่มต้น ( $J_w$ ) อยู่ที่  $18.38 \text{ lm}^{-2} \text{ h}^{-1}$  และสามารถกำจัดสีได้สูงถึง 99.9% เมื่อใช้สารละลายด่าง  $NaCl$  1 M และน้ำทิ้งสีย้อมสังเคราะห์ (สีค้ำสีน้ำเงินและสีแดง) ที่ความเข้มข้น 200, 400, 600, 800 ADMI รวมทั้งในการศึกษาผลของมลสารไอออนลบ PVA และ HCOH ในความเข้มข้นที่ต่างกันภายใต้โหมดการทำงานของ FO นอกจากนี้ค่าอัตราการกรองน้ำฟลักซ์ของเมมเบรนทั้ง 2 ชนิดเพิ่มขึ้นและสมรรถนะของเมมเบรน CTA ในการกำจัดสารอินทรีย์เพิ่มขึ้นอย่างมากหลังจากการดัดแปลงพื้นผิว การทดลองยังแสดงให้เห็นว่าเมมเบรน CTA ช่วยให้น้ำมีเทนสูงกว่าเมมเบรนของ aquaporin สำหรับการบำบัดน้ำเสียสังเคราะห์ การเพิ่มน้ำใน aquaporin ประมาณ 5.13% จาก CTA

จุฬาลงกรณ์มหาวิทยาลัย  
CHULALONGKORN UNIVERSITY

สาขาวิชา วิศวกรรมสิ่งแวดล้อม

ลายมือชื่อนิติ

ปีการศึกษา 2561

ลายมือชื่อ อ.ที่ปรึกษาหลัก

## 5970419021 : MAJOR ENVIRONMENTAL ENGINEERING

KEYWORD: Forward Osmosis technology, cellulose triacetate(CTA) membrane, aquaporin(AqP) membrane, polyvinyl alcohol(PVA), formaldehyde(HCHO), textile wastewater

Kaung Ko Ko Sint : TiO<sub>2</sub> NANOPARTICLES COATED FORWARD OSMOSIS MEMBRANES FOR TREATMENT OF INDUSTRIAL TEXTILE EFFLUENT. Advisor: Assoc. Prof. Chavalit Ratanatamskul, Ph.D. Co-advisor: Dr. Wencho Xue

Textile wastewater occur as demanding water bodies to be treated by membrane separation due to the complex composition and presence of reactive constituents such as heavy metals and salts as well as nutrients, e.g. nitrogen, sulphate and phosphate. Numerous combination of osmosis process with photocatalysts has been experimentally conceived for the water and wastewater treatment and reuse of textile wastewater. The present work was devoted to study the operating feasibility using photocatalyst as TiO<sub>2</sub> nano-particles were coated onto two commercially available FO membranes, a cellulose triacetate (CTA) membrane and an aquaporin (AqP) membrane through a specially designed 3-(trimethoxysilyl) propyl methacrylate–polymethyl methacrylate–bromide (MEMO–PMMA–Br) monomer chain as an alternative forward osmosis treatment method of conventionally treated wastewater discharged from textile plants. Effects of dye concentration, dissolved ions and TOC and reactive dye removing were studied. An initial water flux ( $J_w$ ) of 18.38 L m<sup>-2</sup> h<sup>-1</sup> with a dye rejection of 99.9% has been demonstrated by using 1 M NaCl as the draw solution and synthetic textile wastewater containing reactive textile dyes (black, blue and red) 200, 400, 600, 800 ppm, inorganic salts, varying amounts of PVA and HCOH as interferences in the feed under the FO mode. The water flux of both membranes and the performance of the CTA membrane were greatly enhanced after surface modification. The experiments also show that CTA membrane gives higher water flux than aquaporin membrane for forward osmosis operation of synthetic textile wastewater. The increase in water flux for aquaporin is about 5.13% than CTA.



Field of Study: Environmental Engineering  
Academic Year: 2018

Student's Signature .....  
Advisor's Signature .....  
Co-advisor's Signature .....

## ACKNOWLEDGEMENTS

First of all, I would like to express my deep gratitude to my advisor, Assoc. Prof. Chavalit Ratanatamskul, Ph.D from Chulalongkorn University for his kind support not only for technical knowledge but also for critical thinking idea during my whole studying. Because of his encouragement, inspiration and useful guide, I could carry on looking for the special idea, motivation and I could conduct to do my research. I also would like to say my sincere thankful to my committee members, for their valuable comments and kind suggestions in completion of my work. Moreover, I would like to express my appreciation to all my friends from our Research Laboratory in Chulalongkorn University, Bangkok. My expression for gratitude also extends to all the staffs from International School of Engineering (ISE), Chulalongkorn University and AUN/SEED-Net for their support. At last but not least, I would like to pay my sincere respect to my parents, my teacher Dr. Sandar Tun and thank to my family for their pure love, understanding and motivation. My research dissertation could not be possible and finished in time without their kind support and encouragement.

Kaung Ko Ko Sint

## TABLE OF CONTENTS

	<b>Page</b>
.....	iii
ABSTRACT (THAI) .....	iii
.....	iv
ABSTRACT (ENGLISH) .....	iv
ACKNOWLEDGEMENTS .....	v
TABLE OF CONTENTS .....	vi
List of Tables .....	ix
List of Figures .....	xi
Chapter 1 .....	1
Introduction .....	1
1.1 Rational .....	1
1.2 Objective of this Study .....	2
Chapter 2 .....	4
Theories and Literature Reviews .....	4
2.1 Textile wastewater .....	4
2.1.1 The characteristics of textile wastewater .....	4
2.1.2 Reactive dyes .....	9
2.1.3 Polyvinyl Alcohol in textile wastewater .....	10
2.1.4 Formaldehyde in textile wastewater .....	11
2.1.5 Color measurement of textile wastewaters .....	12
2.1.6 Conventional Treatments of textile wastewater .....	13
2.2 Forward osmosis .....	13
2.2.1 Osmotic phenomena .....	13
2.2.2 Forward osmosis processes .....	15
2.2.3 Forward osmosis membranes .....	17

2.2.4 Forward osmosis for application in wastewater treatment .....	18
2.2.5 Membrane fouling in forward osmosis .....	19
2.3.1 Mechanisms of TiO <sub>2</sub> photocatalytic reactions.....	22
2.3.2 Applications of TiO <sub>2</sub> modified membrane for Textile wastewater treatment .....	23
Chapter 3 .....	25
Methodology .....	25
3.1 Flow chart of research methodology .....	25
3.2 Material and Chemicals .....	26
3.2.1 Forward osmosis membranes .....	26
3.2.2 Reactive dyes.....	26
3.2.3 Synthetic textile effluent .....	28
3.3 Forward osmosis membrane's surface coating.....	29
3.3.1 Surface coating procedure .....	29
3.3.2 Membrane surface characterization.....	30
3.4 FO filtration system set up operation .....	31
3.4.1 Laboratory scale FO system set up.....	31
3.4.2 Pure water filtration test .....	32
3.4.3 Membrane fouling test.....	33
3.4.4 Filtration test of synthetic textile effluent .....	36
3.4.5 Filtration test of selected textile effluent .....	37
3.4.5.1 Characterization of selected textile effluent.....	37
3.5 Analytical methods .....	46
3.5.1 TOC .....	46
3.5.2 Determination of Color .....	46
3.5.3 Electrical conductivity (EC).....	47
3.5.4 IC analysis .....	47
3.5.5 Formaldehyde Analysis .....	48
3.5.5 PVA Analysis .....	48



Chapter 4.....	49
Results and Discussion .....	49
4.1 FO membrane surface modification and characterization.....	49
4.2 Effects of Original and TiO <sub>2</sub> coated FO membranes on colour, TOC removal of synthetic textile wastewater .....	65
4.3 Effect of TiO <sub>2</sub> coating on membrane filtration performance .....	66
4.4 Effects of Original and TiO <sub>2</sub> coated FO membranes on anion pollutants removal of synthetic textile wastewater with reactive dyes .....	71
4.5 The interferences of Polyvinyl alcohol (PVA) on dyes removal using TiO <sub>2</sub> coated membrane .....	87
4.6 Feasible application of original and modified both CTA and AqP membranes for water quality improvement of treated textile effluent .....	96
Chapter 5.....	100
Conclusion .....	100
REFERENCES .....	102
APPENDIX.....	111
VITA.....	117

## List of Tables

	<b>Page</b>
Table 2- 1 Characteristics of typical unused textile wastewater (Eswaramoorthi et al., 2008) .....	7
Table 2- 2 Characteristics of textile effluent after of biological treatment (Ali and Nadeem, 2006) and Guideline for color removal from Textile wastewater, Department of Industry, Thailand, 2556 (in Thai)) .....	8
Table 2- 3 Toxic aromatic amines derivatives from azo dyes(Growth and Meenakshi, 2011).....	9
Table 2- 4 Specific Pollutants from Textile Wet Processing (Imtiazuddin et al., 2012) .....	11
Table 2- 5 Osmotic pressure as a function of solution concentration at 25°C for various potential draw solutions (Cath et al., 2006) .....	17
Table 2- 6 Advanced oxidation processes (Kazner et al., 2014) .....	23
Table 3- 1 Effect of Foulant (Humic Acid) on Original and Coated FO membrane ...	35
Table 3- 2 Investigation on removal efficiency of individual reactive dye (Reactive Black-5/Reactive Red-10/Reactive Blue-2) by original and modified FO Membranes .....	37
Table 3- 3 Investigation on removal efficiency of real textile effluent by original and modified FO Membranes .....	39
Table 3- 4 Investigation on removal efficiency of individual reactive dye (Reactive Black-5/Reactive Red-10/Reactive Blue-2) with effects of formaldehyde by original and modified FO Membranes. ....	41
Table 3- 5 Investigation on removal efficiency of individual reactive dye (Reactive Black-5/Reactive Red-10/Reactive Blue-2) with effects of PVA by original and modified FO Membranes .....	42
Table 3- 6 Investigation on color removal efficiencies of textile effluent with effect	44
Table 3- 7 Investigation on color removal efficiencies of textile effluent with effect	45
Table 4-1 Surface element coverages on the virgin, used , and modified forward osmosis membranes .....	56
Table 4- 2 Water contact angles of the virgin, used , and modified forward osmosis membranes .....	57

Table 4- 3 Removal efficiencies for color (ADMI value) after treated with both virgin and modified CTA and aquaporin membranes for reactive black, reactive blue and reactive red with interferences (HCOH and PVA). .....66



## List of Figures

	<b>Page</b>
Figure 2- 1 Solvent flows in FO, PRO, and RO. For FO, $\Delta P$ is approximately zero and water diffuses to the more saline side of the membrane(Lee and Baker, 1981).....	14
Figure 2- 2 Relationship between water flux, osmotic pressure differential and hydraulic pressure differential. Adapted from (Lee et al., 2008).....	15
Figure 3- 1 Scope of overall experimental runs.....	25
Figure 3- 2 Structure of Reactive Black(Batchelor et al., 2006) .....	26
Figure 3- 3 Structure of Reactive Blue (Batchelder, 1965) .....	27
Figure 3- 4 Structure of Reactive Red (Batchelder, 1965) .....	27
Figure 3- 5 Proposed Coating of Photocatalysts on membrane active surface.....	30
Figure 3- 6 Schematic diagram of the Laboratory-scale FO system (Xue et al., 2018) .....	31
Figure 4- 1 SEM images of membrane active surfaces: (a) virgin CTA membrane, (b) used CTA membrane, (c) modified CTA membrane, (d) virgin AqP membrane, (e) used AqP membrane, and (f) modified AqP membrane.....	50
Figure 4- 2 SEM images of membrane active surfaces: (a) used modified AqP (blue) (b) used modified AqP (HCHO-red), (c) used modified AqP (PVA-black), (d) used modified CTA (blue), (e) used modified CTA (HCHO-black), and (f) used modified CTA (PVA-red), (g) used TiO <sub>2</sub> modified CTA and (h) used TiO <sub>2</sub> modified AqP....	51
Figure 4- 3 SEM images of membrane active surfaces: (a) used AqP (black) (b) used AqP (HCHO-red), (c) used AqP (PVA-blue), (d) used CTA (red), (e) used CTA (HCHO-blue), and (f) used CTA (PVA-black).....	52
Figure 4- 4 EDX spectra of membrane active surfaces: (a) virgin CTA membrane, (b) used CTA membrane, (c) modified CTA membrane, (d) virgin AqP membrane, (e) used AqP membrane, and (f) modified AqP membrane.....	53
Figure 4- 5 EDX spectra of membrane active surfaces: (a) used modified AqP (blue) (b) used modified AqP (HCHO-red), (c) used modified AqP (PVA-black), (d) used modified CTA (blue), (e) used modified CTA (HCHO-black), and (f) used modified CTA (PVA-red), (g) used TiO <sub>2</sub> modified CTA and (h) used TiO <sub>2</sub> modified AqP....	54
Figure 4- 6 EDX spectra of membrane active surfaces: (a) used AqP (black) (b) used AqP (HCHO-red), (c) used AqP (PVA-blue), (d) used CTA (red), (e) used CTA (HCHO-blue), and (f) used CTA (PVA-black).....	55

Figure 4- 7 AFM images of membrane active surfaces: (a) virgin CTA membrane, (b) modified CTA membrane, (c) virgin AqP membrane, and (d) modified AqP membrane.....	58
Figure 4- 8 Forward osmosis water flux, reverse solute flux, and specific reverse diffusion rate for (a) CTA membrane and (b) AqP membrane. The columns with error bars show the averages and standard deviations of water flux; the scatters with error bars show the averages and standard deviations of reverse salt flux; x is the specific reverse diffusion rate.....	59
Figure 4- 9 Membrane flux variation during organic fouling tests for (a) virgin CTA membrane, (b) modified CTA membrane, (c) virgin AqP membrane, and (d) modified AqP membrane.....	62
Figure 4- 10 The average water flux in the initial 30 min of the baseline and fouling cycle experiments.....	63
Figure 4- 11 Correlation between ADMI and concentration of reactive dyes.....	65
Figure 4- 12 Comparison of effluent TOC values, while varying the initial ADMI values of synthetic textile effluent (reactive black) with original AqP modified AqP , original CTA and modified CTA membrane. ....	68
Figure 4- 13 Comparison of draw solution TOC values, while varying the initial ADMI values of synthetic textile effluent (reactive blue) with original AqP, modified AqP original CTA and modified CTA membrane. ....	68
Figure 4- 14 Comparison of draw solution TOC values, while varying the initial ADMI values of synthetic textile effluent (reactive red) with original CTA , modified CTA membrane , original AqP and modified AqP membrane .....	69
Figure 4- 15 Membrane flux variation during synthetic textile wastewater filtration (reactive black) of modified AqP membrane, original AqP membrane, modified CTA membrane and original CTA membrane.....	70
Figure 4- 16 Total removal efficiency of TOC during synthetic textile wastewater filtration with reactive black for modified AqP membrane, original AqP membrane, modified CTA membrane and original CTA membrane. ....	70
Figure 4- 17 Rejection efficiency for TOC during synthetic textile wastewater filtration reactive black of modified AqP membrane, original AqP membrane, modified CTA membrane and original CTA membrane. ....	71
Figure 4- 18 Total removal of sulfate during synthetic textile wastewater filtration reactive black of modified AqP membrane, original AqP membrane, modified CTA membrane and original CTA membrane.....	72

Figure 4- 19 Rejection efficiency of sulfate during synthetic textile wastewater filtration reactive black of modified AqP membrane, original AqP membrane, modified CTA membrane and original CTA membrane. ....	73
Figure 4- 20 Total removal efficiency of nitrate during synthetic textile wastewater filtration with reactive black of modified AqP membrane, original AqP membrane, modified CTA membrane and original CTA membrane. ....	73
Figure 4- 21 Rejection efficiency of nitrate during synthetic textile wastewater filtration reactive black of modified AqP membrane, original AqP membrane, modified CTA membrane and original CTA membrane. ....	74
Figure 4- 22 Total removal efficiency of phosphate during synthetic textile wastewater filtration with reactive black of modified AqP membrane, original AqP membrane, modified CTA membrane and original CTA membrane. ....	75
Figure 4- 23 Membrane flux variation during synthetic textile wastewater filtration reactive black with varying HCHO interference for modified AqP membrane, original AqP membrane, modified CTA membrane and original CTA membrane. ....	75
Figure 4- 24 Total removal of TOC value during synthetic textile wastewater filtration (reactive black) with varying HCHO interference for modified AqP membrane, original AqP membrane, modified CTA membrane and original CTA membrane.....	76
Figure 4- 25 Rejection efficiency of TOC value during synthetic textile wastewater filtration (reactive black) with varying HCHO interference for modified AqP membrane, original AqP membrane, modified CTA membrane and original CTA membrane.....	76
Figure 4- 26 Total retention of sulfate during synthetic textile wastewater filtration (reactive black) with varying HCHO interference for modified AqP membrane, original AqP membrane, modified CTA membrane and original CTA membrane.....	77
Figure 4- 27 Rejection efficiency of sulfate during synthetic textile wastewater filtration (reactive black) with varying HCHO interference for modified AqP membrane, original AqP membrane, modified CTA membrane and original CTA membrane.....	77
Figure 4- 28 Membrane flux variation during synthetic textile wastewater filtration (reactive blue) with varying HCHO interference of modified AqP membrane, original AqP membrane, modified CTA membrane and original CTA membrane. ....	78
Figure 4- 29 Total removal of TOC during synthetic textile wastewater filtration reactive blue of modified AqP membrane, original AqP membrane, modified CTA membrane and original CTA membrane.....	78

Figure 4- 30 Rejection efficiency of TOC value during synthetic textile wastewater filtration with reactive blue with modified AqP membrane, original AqP membrane, modified CTA membrane and original CTA membrane. ....	79
Figure 4- 31 Total retention of sulfate during synthetic textile wastewater filtration (reactive blue) with modified AqP membrane, original AqP membrane, modified CTA membrane and original CTA membrane.....	80
Figure 4- 32 Rejection efficiency of sulfate during synthetic textile wastewater filtration (reactive blue) of modified AqP membrane, original AqP membrane, modified CTA membrane and original CTA membrane. ....	80
Figure 4- 33 Total retention of sulfate during synthetic textile wastewater filtration (reactive blue) with varying HCHO interference for modified AqP membrane, original AqP membrane, modified CTA membrane and original CTA membrane.....	81
Figure 4- 34 Membrane flux variation during synthetic textile wastewater with different ADMI values (reactive red) tests for modified AqP membrane, original AqP membrane, modified CTA membrane and original CTA membrane. ....	81
Figure 4- 35 Total retention of TOC value during synthetic textile wastewater filtration with reactive red of modified AqP membrane, original AqP membrane, modified CTA membrane and original CTA membrane. ....	82
Figure 4- 36 Rejection efficiency of TOC value during synthetic textile wastewater filtration with reactive red with modified AqP membrane, original AqP membrane, modified CTA membrane and original CTA membrane. ....	82
Figure 4- 37 Total retention of sulfate during synthetic textile wastewater filtration (reactive red) with modified AqP membrane, original AqP membrane, modified CTA membrane and original CTA membrane.....	83
Figure 4- 38 Rejection efficiency of sulfate during synthetic textile wastewater filtration (reactive red) with modified AqP membrane, original AqP membrane, modified CTA membrane and original CTA membrane. ....	83
Figure 4- 39 Membrane flux variation during synthetic textile wastewater ( reactive red) with varying the concentration of interference (HCHO) tests for modified AqP membrane, original AqP membrane, modified CTA membrane and original CTA membrane.....	84
Figure 4- 40 Total retention of TOC value during synthetic textile wastewater filtration (reactive red) with varying HCHO interference for modified AqP membrane, original AqP membrane, modified CTA membrane and original CTA membrane.....	84

Figure 4- 41 Rejection efficiency of TOC value during synthetic textile wastewater filtration (reactive red) with varying HCHO interference for modified AqP membrane, original AqP membrane, modified CTA membrane and original CTA membrane.....	85
Figure 4- 42 Total retention of sulfate during synthetic textile wastewater filtration (reactive red) with varying HCHO interference for modified AqP membrane, original AqP membrane, modified CTA membrane and original CTA membrane .....	85
Figure 4- 43 Rejection efficiency of sulfate during synthetic textile wastewater filtration (reactive blue) of modified AqP membrane, original AqP membrane, modified CTA membrane and original CTA membrane. ....	86
Figure 4- 44 Membrane flux variation during synthetic textile wastewater (blue) with varying the concentration of interference (PVA) tests for modified AqP membrane, original AqP membrane, modified CTA membrane and original CTA membrane.....	86
Figure 4- 45 Membrane flux variation during synthetic textile wastewater (red) with varying the concentration of interference (PVA) tests for modified AqP membrane, original AqP membrane, modified CTA membrane and original CTA membrane.....	87
Figure 4- 46 Total retention of TOC value during synthetic textile wastewater filtration (reactive red) with varying HCHO interference for modified AqP membrane, original AqP membrane, modified CTA membrane and original CTA membrane.....	88
Figure 4- 47 Rejection efficiency of TOC value during synthetic textile wastewater filtration (reactive red) with varying HCHO interference for modified AqP membrane, original AqP membrane, modified CTA membrane and original CTA membrane.....	88
Figure 4- 48 Total removal of sulfate during synthetic textile wastewater filtration (reactive red) with varying HCHO interference for modified AqP membrane, original AqP membrane, modified CTA membrane and original CTA membrane .....	89
Figure 4- 49 Rejection efficiency of sulfate during synthetic textile wastewater filtration (reactive red) of modified AqP membrane, original AqP membrane, modified CTA membrane and original CTA membrane. ....	90
Figure 4- 50 Total removal of nitrate during synthetic textile wastewater filtration (reactive red) with varying HCHO and PVA interference for modified AqP membrane, original AqP membrane, modified CTA membrane and original CTA membrane.....	90
Figure 4- 51 Rejection efficiency of nitrate during synthetic textile wastewater filtration (reactive red) of modified AqP membrane, original AqP membrane, modified CTA membrane and original CTA membrane. ....	91
Figure 4- 52 Total removal of phosphate during synthetic textile wastewater filtration (reactive red) with varying HCHO and PVA interference for modified AqP	



membrane, original AqP membrane, modified CTA membrane and original CTA membrane.....	91
Figure 4- 53 Rejection efficiency of nitrate during synthetic textile wastewater filtration (reactive red) of modified AqP membrane, original AqP membrane, modified CTA membrane and original CTA membrane. ....	92
Figure 4- 55 Characteristic of treated textile wastewater effluent from factory A.....	97
Figure 4- 56 (a) Comparison of ADMI value and after treated with both original and modified FO membranes process.....	98



# Chapter 1

## Introduction

### 1.1 Rational

The textile industry can be considered as one of the largest water consumers (Ulson de Souza et al., 2009). Large amount of wastewater is discharged from textile industry without sufficient treatment. Some of these wastewater are colored despite containing only small amounts of dyes. These dyes are toxic and, in most cases, are difficult to be biodegraded and resistant to physic-chemical treatment. Presence of little amount of dyes in water (less than 1 ppm for some dyes) is highly visible and undesirable (Rahman, 2016). Therefore, it is necessary to eliminate dyes from wastewater before it is discharged into the natural water bodies. Complex aromatic structures of most dyes make it difficult for conventional treatment processes such as activated sludge to be effective in achieving good color removal. However, excellent results were obtained using membrane processes which are proven to be very successful in removing the undesired color (Kumar and Choudhary, 2011). Membrane separation processes have the ability to separate dyes continuously from effluent. Membrane technologies have gained increasing attention in water treatment, wastewater treatment and many other industrial applications. The separation of pure water from wastewater using polymeric membranes has been studied intensively for the past half century. Over this time, pressure driven membrane processes, such as microfiltration (MF), ultrafiltration (UF), nanofiltration (NF), and reverse osmosis (RO) have been applied widely in the field of water and wastewater treatment. Forward osmosis (FO), as an alternative to pressure driven membrane processes, has been gaining some attention in the past few years. In FO, the driving force for mass transportation is the difference in osmotic pressure across the membrane. Water diffuses from the feed solution with lower osmotic pressure to a draw solution with higher osmotic pressure. As water diffuses through the membrane, the feed solution becomes concentrated and the draw solution is diluted.

Applying a semi-permeable membrane between the draw and the feed solutions provides pathways for water molecules while restricts the passage of solutes from one side of the membrane to the other side. An ideal FO membrane exhibits high water permeability and solute rejection, low concentration polarization and fouling propensity as well as high chemical and mechanical stability. The majority of the recent advances in the FO process devoted to membrane materials development with the aim of fabricating high-performance FO membranes. CTA Membranes are less expensive, have a longer life, require less cleaning, and are much more resistant to chlorine. Aquaporin (AqP) FO membrane enables high rejection of contaminants and low reverse back diffusion using only osmotic pressure (Huang and McCutcheon, 2015). Aquaporin proteins embedded in the active layer of an AqP membrane are virtually 100% selective to water molecules, which drastically lower the back diffusion of draw solutes.

Membrane surface modification is one of the well investigated methods for preventing biofilm formation. Different methods of surface modification have been reported including grafting macromolecules preparing antifouling surfaces by functionalization with photocatalytic Nanoparticles such as  $\text{TiO}_2$  and carbon-based nanomaterials and using biocidal Nanoparticles such as silver (Ag) Nanoparticles either incorporated into the support layer or attached to the surface of the TFC membranes (Soroush and Ma, 2015).

The objectives of this work are to develop  $\text{TiO}_2$  nanoparticle coated commercial FO membranes (Aquaporin membrane and CTA membrane) and to study the suitability of these  $\text{TiO}_2$  coated membranes for treatment of textile effluent after biological treatment processes. By comparing the properties and performance between membranes with and without  $\text{TiO}_2$  nanoparticles coating, the mechanisms of enhanced filtration performance due to  $\text{TiO}_2$  nanoparticles coating will be interpreted.

## 1.2 Objective of this Study

1. To develop  $\text{TiO}_2$  nanoparticle coated commercial FO membranes
2. To investigate the effects of surface modification on membrane performance in terms of water permeability and fouling resistance.

3. To evaluate the feasibility of the modified FO membranes for removing reactive dyes from textile effluent
4. To investigate the interferences of PVA (Polyvinyl alcohol) and formaldehyde on dyes removal using  $\text{TiO}_2$  coated membrane

### **1.3 Scope of the Research**

1. Establish and operate a laboratory scale forward osmosis filtration system
2. Characterize membrane surface properties including surface morphology, functional groups, chemical components, zeta potential, and contact angle.
3. Develop the FO membrane surface coating method for 2 membranes (Aquaporin membrane and CTA membrane)
4. Investigate the change in water qualities of synthetic textile effluent (Reactive Dyes i.e. reactive black, reactive red and reactive blue) and effluent from textile plant after biological treatment system
5. Fix conditions (temperature, NaCl (draw solution) vary concentration of chemical interferences

### **1.4 Expected Outcomes**

1. Obtain the  $\text{TiO}_2$  nanoparticle coated FO membranes that effectively enhance the elimination of reactive dyes from textile effluent
2. Obtain the mechanisms of performance enhancement for dye removal by  $\text{TiO}_2$  nanoparticle coated FO membranes
3. Publish one paper on academic conference

## **Chapter 2**

### **Theories and Literature Reviews**

#### **2.1 Textile wastewater**

##### **2.1.1 The characteristics of textile wastewater**

The characteristics of textile wastewater vary and depend on types of textile manufacturing and the chemicals usage. The textile wastewater contains high amounts of agents causing damage to the environment and human health including suspended solids and dissolved solids, biological oxygen demand (BOD), chemical oxygen demand (COD), chemicals, odour and colour. Most of the BOD/COD ratios are found to be around 1:4, indicating the presence of non-biodegradable substances. Typical characteristics of textile wastewater are shown in Table 2.1.

Textile wastewater contains trace metals like Cr, As, Cu and Zn, which are capable of harming the environment (Eswaramoorthi et al., 2008). Dyes in water gives out a bad colour and can cause diseases like haemorrhage, ulceration of skin, nausea, severe irritation of skin and dermatitis (Tüfekci and Sivri, 2007). They can block the penetration of sunlight from water surface preventing photosynthesis (Laxman, 2009). Dyes also increase the biochemical oxygen demand of the receiving water and in turn reduce the reoxygenation process and hence hamper the growth of photoautotrophic organisms (Tüfekci and Sivri, 2007). The suspended solid concentrations in the wastewater play an important role in affecting the environment as they combine with oily scum and interfere with oxygen transfer mechanism in the air-water interface (Laxman, 2009).

Inorganic substances in the textile wastewater make the water unsuitable for use due to the presence of excess concentration of soluble salts. These substances even in a lower quantity are found to be toxic to aquatic life (Masupha, 2008). Some of the inorganic chemicals like hydrochloric acid, sodium hypochlorite, sodium hydroxide, sodium sulphide and reactive dyes are poisonous to marine life (Blomqvist, 1996). The organic components are found to undergo chemical and biological changes that result in the removal of oxygen from water. The seriousness of water pollution

depends on the quantity of water and chemicals used in the wet process (Laxman, 2009). Textile dyestuffs are found to contain a large amount of organic substances which are difficult to degrade and are resistant to aerobic degradation. They are also found to be reduced into carcinogenic agents under anaerobic conditions.

### **-Nitrogen**

Nitrogen can be present in different forms. Dyebath additives containing nitrogen are the main source of nitrogen in textile wastewater. Ammonia sources are printing, coating, preparation, and dyeing processes. Printing pastes contain urea, another compound that can be present in large quantities. From the characterizations it can be concluded that nitrogenous compounds are only present in large quantities in dyeing and printing wastewaters (Bisschops and Spanjers, 2003). In wastewater, the most important nitrogen fractions to be measured are nitrate, nitrite, ammonia and Total Kjeldahl nitrogen (TKN). Organic nitrogen is calculated by subtracting the amount of ammonia from the TKN. Usually those parameters are reported separately, instead of the 'total nitrogen' value.

### **-Phosphorus**

In natural waters and wastewaters, the prevailing forms of phosphorus are orthophosphates, condensed phosphates, and organically bound phosphates. In textile wastewaters, dyebath wastewater containing phosphate buffers are the main source of phosphorus. Phosphates are used in different steps in textile wet processing. For instance, in buffers, scouring, water conditioners, surfactants, and flame-retardant finishes. In many cases the phosphate-containing chemicals can be replaced, which is usually more economic than removal of the phosphate in wastewater treatment. Methods for the analysis of phosphorus are based on the conversion of all phosphorous forms to dissolved orthophosphate. The orthophosphate is then measured calorimetrically.

### **-Sulphur Compounds**

In the process high levels of Sulphur compounds can be present in textile wastewater. If sodium sulphate is used as an auxiliary in reactive dyeing, sulphate levels in the dyebath can be as high as 20 – 42 g /l. Sodium sulphide and sodium hydrosulphite are commonly used as reducing agents when sulphur or vat dyes are used. Another source of sulphur compounds is for instance the use of sulphuric acids in pH control. Sulphur compounds that can be measured in wastewater are sulphide, sulphite and sulphate(Bisschops and Spanjers, 2003) .The most suitable method depends on the form in which the sulphur is present and the concentration. Table 2.1 shows the characteristics of typical unused textile wastewater.

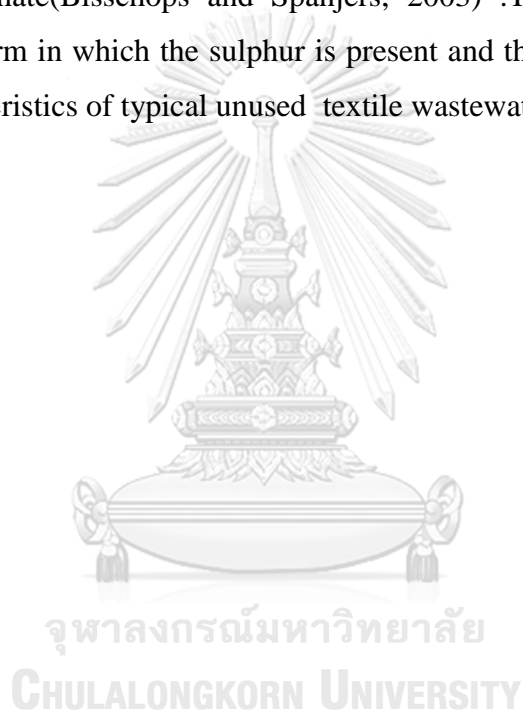


Table 2- 1 Characteristics of typical unused textile wastewater (Eswaramoorthi et al., 2008)

Parameter	Range
pH	6-10
Temperature (°C)	35-45
Total dissolved solids (mg/L)	8,000-12,000
BOD (mg/L)	80-6,000
COD (mg/L)	150-12,000
Total suspended solids (mg/L)	15-8,000
Total Dissolved Solids (mg/L)	2,900-3,100
Chlorine (mg/L)	1,000-6,000
Free chlorine (mg/L)	<10
Sodium (mg/L)	70%
Trace elements (mg/L)	
Fe	<10
Zn	<10
Cu	<10
As	<10
Ni	<10
B	<10
F	<10
Mn	<10
V	<10
Hg	<10
PO <sub>4</sub>	<10
Cn	<10
Oil & grease (mg/L)	10-30
TNK (mg/L)	10-30
NO <sub>3</sub> -N (mg/L)	<5
Free ammonia (mg/L)	<10
SO <sub>4</sub> (mg/L)	600-1000
Silica (mg/L)	<15
Total Kjeldahl Nitrogen (mg/L)	70-80
Color (Pt-Co)	50-2,500

From the report on guideline for color removal from textile wastewater (Department of Industry, Thailand, 2556), it was found that effluents from 98 textile industries after biological wastewater treatment had color in the range of 400-700 ADMI. Also, other effluent quality parameters were reported by Ali and



Nadeem(2006). Here, the characteristics of textile effluent after biological treatment are summarized in Table 2.2.

Table 2- 2 Characteristics of textile effluent after of biological treatment (Ali and Nadeem, 2006) and Guideline for color removal from Textile wastewater, Department of Industry, Thailand, 2556 (in Thai))

<b>Parameter</b>	<b>Range</b>
COD (mg/L)	50-70
TOC (mg/L)	39.5-62.4
Color (ADMI)	400-700
pH	6.2-6.4
Sulphate (mg/L)	200-400
Chloride (mg/L)	100-320
TKN	30-45
TP (mg/L)	1-2
Pb	0.1-0.3
EC ms/cm	2.24-5.10
Ni	BDL
Cu	BDL
Cd	BDL

The values except pH and EC are expressed in mg/l. BDL (below detection limit): less than 2 mg/l.

Human exposure to textile dyes have resulted in lung and skin irritations, headaches, congenital malformations and nausea.(Richardson et al., 2007) detected benzidine, a known carcinogen in a textile effluent which contained disperse orange 37, disperse blue 373 and disperse violet 93 dyes. (Morikawa et al., 1997)tested a total of seven dyes (cremazoles blue S1, cremazoles brown GR, cremazoles orange 3R, direct bordeaux, direct royal blue, direct congo red and direct violet) using AMES tests and witnessed the presence of mutagenic agents. It was noted that direct violet was the only dye with a mutagenicity ratio less than 2:0. They observed that the cremazoles dyes were so toxic to microorganisms. (Morikawa et al., 1997) reported evidence of kidney, liver and urinary bladder cancers on workers after prolonged exposure to textile dyes. It was found that dermatitis, asthma, nasal problems and

rhinitis were acquired by workers after prolonged exposure to reactive dyes. Toxic aromatic amines derivatives from azo dyes are also shown in Table 2.3.

Table 2- 3 Toxic aromatic amines derivatives from azo dyes(Growth and Meenakshi, 2011)

AROMATIC AMINE GROUP	HUMAN CARCINOGEN EVIDENCE (Cartwright R.A., 1983)
1-Naphthylamine	Slight/ Mixed
2-Naphthylamine	Good
2,5-Diaminotoluene	Slight
3,3'-Dichlorobenzidine	Slight/ Mixed
3,3'-Dimethoxybenzidine	Slight/ Mixed
3,3'-Dimethylbenzidine	Slight
4-Biphenylamine	Good
4-Nitrobiphenyl	Slight/ Mixed
4,4'-Methylenebis(2-chloroaniline)	Slight
Auramine	Slight
Benzidine	Good
Magenta	Slight
N-Phenyl-2-naphthylamine	Slight
N,N-Bis(2-chloroethyl)-naphthylamine	Good

### 2.1.2 Reactive dyes

The reactive dyes are sometimes called as fiber reactive dyes. They are most important dyeing class for cellulosic fibers and are also used to dye protein fibers such as wool and silk. Reactive dyes are capable of forming covalent bonds with the fiber molecule and are considered to be the most effective and permanent dyes used. They are found to work well on any cellulose fiber under different temperatures. Reactive dyes are of two types: homobifunctional and heterobifunctional. The homobifunctional reactive dyes contain two monochlorotriazine groups and the

heterobifunctional reactive dyes contain one monochlorotriazine and one vinyl sulphone group. Under alkaline conditions around 50-70% of the dye is fixed onto the fiber using the dyes containing one reactive group and around 80-95% of the dye is fixed onto the fiber using the dyes containing two reactive groups. United Nations Statistics Division reported that the total world imports and export market for reactive dyes and preparations based there on, increased from 125,000 tonnes in 1988 to 350,000 tonnes in 2011 (~3 fold increase in 23 years). The individual production statistics for the reactive dyes are not found in the literature.

### **2.1.3 Polyvinyl Alcohol intextile wastewater**

Sizing and desizing are the key textile processes where the use of polyvinyl alcohol (PVA) is unavoidable due to its functional and economically beneficial characters. Textile processing is the major source of industrial water pollution across the world and sizing – desizing operations account for nearly 30% of the water consumed in a textile plant (Chen et al., 2013a). The main problem resulting from the desizing step is the high load of chemical oxidation demand (COD) found in the polymer containing effluent (Bechtold et al., 2004). These washed polymers include starch, PVA, carboxymethyl cellulose and acrylates. PVA and starch are the major contributors of organic load with 0.01 and 0.67 BOD to COD ratio respectively (Matsumura et al., 1993). China, Japan and the United States continue to be the world's largest producers and consumers of PVA. It is predicted that its consumption will increase at an overall rate of about 3.6% annually during 2012–2017. Though PVA is not toxic, it has a great surface activity and can form large amounts of foam in the water. This foam affects the oxygen content in water body, thereby inhibiting or even undermine the respiratory activity of aquatic organisms (Zhang et al., 2005). The desize pollution streams containing synthetic PVA are hence a threat to the environment (Hao and Zhao, 1994). Although considerable efforts have been made to replace PVA, it has not been possible to develop a warp sizing chemical that can match the sizing performance of PVA and at the same time be cost-effective and biodegradable in effluent treatment plants (Chen et al., 2013b). A number of studies explain the improvement in the biodegradability of PVA using advanced oxidation processes (Oh et al., 2009; Wu et al., 2008; Yan and Meixia, 2008), but their

application and treatment economy needs to be considered for the process viability. Similar attempts to study membrane filtration (Mo et al., 2008), vacuum flash evaporation (VFE) (Gupta, 2009), ultrafiltration (UF) (Porter, 1998) and (Altin, 2008) have been made of PVA recycle and reuse after the treatment. But high initial investment cost and operation – maintenance cost makes these options unattractive to textile industries for implementation and use. Lower COD textile wastewater can be used easily and the water can be reused after any tertiary treatment (He et al., 2013). But for treatment of high COD in wastewater of 10,000 to 20,000 mg/l with 0.5 to 1% PVA concentration need well performing microbial consortia with optimized process. There is no any systematic process research available which will lead towards process optimization of PVA biodegradation and it can be viable for commercialization. Specific Pollutants from Textile Wet Processing (Imtiazuddin et al., 2012) can be summarized in Table 2.4.

Table 2- 4 Specific Pollutants from Textile Wet Processing (Imtiazuddin et al., 2012)

Process	Various Pyhsico-chemicals
Desizing	Enzymes, Starch, Waxes, CMC
Bleaching	H <sub>2</sub> O <sub>2</sub> , Sodium Silicate, Organic Stabilizer, Surfactant
Mercerizing	NaOH, Cotton Wax
Dyeing	Dyes, Salts, Surfactant, Urea, Soda Ash,
Printing	Urea, Dyes, Pigments, Binder, Soda Ash, Thickener
Finishing	Resins, Formaldehyde, PVA, Waxes, Hydrocarbon

#### 2.1.4 Formaldehyde in textile wastewater

Formaldehyde is widely used in various industrial settings such as the manufacture of pentaerythritol, ethylene glycol, synthetic resins, adhesives and glue, paints, and medicines, and the production of textile and wood processing, chemical and petrochemical industries, and paper manufacturing (Tang et al., 2009). These industries that utilize or produce formaldehyde usually generate large volumes of wastewater containing variable concentrations of formaldehyde, ranging from a few

to hundreds of milligrams per liter. Formaldehyde can seriously harm human health and cause damage to the environment (Grafstrom et al., 1985). The US EPA has classified formaldehyde as a “probable human carcinogen”. It was found to critically damage DNA and to mutate in mammalian cells and microorganisms. Due to its wide application in all parts of the world, there is significant risk of releasing large amounts of formaldehyde to the environment through industrial emission. To prevent this from occurring, wastewater containing formaldehyde must be used in an effective and environmentally friendly process before being discharged. Biological treatment processes are the most commonly accepted methods for wastewaters containing organic compounds such as formaldehyde (Eiroa et al., 2004). However, the concentration of formaldehyde in effluents generated from many chemical industries ranges highly from 5000 to 10,000 ppm, even though in the low limit of 100-500 ppm discharge, which is beyond the capacity of biological decomposition processes (Kajitvichyanukul et al., 2006) due to its strong bio-resistance and toxicity to microbes, thus limiting the direct use of biological treatment methods (Cui et al., 2016). Therefore, development of an energy efficient, rapid and sustainable treatment process is essential for proper environmental protection.

### **2.1.5 Color measurement of textile wastewaters**

The electromagnetic spectrum can be divided in three different regions: ultraviolet, visible light and infrared. Although visible light is considered to be between the wavelengths of 350 and 780 nm, the human eye can normally detect radiations between the wavelengths of 380 and 720 nm. Colour in water can be either a result of natural phenomena like the presence of humic substances, natural metallic ions, e.g. iron and manganese, and/or plankton; or the colour can also result from an artificial phenomenon like the discharge of dyes and pigments. Industrial processes such as textile, chemical and pharmaceutical industries may discharge large amounts of coloured wastewaters into water bodies. In general, colour in water is classified in terms of true colour, i.e. when the sample is turbidity-free, or apparent colour, i.e. when the sample is measured without previous treatment (Apha, 1998). The most common methods to measure the colour of water and wastewater are visual

comparison and spectrophotometry, although there is still a lack of a universal method to classify coloured wastewater emissions. By visual comparison, colour is quantified by comparing the sample colour with either known concentrations of coloured standards (normally a platinum–cobalt solution), or properly calibrated colour disks. This method is currently used in water treatment plants as a control parameter mainly because of its simplicity, but it is not applicable for highly coloured industrial wastewaters.

### **2.1.6 Conventional Treatments of textile wastewater**

Effluent discharged from the textile industries undergo various physico-chemical treatments such as flocculation, coagulation and ozonation and biological treatment for the removal of COD, nitrogen, organics, phosphorus and metal removal. The disadvantages of the physicochemical treatment process are: (a) the formation and disposal of sludge and (b) the required space. The disadvantage of biological treatment processes are: (a) the presence of toxic heavy metals in the effluent which affects the growth of microorganism (b) most of the dyes used are a non-biodegradable in nature and (c) the long time required for treating the effluent (Eswaramoorthi et al., 2008). Treatment of textile wastewater involves three treatment processes: primary, secondary and tertiary treatments.

## **2.2 Forward osmosis**

### **2.2.1 Osmotic phenomena**

Osmosis is the transport of water due to a difference in solute activities across a membrane. Osmotic pressure (OP). Osmotic pressure is defined (always with respect to a semipermeable membrane, that is, one permeable to solvent but not to the solute) as “the attractive force of a solute in a solution that is equal to hydrostatic pressure on the solution that is required to prevent water from a pure water chamber from moving across an ideal semi-permeable membrane into the solution”. An alternative definition is “Osmotic pressure is the pressure required to raise the activity of the water in a solution so that activity equals the activity of pure water.” These

statements are thermodynamically equivalent. While the latter does not mention a membrane, an experiment to test whether or not the two definitions can be reconciled would involve a membrane.

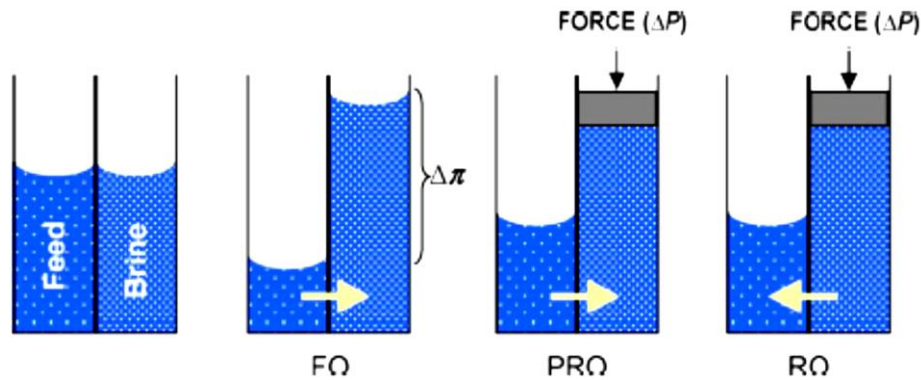


Figure 2- 1 Solvent flows in FO, PRO, and RO. For FO,  $\Delta P$  is approximately zero and water diffuses to the more saline side of the membrane (Lee and Baker, 1981).

Solvent transport can be expressed as:

$$J_w = A (\Delta\pi - \Delta p)$$

Where  $J_w$  is the water flux across the membrane (in this case signed as positive in the direction of osmotic flow),  $A$  is the water permeability coefficient,  $\Delta\pi$  is the osmotic pressure difference across the membrane and  $\Delta P$  is the hydrostatic pressure difference.

(Lee et al., 2008) characterized various osmotic processes, defining Forward Osmosis (FO) when  $\Delta P = 0$ , Pressure Retarded Osmosis (PRO) as  $\Delta\pi > \Delta P$  and Reverse Osmosis (RO) when  $\Delta P > \Delta\pi$ . For practical purposes there are few situations where forward osmosis occurs with this definition (no applied hydraulic pressure on either side of the membrane) and more recently it is generally been assumed that FO relates to water treatment applications and PRO relates to osmotic power applications or applications where the membrane active layer faces the draw solution. What is not defined by (Lee et al., 1999), is the case where hydraulic pressure is applied to the draw solution, Pressure Enhanced Osmosis (PEO) (or Pressure Assisted Osmosis

(PAO)). For the purposes of this paper Forward Osmosis is a general description given for all osmotically driven membrane processes (ODMPs).

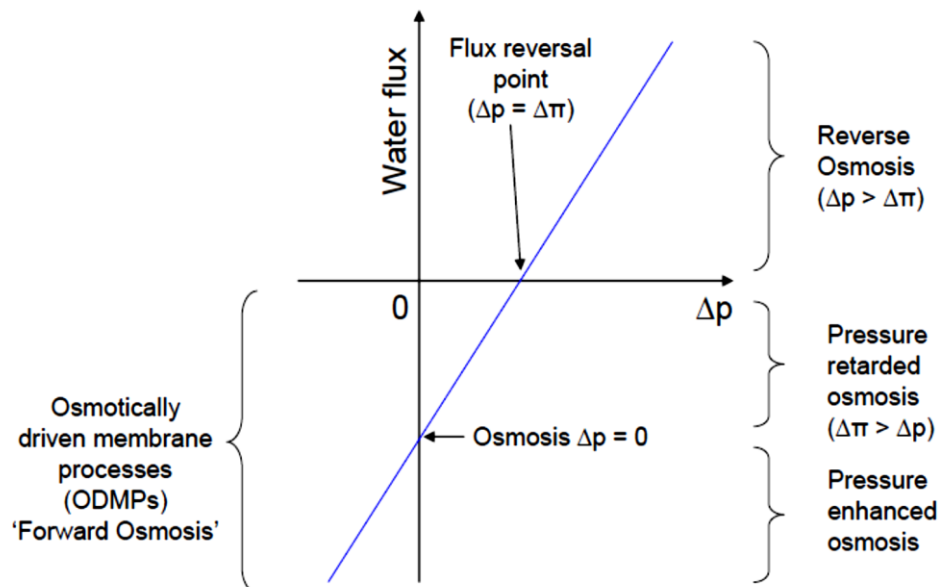


Figure 2- 2 Relationship between water flux, osmotic pressure differential and hydraulic pressure differential. Adapted from (Lee et al., 2008)

### 2.2.2 Forward osmosis processes

Forward Osmosis (also known as Engineered Osmosis (EO), Direct Osmosis (DO) or Manipulated Osmosis (MO)), is a membrane technology utilizing the natural process of osmosis. FO requires two solutions: a feed solution and an osmotic (draw) solution, together with a semipermeable membrane. The draw solution requires an osmotic concentration higher than that of the feed, in order to induce a net water flow through the semi- permeable membrane towards the draw side. In this way, water can be effectively separated from the rest of the feed water constituents. The driving force, unlike other state-of-the-art technologies, is the osmotic pressure gradient over the membrane and not hydraulic pressure. FO is therefore expected to operate with a low energy demand; the challenge is more the energy demand of the reconcentration system. FO also offers additional potential advantages for the subsequent reconcentration step, such as a lower risk of scaling and biofouling than for example



an RO process. The key to achieving high performance in FO is the composition of important factors influencing the osmotically-driven process; amongst others: temperature; membrane type and orientation; the osmotic solution (type and concentration) and feed water type. Despite the availability of over 1000 publications on FO since the 18th century (Alsvik and Hägg, 2013), research in this field has grown significantly since 2005. The growing interest was sparked by the commercialization of membranes specifically tailored to the FO process.

The vast majority of FO studies have tested inorganic-based compounds as DS, and they are still widely used nowadays. Inorganic-based compounds are mainly composed of electrolyte solutions although some non-electrolyte solutions could be also encountered. The use of inorganic compounds as DS has attracted many researchers since they can generally produce reasonably high water fluxes and can be easily recovered by RO or NF or used directly without further treatment (e.g. for fertigation).

Very often a NaCl draw solution is used because it is highly soluble, nontoxic at low concentration and relatively easy to reconcentration using conventional processes without the risk of scaling. Other chemical has also been suggested and tested as draw solutes including  $\text{CaCl}_2$ ,  $\text{Ca}(\text{NO}_2)_3$ ,  $\text{KBr}$ ,  $\text{KCl}$ ,  $\text{KHCO}_3$ ,  $\text{K}_2\text{SO}_4$ ,  $\text{MgCl}_2$ ,  $\text{MgSO}_4$ ,  $\text{NaCl}$ ,  $\text{NaHCO}_3$ ,  $\text{Na}_2\text{SO}_4$ ,  $\text{NH}_4\text{Cl}$ ,  $\text{NH}_4\text{HCO}_3$ , and  $(\text{NH}_4)_2\text{SO}_4$ . Recent investigations have established that internal concentration polarization is a major factor in limiting water flux in osmotically driven membrane processes. McCutcheon and Elimelech (McCutcheon and Elimelech, 2006) improved a model that was initially developed by (Lee et al., 2008). (Lee and Baker, 1981) in which the solution diffusion coefficient and the membrane support layer characteristics contribute to internal concentration polarization, while Tan and Ng (Tan and Ng, 2008) suggest that only the membrane characteristics influence water flux. In both investigations, NaCl was the only draw solution evaluated, and therefore, it was not possible to decisively determine the role of the draw solution diffusion coefficient. In a recent study by (Chekli et al., 2015), the draw solution of 1 M of KCl and NaCl exhibit the highest water flux of more than 25 LMH while  $\text{MgCl}_2$  and  $\text{CaCl}_2$  produced the highest osmotic pressure due to their high solubility in water. Sodium chloride (i.e. NaCl) has been widely used as DS in a variety of applications, including food production and water and wastewater

treatment. The advantages of NaCl are that it is abundant on earth, making seawater a natural and inexpensive source of DS, it is relatively easy to reconcentrate with RO process and it has high water solubility and osmotic pressure. Besides, the thermodynamic properties of NaCl have been widely investigated, making it easier to study.

Table 2- 5 Osmotic pressure as a function of solution concentration at 25°C for various potential draw solutions (Cath et al., 2006)

Draw solute(s)	Concentration	Osmotic pressure (atm)	Molecular weight	Feed solution	Water flux (LMH)	Remark
NaCl	0.60 M	28	58.5 g/mol	DI water	9.6	CTA flat sheet membrane, FO mode
MgCl <sub>2</sub>	0.36 M	28	95 g/mol	DI water	8.4	CTA flat sheet membrane, FO mode
KCl	2 M	89.3	74.6 g/mol	DI water	22.6	CTA flat sheet membrane, FO mode
NH <sub>4</sub> HCO <sub>3</sub>	0.67 M	28	79 g/mol	DI water	7.3	CTA flat sheet membrane, FO mode
Sucrose	1 M	26.7	342.3 g/mol	DI water	12.9	CA hollow fiber, FO mode
PAA-Na 1200	0.72 g/mL	44	1200 Da	DI water	22	CA hollow fiber, PRO mode
PEG-(COOH) <sub>2</sub> -MNPs 250	0.065 M	73	None	DI water	13	CTA flat sheet membrane, PRO mode
1,2,3-Trimethylimidazolium iodide	1M	50	238 g/mol	DI water	13	CTA flat sheet membrane, PRO mode
Sodium formate	0.68 M	28	68 g/mol	DI water	9.4	CTA flat sheet membrane, FO mode
Polyglycol copolymer	30~70%	40~95	> 500 Da	3.5%NaCl	> =4	CTA flat sheet membrane, FO mode
Sodium hexa- carboxylatophenoxy phosphazene	0.067 M	None	1089 g/mol	DI water	6	CTA flat sheet membrane, FO mode

### 2.2.3 Forward osmosis membranes

The first recorded investigations of membrane phenomena date back to the accidental discovery of osmotic pressure in 1748 using pigs' bladders (Alsvik and Hägg, 2013). Thereafter, studies focused on the mechanism of osmosis through natural materials. Membranes and osmotic processes have since evolved. Special attention was given specifically to FO, to avoid the need of energy sources for pressure-driven production. FO was trialed through synthetic materials, which began

with the first asymmetric cellulose acetate (CA) RO membranes developed in the 1960's. These were initially intended for FO, however, due to inherent transport limitations were considered ineffective. Other RO membranes too, have not shown convincing results in FO due to hydrophobicity and relatively thick support layers (150  $\mu\text{m}$ ). Thick support layers lead to poor performance of osmotically driven membrane processes, which is mainly related to concentration polarization (CP). Both internal CP (ICP) and external CP (ECP) exist. CP is caused by a balance between flux, rejection and diffusion, and lowers flux and membrane selectivity (intrinsic membrane selectivity remains unaltered). ICP is exclusive to FO and generally occurs within the porous support layer of the membrane, while ECP is present at the surface of the dense active layer (AL). The breakthrough for FO came with the development of thin, FO-tailored CTA membranes ( $\sim 50 \mu\text{m}$ ) by HTI, allowing higher fluxes through reduced ICP (Lutchmiah et al., 2014). ICP, however, is still an issue for FO and the main driver for further membrane development.

#### **2.2.4 Forward osmosis for application in wastewater treatment**

Drinking water is produced mainly from safe water sources, i.e. groundwater, but due to population growth and economic development, exploitation of aquifers and declining groundwater levels have diminished fresh water sources. The unsustainable use of drinking water for purposes other than sustenance, i.e. industrial processes, is therefore of great concern. A possible alternative source is wastewater. Via microfiltration (MF), ultrafiltration (UF), nanofiltration (NF) or reverse osmosis (RO), high quality water can be produced. Forward Osmosis (FO), an alternative membrane process, also has the potential to treat wastewater, producing high quality water. FO is a technical term describing the natural phenomenon of osmosis: the transport of water molecules across a semipermeable membrane. The osmotic pressure difference is the driving force of water transport, as opposed to pressure-driven membrane processes.

Another major part of impaired-quality water treatment and reclamation is industrial wastewater. A company in the US has successfully piloted a system, based on forward osmosis, that recycles wastewater generated by textile and carpet mills using dyeing processes (R Valladares Linares et al., 2014). Another FO application is to remove

heavy metals from industrial waste water or other impaired-quality water. The effects of hydrodynamic conditions, organic fouling, temperature, feed and draw solution properties have been studied. FO membrane shows a nearly complete rejection to the metals tested (e.g. Pb, Zn, Cu, Cd), indicating its potential to be a convenient and economic method for industrial wastewater treatment. (Rassoul et al., 2012)

Nowadays, most efforts of FO applications for industrial wastewater treatment have been dedicated to the treatment and reclamation of produced water from oil and gas (O&G) industry. Bench scale testing indicates the capacity of FO process for the separation of emulsified oily water (Duong and Chung, 2014).

Fresh water can be recovered from high concentration (up to 200,000 ppm) synthetic oily solution by a customized TFC FO membrane, at a reasonable flux of about 11.8 l/m<sup>2</sup>/h. Some tests from bench to commercial scale have been conducted directly to the real produced water from O&G processing. FO combined with RO in a closed loop has been used to reclaim drilling wastewater from gas exploration operations (R Valladares Linares et al., 2014) , and it is capable of recycling 242,000 gallons drilling wastewater per day, consequently reducing the need for additional fresh water and truck traffic. Similar studies and applications have been conducted by individual research teams and companies using different membrane materials, membrane modules, draw solutions and process configurations (Abousnina, 2012).

Major benefits were achieved by the use of FO: the volume of the waste stream and the need for a fresh water source were greatly reduced in all cases, for feed solutions having a dissolved contaminant concentration greater than 10,000 ppm, a well-designed FO process can economically outperform an RO process, and a high rejection of organic and inorganic contaminants was obtained. However, due to the complexity of both organic and inorganic compounds in the produced water, a relatively complicated pre-treatment process may be required (McGinnis et al., 2013).

### **2.2.5 Membrane fouling in forward osmosis**

This is a key differentiator between osmotically driven processes and reverse osmosis, which has been investigated by a number of academic researchers and reported by commercial organizations based on real operating experience. The general

conclusion is that fouling under FO conditions is less than under a pressure drive RO process and moreover is often entirely reversible.

(Cath et al., 2006) studied fouling in FO for long term space missions, where they reported there was no sign of flux reduction as a result of membrane fouling, thus giving the first indication of the low fouling propensity of the process.

(Cornelissen et al., 2011) used an osmotic membrane bio reactor system to treat activated sludge, where they reported that neither reversible nor irreversible fouling was observed when the membrane active layer was facing the sludge.

(Lee and Baker, 1981) and reported in a comparison between forward osmosis and reverse osmosis organic fouling that organic fouling under FO conditions could be controlled entirely by increasing the crossflow velocity on a flat sheet membrane, while no noticeable change was observed for the RO system.

The Comparison of FO and RO membrane fouling (operating at the same initial flux rates) on the concentration of anaerobic digester concentrate has been investigated (Holloway et al., 2007). They reported that the rate of flux decline was higher with RO than FO and that the FO fouling was reversible, whereas the RO fouling was not. They further speculated that the reason for both the lower rate of fouling and its reversibility was due to the affects of pressure on the foulants on the membrane surface, which occurs rapidly in RO.

### 2.3 TiO<sub>2</sub> modified membrane

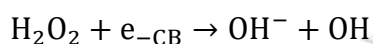
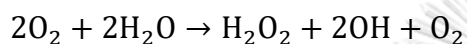
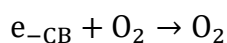
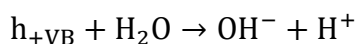
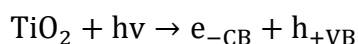
The separation and removal of volatile organic compounds (VOCs) from wastewater are very important processes in environmental applications. For example, benzene is a commonly used VOC as a starting material for the synthesis of aromatic compounds such as phenol and styrene in the petrochemical industry and Dye industry (Qu et al., 2014). However, benzene has severe effects on the environment and human body. Several conventional separation techniques for removal of benzene from water are currently used in industries. However, these processes are cost-intensive and often inefficient. Membrane techniques are expected to be more energy efficient. Many studies have reported the removal of VOCs from water through various polymer membranes using pervaporation. In this study, we used TiO<sub>2</sub> coated

membranes for Photocatalytic Oxidation of PVA and HCOH in wastewater under light.

Here some other useful nanoparticles are studied, in one of the newest works of (Peternel et al., 2007), a novel TFN membrane was prepared and the effects of SAPO-34 nanoparticles were studied. The substrate of this hollow fiber membrane was a dual-layer of PES/PVDF. The membrane showed a large nano-porosity and due to this porosity, high rejection and flux were achieved. In the future it can be a good nanoparticle for the anti-fouling agent on the surface of membranes. For the water purification, another work has been studied by (Al-Amoudi et al., 2008). In this experiment, the nanoparticles of magnesium titanium oxide ( $\text{MgTiO}_3$ ) were used as a filler with different concentrations to achieve a better performance. Water flux and the salt rejection were observed and the TFN membrane showed a high performance in these two parameters. The permeability was increased from 26 to  $44.6 \text{ L/m}^2$  and rejection of about 98% was prepared with a low concentration of nanoparticles. However, one of the useful nanoparticles as an anti-fouling agent is silver. The photo reduction and soft reduction methods were used to synthesize Ag nanoparticles, 4-mercaptopyridine was used as the probe molecule. Ag nanoparticles showed a stable performance on prohibition of bacterial growth. Another work also used Ag nanoparticles for bio-fouling mitigation. Although the roughness, hydrophilicity and salt selectivity were not impacted, about 75 percent of live bacteria was attached to the surface. However, slight reduction in flux was observed. To increase the water flux in an experiment, a hydrophobic zeolite imidazolate framework-8 (ZIF-8) was employed as nanoparticle in the PA selective layer. The membrane including lab made nanoparticles showed a water permeate increase to  $3.35 \text{ l/m}^2 \cdot \text{h} \cdot \text{bar}$ . Generally, among methods of TFN membrane fabrication (i.e. interfacial polymerization, layer-by-layer modifications, UV grafting or UV photografting, electron beam irradiation and plasma treatment), interfacial polymerization is the best choice besides using additive or nanoparticle additives.

### 2.3.1 Mechanisms of TiO<sub>2</sub> photocatalytic reactions

First step of photocatalytic degradation of the aromatic compounds results in the formation of hydroxyl derivatives, which in turn modifies the product distribution in the solution. Photocatalytic degradation is carried out by two types of oxidizing species: the hydroxyl radicals and the positive holes (Ghaly et al., 2014).



Where:

TiO<sub>2</sub> (h<sub>+VB</sub>) - Valence-band holes

TiO<sub>2</sub> (e<sub>-CB</sub>) - Conduction-band Electrons

Upon irradiation by UV, the electrons on the surface of the semiconductor gets excited to the conduction band forming positive holes in the valance band (Equation 19). The valance band holes thus formed are good oxidizers; they have the potential to oxidize water or OH ions into OH radicals as shown in Equations. The conduction band electrons on the other hand act as reducers Chain termination would occur as shown in Equations. Oxidation of TiO<sub>2</sub>/UV is suggested to have a larger advantage over H<sub>2</sub>O<sub>2</sub>/UV, this is because titanium dioxide is found to absorb light up to 385 nm which is greater than that absorbed by H<sub>2</sub>O<sub>2</sub>(Lafond, 2008).

(Halmann et al., 1992) reported that the dye Acid Orange 5 which is normally found in wastewater in concentrations of 10<sup>-4</sup> to 10<sup>-6</sup> M can be completely degraded using black-light mercury lamp as a UV radiation source. (Peternel et al., 2007) reported a 71% reduction in colour when the effluent was used at a pH of 3 under UV/TiO<sub>2</sub>. (Liu et al., 2008) stated that a highest of 70.6% reduction and a lowest of 44.3% reduction of acid yellow 17 was achieved when the effluent was used under UV/TiO<sub>2</sub>.

Table 2- 6 Advanced oxidation processes (Kazner et al., 2014)

Oxidants *	Use
H <sub>2</sub> O <sub>2</sub> / Fe <sup>2+</sup>	Fenton
H <sub>2</sub> O <sub>2</sub> / UV/ Fe <sup>2+</sup>	Photo assisted Fenton
O <sub>3</sub> / UV	Also applicable in gas phase
O <sub>3</sub> / H <sub>2</sub> O <sub>2</sub>	Advance Oxidation
O <sub>3</sub> /UV/H <sub>2</sub> O <sub>2</sub>	Advance Oxidation
O <sub>3</sub> /TiO <sub>2</sub> /Electron beam irradiation	Advance Oxidation
O <sub>3</sub> /TiO <sub>2</sub> /H <sub>2</sub> O <sub>2</sub>	Advance Oxidation
O <sub>3</sub> + Electron beam irradiation	Advance Oxidation
O <sub>3</sub> /Ultrasonic	Advance Oxidation
H <sub>2</sub> O <sub>2</sub> /UV	Advance Oxidation

### 2.3.2 Applications of TiO<sub>2</sub> modified membrane for Textile wastewater treatment

Nano-scale materials embedded in the polyamide barrier layer can improve the performance of Thin Film Composite RO membrane (Jeong et al., 2007). Many researchers have attempted to synthesize Thin Film Composite RO membrane and evaluate their performance. For example, it has been reported that thin film nanocomposite membrane comprised of NaA zeolite exhibited smoother and more hydrophilic, negatively charged surfaces. It was shown that nanoparticle pores played an active role in water permeation and solute rejection (Ma et al., 2012). Zeolite-polyamide thin film nanocomposite (TFN) membrane was prepared on a polysulfone (PSf) porous substrate tailored for forward osmosis i.e. thin support, high porosity, and straight needle-like pores. The embedded NaY zeolite nanoparticles in the polyamide barrier layer significantly increased its water permeability (Jeong et al., 2007). Thin Film Nanocomposite formed with higher loading (~5 w %) of TiO<sub>2</sub> nanoparticles and more robust structure of PA-TiO<sub>2</sub> nanocomposite membrane has been reported. Nanocomposite with silica exhibited superior thermal stability than the pure polyamide membranes and better performance in terms of separation efficiency and water flux (Jadav and Singh, 2009). Loading silver nanoparticles on thin-film composite (TFC) reverse osmosis membrane reduced its permeability but showed strong anti-bacterial activity leading to reduction of more than 75% in the number of



live bacteria attached to the membrane (Ben-Sasson et al., 2014). PolysulfoneTiO<sub>2</sub> substrate was prepared for forward osmosis application and it was found that both and porosity of the substrate were increased upon addition of TiO<sub>2</sub>(Emadzadeh et al., 2014). Results revealed that both hydrophilicity and porosity of the substrate were increased upon addition of TiO<sub>2</sub> nanoparticles. PSf-TiO<sub>2</sub> substrate was formed and the results revealed that the hydrophilicity and the porosity of the substrate were improved upon the TiO<sub>2</sub> addition, leading to significant enhancement in water-flux (Emadzadeh et al., 2013).



# Chapter 3

## Methodology

### 3.1 Flow chart of research methodology

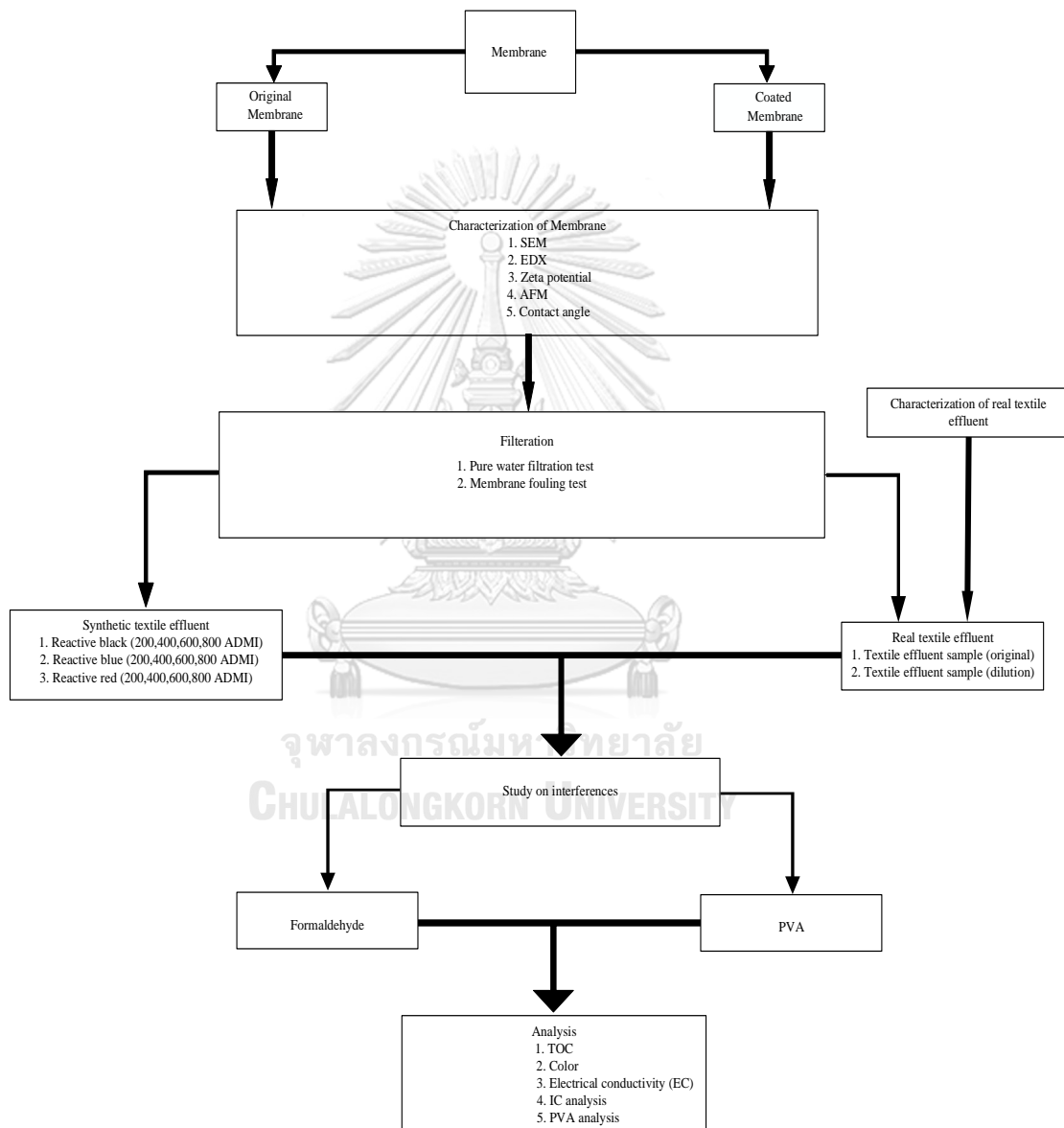


Figure 3- 1 Scope of overall experimental runs

## 3.2 Material and Chemicals

### 3.2.1 Forward osmosis membranes

Two commercially available FO membranes are used in this study: an asymmetric cellulose triacetate (CTA) FO membrane acquired from Hydration Technology Innovations (Albany, OR) and Aquaporin flat Sheet TFC membrane (AqP membrane). The CTA membrane has been the subject of numerous previous FO studies and is composed of a cellulose triacetate layer with an embedded woven support mesh. On the other hand, the AqP membrane is a relatively new product. It is reported to have a thin selective Aquaporin Protein active layer on top of a porous support layer. All the tested membranes are specially designed for FO applications, which have been extensively evaluated for FO treatment processes. However, the performance of TiO<sub>2</sub> coated FO membrane has not been widely considered and investigated yet.

### 3.2.2 Reactive dyes

#### 1. Reactive Black

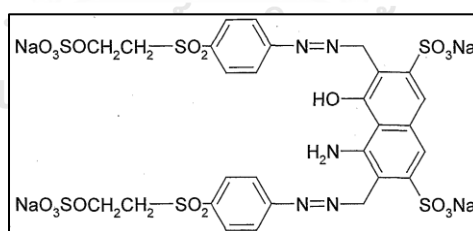


Figure 3- 2 Structure of Reactive Black(Batchelor et al., 2006)

<b>Molecular Formula</b>	:C <sub>26</sub> H <sub>21</sub> N <sub>5</sub> Na <sub>4</sub> O <sub>19</sub> S <sub>6</sub>
<b>Molecular Weight</b>	: 991.82
<b>CI</b>	: Reactive Black 5
<b>Synonym</b>	: Remazol Black B

Chemical Name : 2,7-naphthalenedisulfonic acid, 4-amino-5-hydroxy-3,6-bis(2-(4-((2-(sulfooxy)ethyl)sulfonyl)phenyl)diazenyl)-, sodium salt (1:4)

$\lambda_{\max}$  : 597 nm

## 2. Reactive Blue

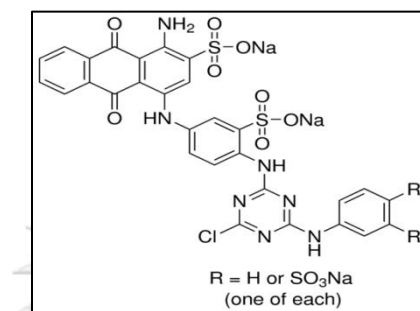


Figure 3- 3 Structure of Reactive Blue (Batchelder, 1965)

## 3.Reactive Red

Molecular Formula : C<sub>29</sub>H<sub>17</sub>ClN<sub>7</sub>Na<sub>3</sub>O<sub>11</sub>S<sub>3</sub>

Molecular Weight : 991.82

CI : Reactive Blue 2

Synonym : Basilen Blue E-3G

Chemical Nam : 1-Amino-4-[[4-[[4-chloro-6-[[3 (or 4)-sulfophenyl]amino]-1,3,5-triazin-2-yl]amino]-3-sulfophenyl]amino]-9,10-dihydro-9,10-dioxo-2-anthracenesulfonic acid

$\lambda_{\max}$  : 615 nm

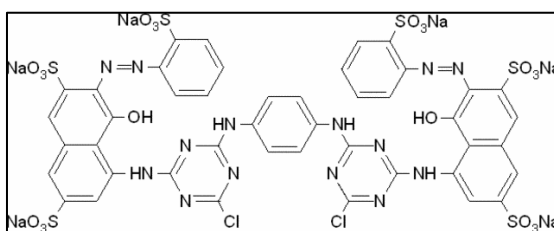


Figure 3- 4 Structure of Reactive Red (Batchelder, 1965)

<b>Molecular Formula</b>	: C <sub>44</sub> H <sub>24</sub> Cl <sub>2</sub> N <sub>14</sub> O <sub>20</sub> S <sub>6</sub> Na <sub>6</sub>
<b>Molecular Weight</b>	: 1469.98
<b>CI</b>	: Reactive Red 120
<b>Synonym</b>	: Red A gel (Amicon)
<b>Chemical Name</b>	: (3Z)-5-[[4-chloro-6-[4-[[4-chloro-6-[[7Z)-8-oxo-3,6-disulfo-7-[(2-sulphophenyl)hydrazinylidene]naphthalen-1-yl]amino]-1,3,5-triazin-2-yl]amino]anilino]-1,3,5-triazin-2-yl]amino]-4-oxo-3-[(2-sulphophenyl)hydrazinylidene]naphthalene-2,7-disulfonic acid
$\lambda_{\max}$	: 482 nm

### 3.2.3 Synthetic textile effluent

The synthetic textile effluents are prepared from two reactive dyes (Reactive Black 5, Reactive Red 10 and Reactive Blue 2) (Sigma-aldrich) through this research. Reactive dye concentrations of the feed solutions are varied from 200 to 800 ADMI (common range of colour in textile effluent) to know effect of reactive dye concentration on treatment performance of TiO<sub>2</sub>-coated FO membrane as shown in Table 3.2 and 3.3. Reactive Black 5, Reactive Red 10 and Reactive Blue 2 are obtained from SIGMA-ALDRICH company. 1M NaCl (reagent grade) is used for draw solution.

Additional trace ions commonly found in textile effluent are also added to the synthetic textile wastewater as follows: Phosphorus prepared from potassium phosphate K<sub>2</sub>HPO<sub>4</sub> for 2 mgP/L, Chloride prepared from Calcium chloride: CaCl<sub>2</sub> for 150 mgCl/L, sulphate prepared from Magnesium sulfate MgSO<sub>4</sub> for 300 mgSO<sub>4</sub>/L. Reactive dye solutions are prepared by dissolving requisite quantity of dye and abovementioned ions in denoised water from Millipore purification system. pH of the reaction is adjusted to 7.0 using H<sub>2</sub>SO<sub>4</sub> and NaOH solutions. pH of the solution is monitored using a Basic pH meter.

In operation the FO system, the feed water and draw solution are pumped in to the FO membrane unit. The permeate will be collected after the steady state condition.

(3 hrs. or steady state time). When possible, all samples will be analyzed immediately after being withdrawn from the reactor; however, some samples are preserved in accordance with standard methods 1998 (Standard, 1998). The filtrate is collected in a clean container and further be prepared for the analysis.

### **3.3 Forward osmosis membrane's surface coating**

#### **3.3.1 Surface coating procedure**

The PMMA-g-MEMO-PMMA-Br binding agent is prepared following the procedure described by Klaysri et al. (2016). Prior to the membrane coating experiment, the PMMA-g-MEMO-PMMA-Br gel is diluted using Tetrahydrofuran (THF) at 1:1 volume ratio. The diluted PMMA-g-MEMO-PMMA-Br glue is then uniformly sprayed over the designed coating surface of the TFC FO membrane. After dried for 30 min in a fume cupboard, the designed coating surface is dipped in a sulphate acid solution with pH 3 to hydrogenate the glue molecules for 30 min. The hydrogenated PMMA-g-MEMO-PMMA-Br glue contains three OH groups in the position of the Si atom, which make a strong binding with coordinative unsaturated Ti atoms at the surface of nanoparticles.

A suspension of  $\text{TiO}_2$  nanoparticles is prepared using commercial  $\text{TiO}_2$  nanopowder. The nanopowder is dissolved to ethanol at pH 10 adjusted using ammonia solution. After agitated for 1 h at 1000 rpm using a magnetic stirring plate, the  $\text{TiO}_2$  solution is further used using ultrasonic for 15 min in a water bath at  $25^\circ\text{C}$  to get a well dispersed  $\text{TiO}_2$  nanoparticle suspension. The hydrogenated FO membrane is substitute immersed in the  $\text{TiO}_2$  nanoparticle suspension for 30 min. After three cycles of ultrasonic and dip treatment, the membrane is rinsed by ethanol and stocked in distilled water at  $4^\circ\text{C}$  in dark for further examination. (Klaysri et al., 2016)

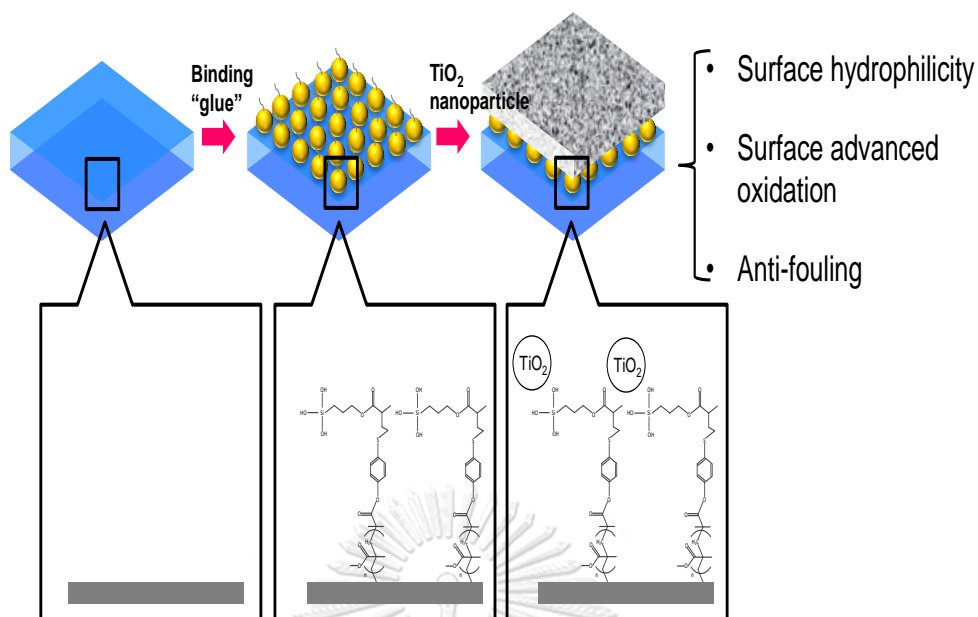


Figure 3- 5 Proposed Coating of Photocatalysts on membrane active surface.

### 3.3.2 Membrane surface characterization

The surface morphology and cross-sectional structure of the Aquaporin (AqP) membranes and cellulose triacetate (CTA) membranes (analyze every time per coating processes) is imaged with scanning electron microscopy (SEM) (S-3400N, Hitachi) to know lower magnification micrograph and higher magnification image of the both coated and original membranes.

Energy-dispersive X-ray spectroscopy (EDX) (Apollo X, Edax) is applied for elemental analysis of both coated and original membrane.

Zeta potential is a measure of the effective electric charge on the nanoparticle surface. The magnitude of the zeta potential provides information about particle stability, with particles with higher magnitude zeta potentials exhibiting increased stability due to a larger electrostatic repulsion between particles. In our research, we use Zeta potential instrument (ZetaPlus) for zeta potential determinations in coated and original membranes.

Atomic Force Microscopes (TT-2 AFM) for Nanoparticle Characterization and contact angle measurement for the surface characterization of FO membrane.

To know the hydrophilicity of coated and original membranes, we can use contact angle meter (CAM-PLUS IMAGE, C1221105, TanteInc), respectively.

### 3.4 FO filtration system set up operation

#### 3.4.1 Laboratory scale FO system set up

A schematic diagram of the laboratory scale FO unit is shown in Fig 3.5. A cross flow membrane unit that accepted flat membranes having an effective area of  $60\text{cm}^2$  (C10-T, Nitto Denko, Japan) is applied. This membrane module contains channels on both sides of the membrane for feed and draw solution, respectively. Spacers are installed at draw solution side to support membrane as well as serve to increase turbulence to decrease the effect of external concentration polarization during filtration. Co-current circulation of draw solution and feed solution is controlled via peristaltic pumps (Nitto Denko, Japan). Water flux is determined by measuring the rate at which the weight of feed solution decreases via an electronic balance.

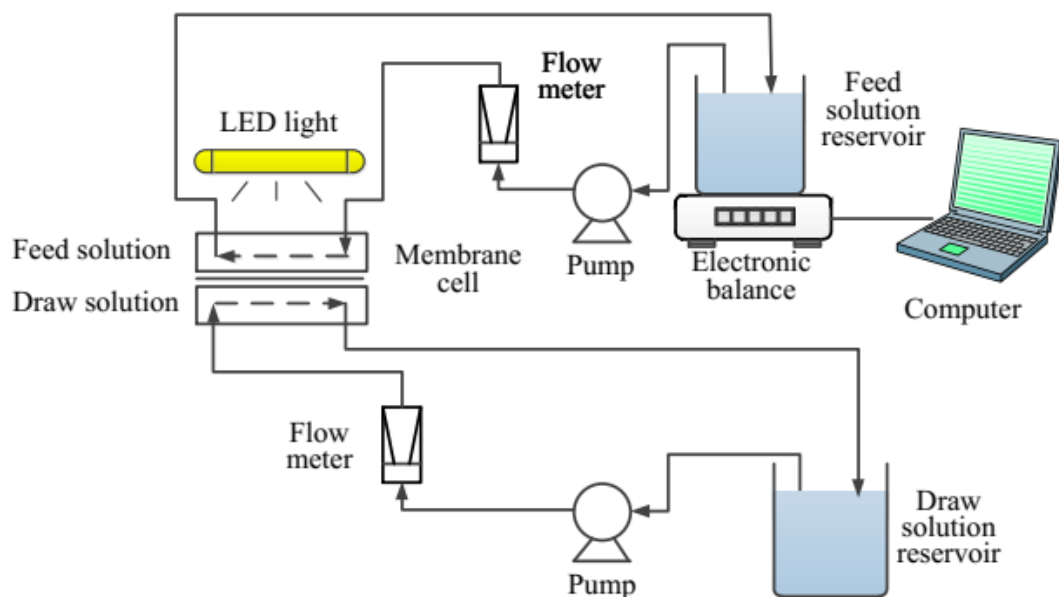


Figure 3- 6 Schematic diagram of the Laboratory-scale FO system (Xue et al., 2018)

The permeation performance of membranes is evaluated using across-flow FO filtration set up which is illustrated schematically in Figure 3.5. An FO membrane coupon with an effective membrane area of  $60\text{ cm}^2$  is set in a cross-flow membrane cell (C10-T, Nitto Denko, Japan). Diamond-patterned spacers are placed on both side of the membrane to allow cross flows of the feed water as well as the draw solution.



Two variable-speed peristaltic pumps are used to recirculate the respective feed and draw solutions and to control the respective cross-flow velocities. Membrane permeate flux (i.e., volumetric flux of water) is determined at regular time intervals by measuring the weight changes of the feed tank with a digital mass balance connected to a computer data logging system (Kazner et al., 2014).

### 3.4.2 Pure water filtration test

Water permeation of the membrane in FO unit is measured using salt water NaCl as draw solute for dye wastewater reclamation in forward osmosis (FO) process will be investigated. DI water is used as feed solution. The test is first conducted with DI water on both sides of the membranes. All membranes are tested in both orientations, i.e., with the active layer facing the feed solution (AL-FS) and the active layer facing the draw solution (AL-DS). The membrane performance parameters, including the water and solute permeabilities, A and B and also the resistance to solute diffusion within the membrane porous support layer will be determined respectively. In the experiment, the draw solution contained 1L of 1 M NaCl and initial volume of DI water is 0.5L. The apparatus will be operated in a closed loop. The cross-flow velocity is set at 8.3 cm/s in all the experiments. The temperatures of the feed and draw solutions are in the range of 20±2°C.

$$J_w = \frac{\Delta \text{Weight of the feed solution}}{\text{density of draw solution} \cdot \text{Effective area} \cdot \Delta \text{time}}$$

$$J_w = \frac{\Delta m_F}{\rho D A_m \Delta t}$$

Water flux is determined using an electronic balance by measuring the rate at which the weight of the feed solution decreased. The water flux through the membrane will be calculated by measuring the change in the weight of the feed solution ( $\Delta$ ) mf passed through the effective surface area ( $A_m$ ) of the membrane over a specific time period of the experiment ( $\Delta t$ ) which is about 30s for each draw solution concentration.

$$JD_s = \frac{\Delta m D_s}{A * \Delta T}$$

The reverse salt flux,  $J_s$  in  $\text{gm}^2/\text{h}$  is calculated by dividing the mass flow rate of NaCl (obtained via measuring the feed conductivity) by the membrane effective surface area.

The reverse salt diffusion  $J_s$  was determined from the feed conductivity changes over the predetermined time by using the following equation:

$$J_s = \frac{\Delta(C_f \times V_f)}{A \times \Delta t}$$

where,  $C_f$  is NaCl concentration in feed solution and  $V_f$  is the volume at the end of FO test,  $\Delta$

During the FO process, concentration differences across the membrane for the feed and draw solutes can result in solute cross-migration. As a consequence, draw solute which can diffuse to the feed side of the membrane channel may be lost in the concentrate stream, if not recovered. Also, salt ions that diffuse from the feed-side to the draw solution will reduce the quality of the produced permeate and could also negatively impact reclamation of the draw solute. Moreover, the permeate water stream dilutes the draw solute concentration, while the salt concentration increases axially in the membrane channel. The draw solution may be further diluted due to draw solute cross-migration from the draw to the feed channel. Depending on the intended use of the product water (which may contain the draw solute, unless it is removed by an additional separation process) draw solute/solution make-up may be needed in order to compensate for losses during both draw solution regeneration and draw solute loss due to cross-migration.

Other experimental conditions are: draw solution (1M NaCl for DS, and feed solution (7mmol/L NaCl+0.5 mmol/L CaCl<sub>2</sub>+1 mmol/L NaHCO<sub>3</sub>); cross-flow velocity 30 cm/s on both side of the FO membrane, and temperature 22–24°C.

### 3.4.3 Membrane fouling test

The osmotic driving force for water flux is decreasing due to the dilution of draw solution and concentration of feed solution. Therefore, the flux decline in the fouling experiments is caused not only by membrane fouling but also by the decrease

in osmotic driving force. In order to separate the effects of fouling and decreasing of osmotic driving force, we conduct the baseline experiments (with feed solution without any foulants) before the fouling experiments.

After the baseline measurement, solution with humic acid (1.5 mg/l) is employed as the feed. The fouling layer will form on the active layer of the membrane. The baseline experiments are followed the same protocol as that for the fouling experiments except that no foulant will be added to the feed solution (7mmol/L of NaCl , 0.5 mmol/L of CaCl<sub>2</sub> and 1 mmol/L NaHCO<sub>3</sub>) and, 1M NaCl solution (1Liter) used as draw solution, to quantify the flux decline due to the progressive decrease in the osmotic driving force. The flux curves obtained from the baseline tests are used to correct the flux curves obtained during fouling runs. The conductivity of the feed and DS is monitored via digital conductivity meter.

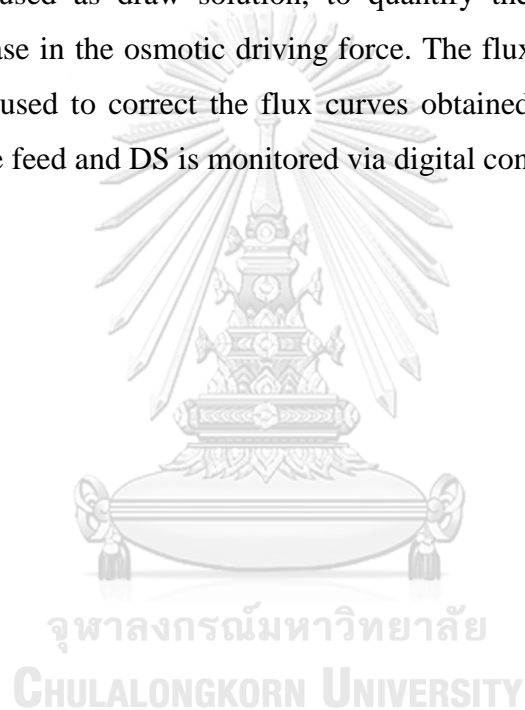


Table 3- 1 Effect of Foulant (Humic Acid) on Original and Coated FO membrane

Membrane		Draw Solution	Feed Solution	
			Baseline test	Fouling test
CTA	Coating	1 M NaCl	(7mmol/L NaCl + 0.5 mmol/L CaCl <sub>2</sub> + mmol/L NaHCO <sub>3</sub> )	(1.5 mg humic acids + 0.5 mmol/L CaCl <sub>2</sub> + 1 mmol/L NaHCO <sub>3</sub> )
	Without coating	1 M NaCl	(7mmol/L NaCl + 0.5 mmol/L CaCl <sub>2</sub> + mmol/L NaHCO <sub>3</sub> )	(1.5 mg humic acids + 0.5 mmol/L CaCl <sub>2</sub> + 1 mmol/L NaHCO <sub>3</sub> )
Aqp	Coating	1 M NaCl	(7mmol/L NaCl + 0.5 /L CaCl <sub>2</sub> + mmol/L NaHCO <sub>3</sub> )	(1.5 mg humic acids + 0.5 mmol/L CaCl <sub>2</sub> + 1 mmol/L NaHCO <sub>3</sub> )
	Without coating	1 M NaCl	(7mmol/L NaCl + 0.5 mmol/L CaCl <sub>2</sub> + mmol/L NaHCO <sub>3</sub> )	(1.5 mg humic acids + 0.5 mmol/L CaCl <sub>2</sub> + 1 mmol/L NaHCO <sub>3</sub> )

Table 3-2 exhibits the experiment procedure to investigate the effect of Humic acid on FO membranes (both original and modified) fouling, FO flux versus filtration time. Other experimental conditions are: draw solution (1M NaCl for DS, and ; feed solution (7mmol/L NaCl, 0.5 mmol/L CaCl<sub>2</sub> and1 mmol/L NaHCO<sub>3</sub>)for baseline test and feed solution (1.5 mg humic acids, 0.5 mmol/L CaCl<sub>2</sub> and 1 mmol/L NaHCO<sub>3</sub>) for fouling test; cross-flow velocity 30 cm/s on both side of the FO membrane, and temperature 22–24 degree Celsius.

### 3.4.4 Filtration test of synthetic textile effluent

(1) Investigation on removal efficiency of individual reactive dye in synthetic textile effluent

Laboratory feed solutions influent were used for all testing. The feed solutions used in this study are synthetic textile effluents with reactive dyes having concentrations of 200,400,600,800 ADMI as described in Table 3.2. Two FO membranes with and without coating are used in this research.



Table 3- 2 Investigation on removal efficiency of individual reactive dye (Reactive Black-5/Reactive Red-10/Reactive Blue-2) by original and modified FO Membranes

Membrane		Draw Solution	Reactive Black-5/Reactive Red-10/Reactive Blue-2 (ADMI)
CTA	Coating	1 M NaCl	200
			400
			600
			800
	Without coating	1 M NaCl	200
			400
			600
			800
Aqp	Coating	1 M NaCl	200
			400
			600
			800
	Without coating	1 M NaCl	200
			400
			600
			800

### 3.4.5 Filtration test of selected textile effluent

#### 3.4.5.1 Characterization of selected textile effluent

In this study, the effluent from textile factory “A”, located at Sahapat Industrial Estate, Cholburi province is selected for FO filtration test. The analysis of water quality of textile effluent is the prime consideration to assess its effect on the

entire ecosystem. Various important parameters and methods in general practice are given below.

- (1) Color
- (2) pH
- (3) Electrical conductivity (EC)
- (4) TOC
- (5) Nitrate
- (6) Sulfate
- (7) Phosphate

#### **-Investigation on color removal efficiency of real textile effluent**

Textile effluent will be collected from textile factory “A”, which is located at Sahapat Industrial Estate, Cholburi Province. Composite samples are taken from the tank after biological treatment process, where effluent streams from various wet processing sections of the plant are collected and combined. To obtain representative samples, sampling is done after the shutdown of textile plant and mixing of effluent in the effluent tank. Sampling is carried out in a 10 L plastic container. The analysis of the effluent is performed within 48 h after sampling.

Table 3- 3 Investigation on removal efficiency of real textile effluent by original and modified FO Membranes

Membrane		Draw Solution	Selected textile effluent as a feed solution
<b>CTA</b>	Coating	1 M NaCl (1liter)	1 liter of textile effluent
	Without coating	1 M NaCl (1liter)	1 liter of textile effluent
<b>Aqp</b>	Coating	1 M NaCl (1liter)	1 liter of textile effluent
	Without coating	1 M NaCl (1liter)	1 liter of textile effluent

The membrane filtration test is already mentioned in the previous section. The permeate quality will be measured for TOC, colour (ADMI), Electrical conductivity (EC), pH, all anions will be measured by Ion Chromatography (IC) machine.

#### **-Investigation on effect of formaldehyde as inference on removal efficiency of individual reactive dye**

The following experiment aims to investigate the effect of formaldehyde as inference of Dyes (Reactive Black-5, Reactive Blue-2, Reactive Red-10) removal efficiency with varying the concentration of formaldehyde from 1 to 10 mg/L as shown in Table 3.4. Two FO membranes with original and modified membrane were used. Experimental conditions: draw solution (1M NaCl for DS, and ; feed solutions (



1,2,5 and 10 ppm formaldehyde + 800 ADMI Reactive Black 5, ,Reactive Blue-2, Reactive Red-10 for the experiment; pH of the reaction solutions was adjusted using  $H_2SO_4$  and NaOH solutions. Initial pH of the solution was monitored using a Basic pH meter, and temperature 22–24°C.

In operation the FO system, the feed water and draw solution are pumped in to the FO membrane unit. The permeate will be collected after the steady state condition. (3 hrs. or steady state time). When possible, all samples are analyzed immediately after being withdrawn from the reactor; however, some samples were preserved in accordance with Standard Methods (1998). The filtrate is collected in a clean container and further prepared for the analysis.



Table 3- 4 Investigation on removal efficiency of individual reactive dye (Reactive Black-5/Reactive Red-10/Reactive Blue-2) with effects of formaldehyde by original and modified FO Membranes.

Membrane		Draw Solution	formaldehyde (mg/l)	Reactive Black-5/Reactive Red-10/Reactive Blue-2 (ADMI)
CTA	Coating		1 mg/l	800
		1 M NaCl	2 mg/l	800
			5 mg/l	800
			10 mg/l	800
	Without coating		1 mg/l	800
		1 M NaCl	2 mg/l	800
			5 mg/l	800
			10 mg/l	800
Aqp	Coating	1 M NaCl	1 mg/l	800
			2 mg/l	800
			5 mg/l	800
			10 mg/l	800
	Without coating	1 M NaCl	1 mg/l	800
			2 mg/l	800
			5 mg/l	800
			10 mg/l	800

(3) Investigation on effect of PVA as inference on removal efficiency of individual reactive dye

Prepare PVA solutions with varying concentrations according to the following table. Standard solutions prepared by mixing PVA and heated to 70° C to promote dissolution for 1 h, then cooled to room temperature and stirred for 1 h at room temperature to ensure homogeneity. The following experiment aims to investigate the effect of PVA as inference of Dyes (Reactive Black-5, Reactive Blue-2, Reactive Red-10) removal efficiency with varying the concentration of PVA from 1 to 10 mg/L as shown in Table 3.4. Two FO membranes with original and modified membrane are used. Experimental conditions: draw solution (1M NaCl for DS, and ; feed solutions (

1,2,5 and 10 ppm PVA + 800 ADMI Reactive Black 5, ,Reactive Blue-2, Reactive Red-10 for the experiment; pH of the reaction solutions is adjusted using H<sub>2</sub>SO<sub>4</sub> and NaOH solutions. Initial pH of the solution is monitored using a Basic pH meter, and temperature 22–24°C.

Table 3- 5 Investigation on removal efficiency of individual reactive dye (Reactive Black-5/Reactive Red-10/Reactive Blue-2) with effects of PVA by original and modified FO Membranes

Membrane		Draw Solution	PVA (mg/l)	Reactive Black-5/Reactive Red-10/Reactive Blue-2
CTA	Coating	1 M NaCl	1 mg/l	800
			2 mg/l	800
			5 mg/l	800
			10 mg/l	800
	Without coating	1 M NaCl	1 mg/l	800
			2 mg/l	800
			5 mg/l	800
			10 mg/l	800
Aqp	Coating	1 M NaCl	1 mg/l	800
			2 mg/l	800
			5 mg/l	800
			10 mg/l	800
	Without coating	1 M NaCl	1 mg/l	800
			2 mg/l	800
			5 mg/l	800
			10 mg/l	800

In operation the FO system, the feed water and draw solution are pumped in to the FO membrane unit. The permeate will be collected after the steady state condition. (3 hrs. or steady state time). When possible, all samples are analyzed immediately after being withdrawn from the reactor; however, some samples are preserved in accordance with Standard Methods (1998). The filtrate is collected in a clean container and further prepared for the analysis.

### **-Investigation on effects of formaldehyde and PVA as inferences on color removal efficiencies of real textile effluent**

The following experiment aims to investigate the effects of formaldehyde and PVA as inferences on color removal efficiencies of real textile effluent. The concentrations of formaldehyde and PVA will be selected for optimal concentrations from the previous experiments with synthetic reactive dyes as shown in Table 3.6 and 3.7. Two FO membranes with original and modified membrane were used. Experimental conditions: draw solution (1M NaCl for DS, and; feed solutions (real textile effluent with formaldehyde/ PVA at optimal concentrations for the experiment; pH of the reaction solutions was adjusted using H<sub>2</sub>SO<sub>4</sub> and NaOH solutions. Initial pH of the solution was monitored using a Basic pH meter, and temperature.



Table 3- 6 Investigation on color removal efficiencies of textile effluent with effect of formaldehyde as interferences by original and modified FO Membranes

Membrane		Draw Solution	Feed Solution	
CTA	Coating	1 M NaCl	Optimum concentration of formaldehyde obtained from the previous experiment that used formaldehyde as interference in the removal efficiency of individual reactive dye (Reactive Black-5/Reactive Red-10/Reactive Blue-20	Selected textile effluent
	Without coating	1 M NaCl		
Aqp	Coating	1 M NaCl		
	Without coating	1 M NaCl		

Table 3- 7 Investigation on color removal efficiencies of textile effluent with effect of PVA as interferences by original and modified FO Membranes.

Membrane		Draw Solution	Feed Solution		
CTA	Coating	1 M NaCl	Optimum concentration of formaldehyde obtained from the previous experiment that used PVA as interference in the removal efficiency of individual reactive dye (Reactive Black-5/Reactive Red-10/Reactive Blue-20	Selected textile effluent	
	Without coating	1 M NaCl			
Aqp	Coating	1 M NaCl			
	Without coating	1 M NaCl			

### 3.5 Analytical methods

#### 3.5.1 TOC

TOC is determined with a TOC analyzer. Total carbon (TC) is the sum of organically and inorganically bound carbon present in water. It can be divided into different fractions: inorganic carbon, total organic carbon (TOC), dissolved organic carbon (DOC), particulate organic carbon, volatile organic carbon, and nonpurgeable organic carbon. Usually organic carbon is not measured in textile processing. It is a general wastewater treatment parameter, and has no specific relation to textile wastewater. TOC is a measure of all carbon atoms that are covalently bound in organic molecules and cannot be measured with BOD or COD methods, as part of the carbon is not accounted for in those tests.

#### 3.5.2 Determination of Color

Color is determined with a Spectrophotometer Model 5 in accordance with the ADMI Tristimulus method 2120 D detailed in Standard Methods (1998). Textile dyes possess characteristic chromophoric groups which are responsible to impart colors to compounds. Each dye therefore shows independent absorbance maxima ( $\lambda_{\max}$ ) at particular wavelengths of light. This property makes it easier to monitor dye removal over time. Decrease in absorbance clearly means that the dye is being removed or transformed and can easily be measured using a simple colorimeter or UV-visible spectrophotometer. The ADMI color values are calculated with a computer program. The spectrophotometer is calibrated before each use with standard platinum cobalt color solutions (Fisher Scientific) of 100, 200, 300, 400, and 500 ADMI color units. Change in the absorbance and loss of the peak at  $\lambda_{\max}$  gives the first evidence of dye removal and decolorization. The decolorization percentage was thus calculated using Eq. (1).

$$\text{Decolorization \%} = \frac{\text{Initial absorbance} - \text{Final absorbance}}{\text{Initial absorbance}} \times 100$$

It is however difficult to measure decolorization of dye mixtures and/or real textile wastewater as they do not have any particular color and thus wavelength of maximum absorption. A tristimulus method approved by American Dye Manufacturers Institute (ADMI) called as ADMI value is therefore employed for measuring dye removal from mixtures and wastewater. This method uses three different wavelengths to calculate the color value independent of the hue of the samples and color removal is measured using Eq. (2).

$$ADMI \text{ removal } \% = \frac{\text{Initial ADMI} - \text{Final ADMI}}{\text{Initial ADMI}} \times 100$$

### 3.5.3 Electrical conductivity (EC)

EC is a numerical expression of the ability of an aqueous solution to carry an electric current. This ability depends on the presence of ions, their total concentration, mobility, valence, and relative concentration and on the temperature of measurement. Conductivity in water is affected by the presence of inorganic dissolved solids such as chloride, nitrate, sulfate, and phosphate anions or sodium, magnesium, calcium, iron, and aluminum cations. Digital conductivity meter is used for detection of conductivity of water sample. The conductivity cell is washed thoroughly by distilled water and cleaned by filter paper before each measurement for sample and for KCl standard solution. All measurements of conductance are made at room temperature. For sample measurement, 100 mL of thoroughly mixed homogeneous sample is taken out in 100 mL glass beaker. The conductivity cell is dipped in the beaker and EC is noted.

### 3.5.4 IC analysis

All anions (phosphate, chloride, sulfate) are measured by IC machine. The determinations were made on a Dionex 4000i Ion Chromatograph using an AS14 analytical column with both conductivity and UV/visible absorbance detection. The method is accredited by the United Kingdom Accreditation Service (UKAS) according to the requirements of BS EN ISO 17025. The samples are filtered to 0.45  $\mu\text{m}$  before analysis. After chromatographic separation, all of the anions were measured using the conductivity detector. For all anions, the accuracy of the method



is better than  $\pm 10\%$ , the bias is within  $\pm 3\%$  and the precision at the 95% confidence interval is better than 5% at concentrations an order of magnitude above the limit of quantification.

### 3.5.5 Formaldehyde Analysis

An aliquot of the sample containing of formaldehyde is combined with an equal volume of the acetylacetone reagent in a test tube. The tube is capped, shaken, and reacted at  $60^{\circ}\text{C}$  for 10 min. After cooling, the absorbance of the solution is read at 412 nm. Colored or turbid samples are extracted with n-butanol prior to reading the absorbance, and the reading then is taken on the n-butanol extract. Concentration is calculated from a curve of standard formaldehyde solutions. The chemical reaction is based on the Hantzsch reaction. Formaldehyde reacts with acetylacetone in the presence of ammonium ion to form the yellow compound, 3,5-diacetyl-1,4-dihydrolutidine. Then, detect with a spectrophotometer, suitable for use at 412 nm. (Nash, 1953)

### 3.5.5 PVA Analysis

Iodine Method is used for PVA analysis. Take PVA containing the sample and dilute it to a volume of 10 ml. Add 5 mL of 4% boric acid and 2 ml of I<sub>2</sub>-KI (1.27 g of I<sub>2</sub> and 25 g of KI in 1 liter). Solutions are equilibrated for 5 min exactly for each sample and then dilute to 25 ml of double distilled water. PVA concentration is analyzed at 690 nm (in triplicates) in spectrophotometer. (Magdum et al., 2013).

## Chapter 4

### Results and Discussion

#### 4.1 FO membrane surface modification and characterization

In our work, we investigated the effects of TiO<sub>2</sub> coating on membrane surface and its characteristics were measured by the following analyses and experiments. FT-IR analysis was conducted to evaluate the variation in functional groups during surface modification. SEM-EDX and AFM are used to confirm that the TiO<sub>2</sub> nanoparticles were successfully coated onto the active layers of CTA and AqP membranes and to visualize the variation of surface roughness before and after modification and Zeta potential is used to measure the effective electric charge on the nanoparticle surface. The water contact angles analysis, membrane filtration performance and antifouling performance of the virgin, used, and TiO<sub>2</sub> modified FO membranes were also already done in our research works.

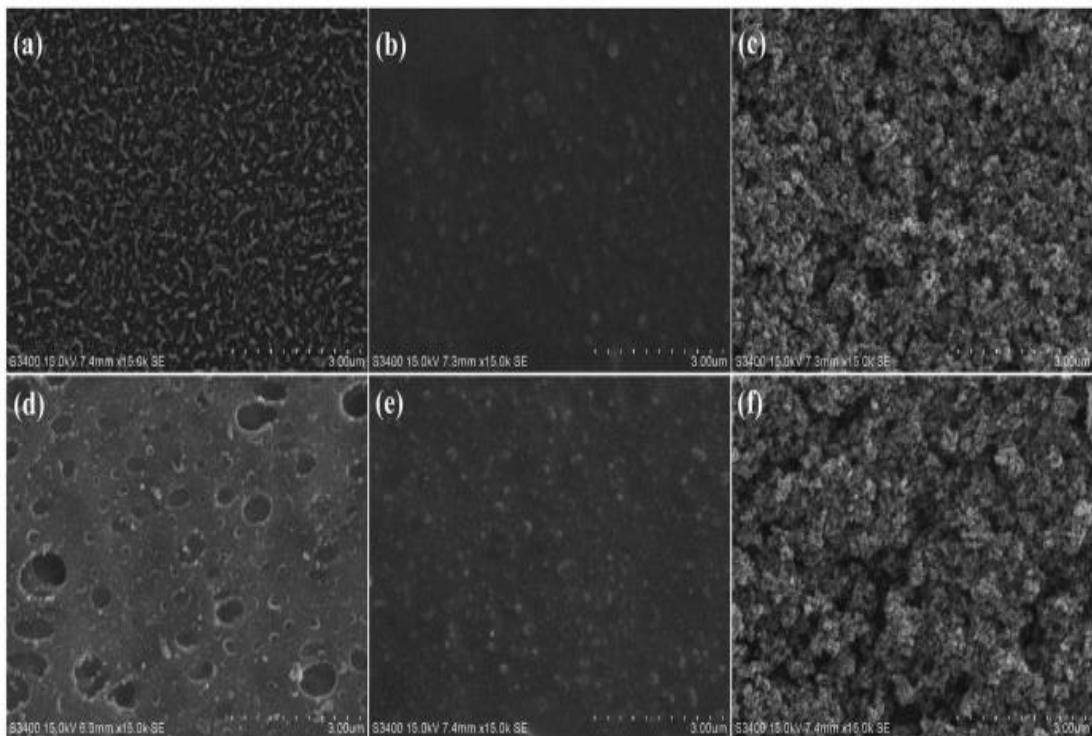


Figure 4- 1 SEM images of membrane active surfaces: (a) virgin CTA membrane, (b) used CTA membrane, (c) modified CTA membrane, (d) virgin AqP membrane, (e) used AqP membrane, and (f) modified AqP membrane.

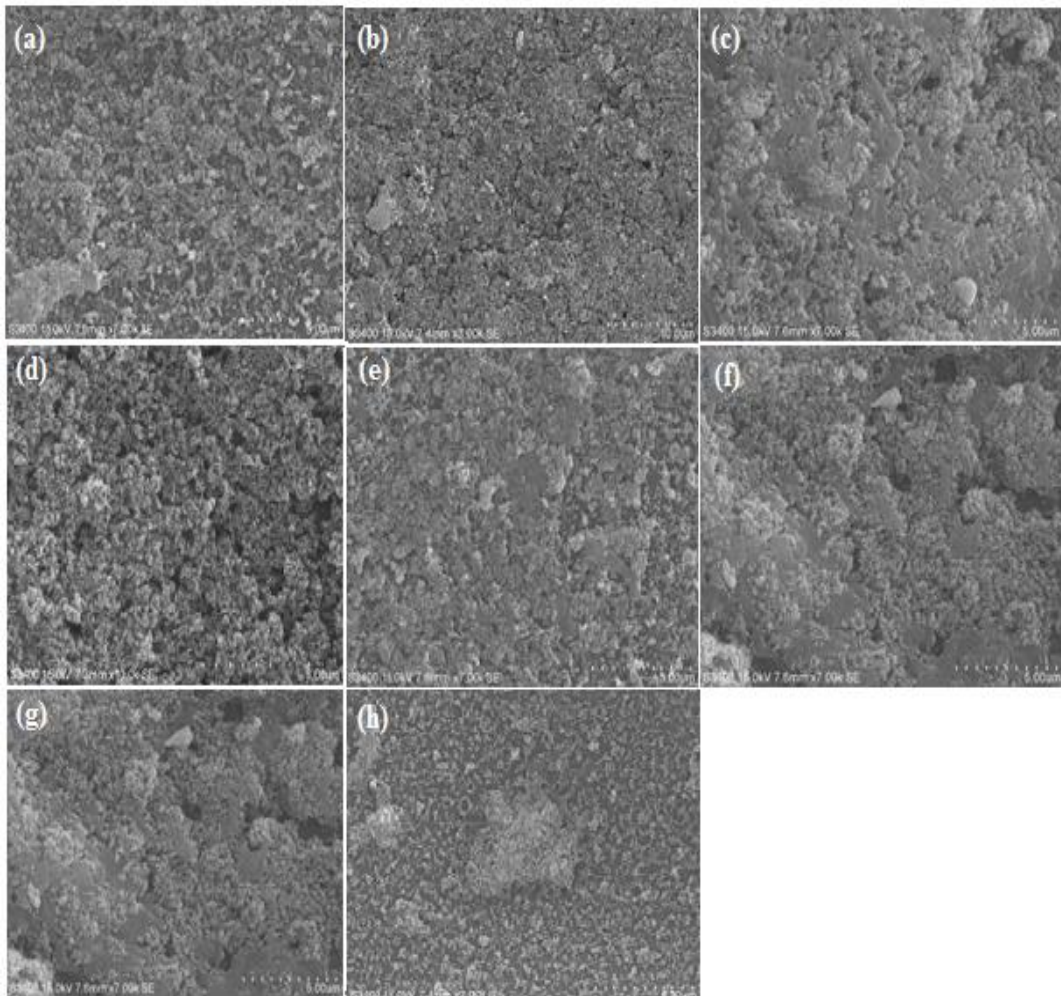


Figure 4- 2 SEM images of membrane active surfaces: (a) used modified AqP (blue) (b) used modified AqP (HCHO-red), (c) used modified AqP (PVA-black), (d) used modified CTA (blue), (e) used modified CTA (HCHO-black), and (f) used modified CTA (PVA-red), (g) used  $\text{TiO}_2$  modified CTA and (h) used  $\text{TiO}_2$  modified AqP.

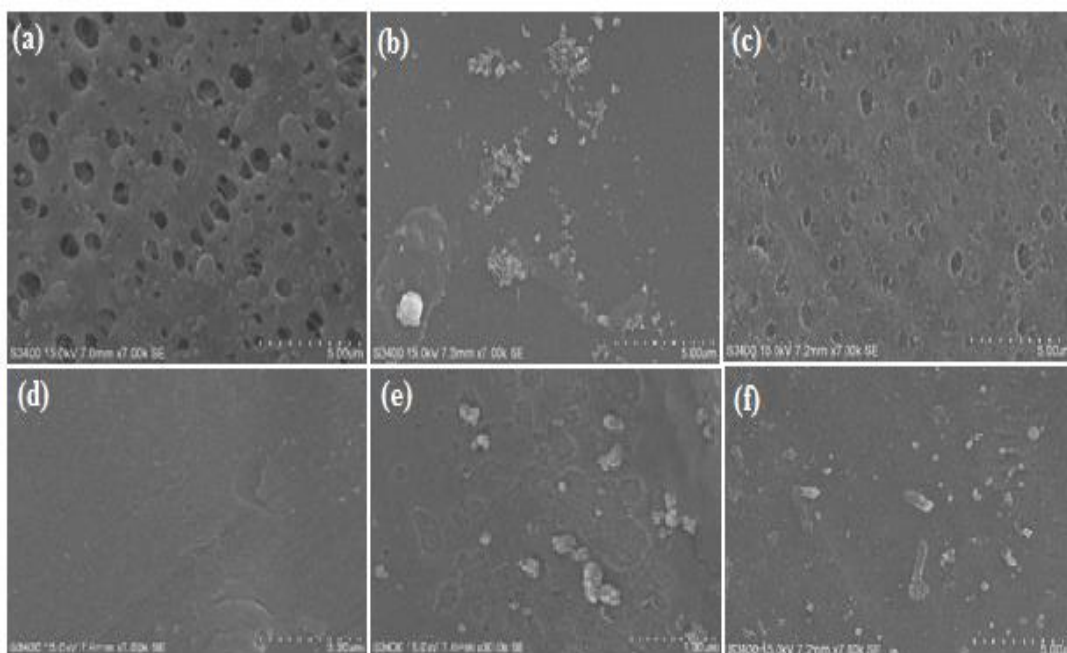


Figure 4- 3 SEM images of membrane active surfaces: (a) used AqP (black) (b) used AqP (HCHO-red), (c) used AqP (PVA-blue), (d) used CTA (red), (e) used CTA (HCHO-blue), and (f) used CTA (PVA-black).

The SEM images from (Figs. 4.1 to 4.3) illustrated the effective deposition of  $\text{TiO}_2$  nanoparticles on FO membranes after the modification procedure.  $\text{TiO}_2$  nanoparticles were uniformly scattered on both CTA and AqP membranes, turning the smooth active surfaces into ones covered by clusters and possessed porous structures. To quantitatively evaluate the coverage of titanium on both membranes, EDX spectra measurements were performed. Four major elements, carbon (C), oxygen (O), silicon (Si), and titanium (Ti), were identified from the EDX spectra. The increase of silicon coverage after spraying the MEMO-PMMA-Br reagent on the membrane surface showed good binding between the membrane surface and the monomer chains. The comparable coverage of silicon on the AqP and CTA membrane surfaces (Table 4.1) indicates the equivalent binding ability of the MEMO-PMMA-Br monomer on both polyamide and cellulose triacetate active layers. The surface atomic percentages of titanium increased to approximately 30% after modification by  $\text{TiO}_2$  nanoparticles for both membranes. Meanwhile, the surface silicon coverage decreased, which was

probably blocked by TiO<sub>2</sub> nanoparticles, suggesting the bonding between TiO<sub>2</sub> and MEMO-PMMA-Br monomer chains was through the silanols.

AFM was performed to visualize the variation of surface roughness before and after modification (Fig. 4.7). A significant increased surface roughness was observed in the modified membranes. This result generally supports the observations of the SEM images and indicates the successful surface coating of TiO<sub>2</sub> on both FO membranes. Additional surface roughness information provided by a two-dimensional stylus profilometer supported the results obtained from AFM, with the average roughness of the CTA membrane increased from 554.84 nm to 622.51 nm, and that for the AqP membrane increased from 303.23 nm to 440.64 nm.

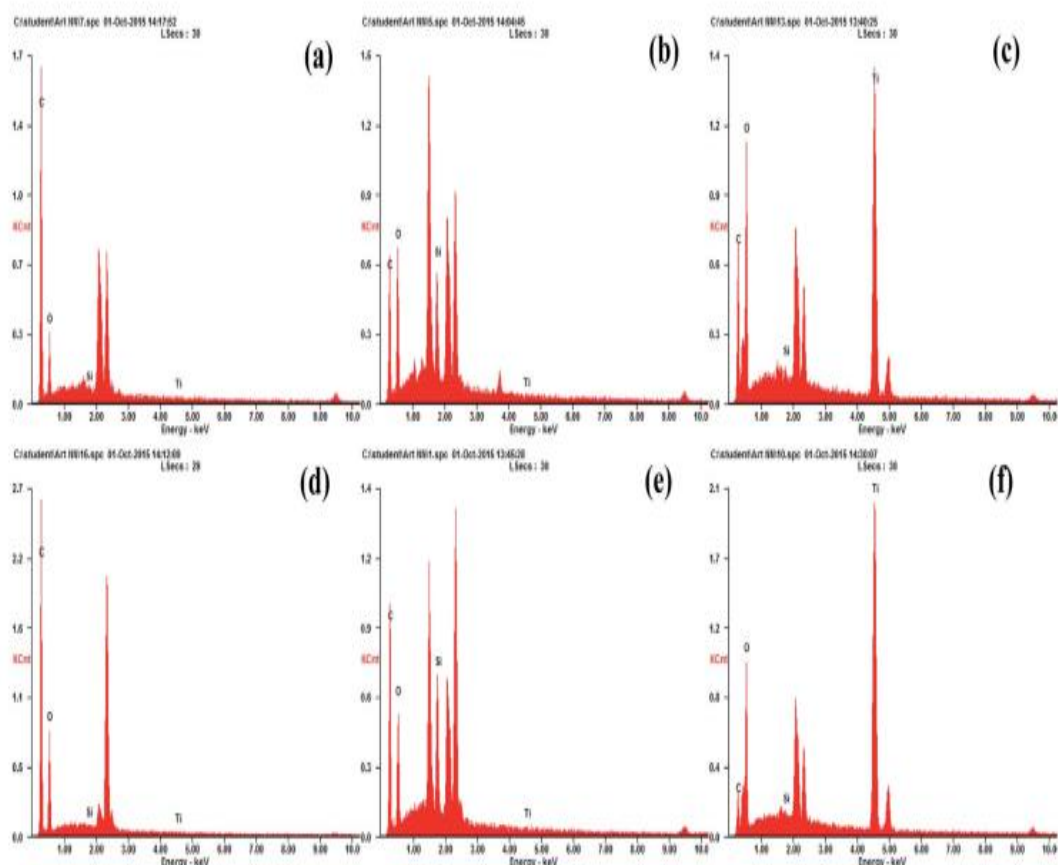


Figure 4- 4 EDX spectra of membrane active surfaces: (a) virgin CTA membrane, (b) used CTA membrane, (c) modified CTA membrane, (d) virgin AqP membrane, (e) used AqP membrane, and (f) modified AqP membrane.

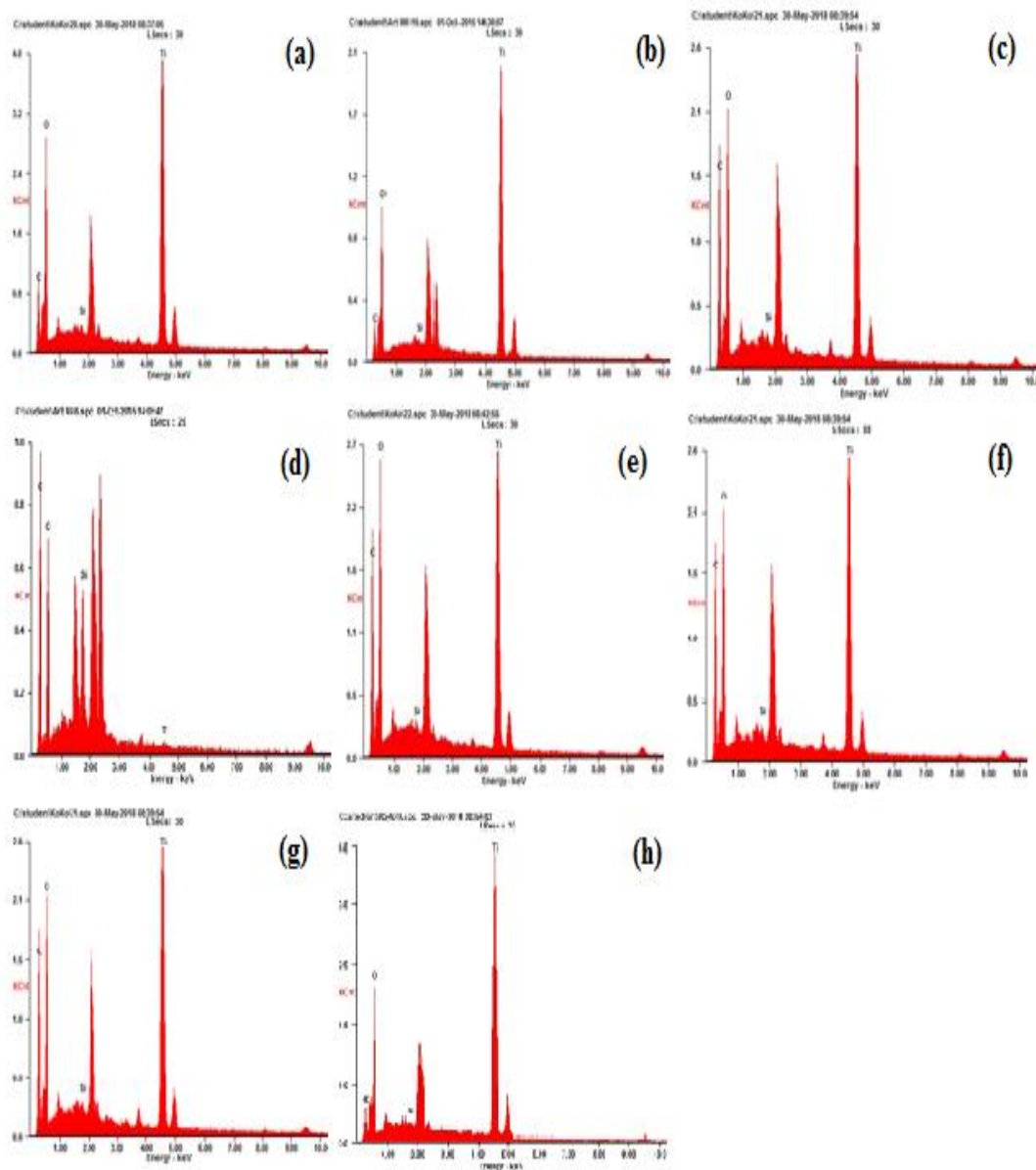


Figure 4- 5 EDX spectra of membrane active surfaces: (a) used modified AqP (blue) (b) used modified AqP (HCHO-red), (c) used modified AqP (PVA-black), (d) used modified CTA (blue), (e) used modified CTA (HCHO-black), and (f) used modified CTA (PVA-red), (g) used  $\text{TiO}_2$  modified CTA and (h) used  $\text{TiO}_2$  modified AqP.



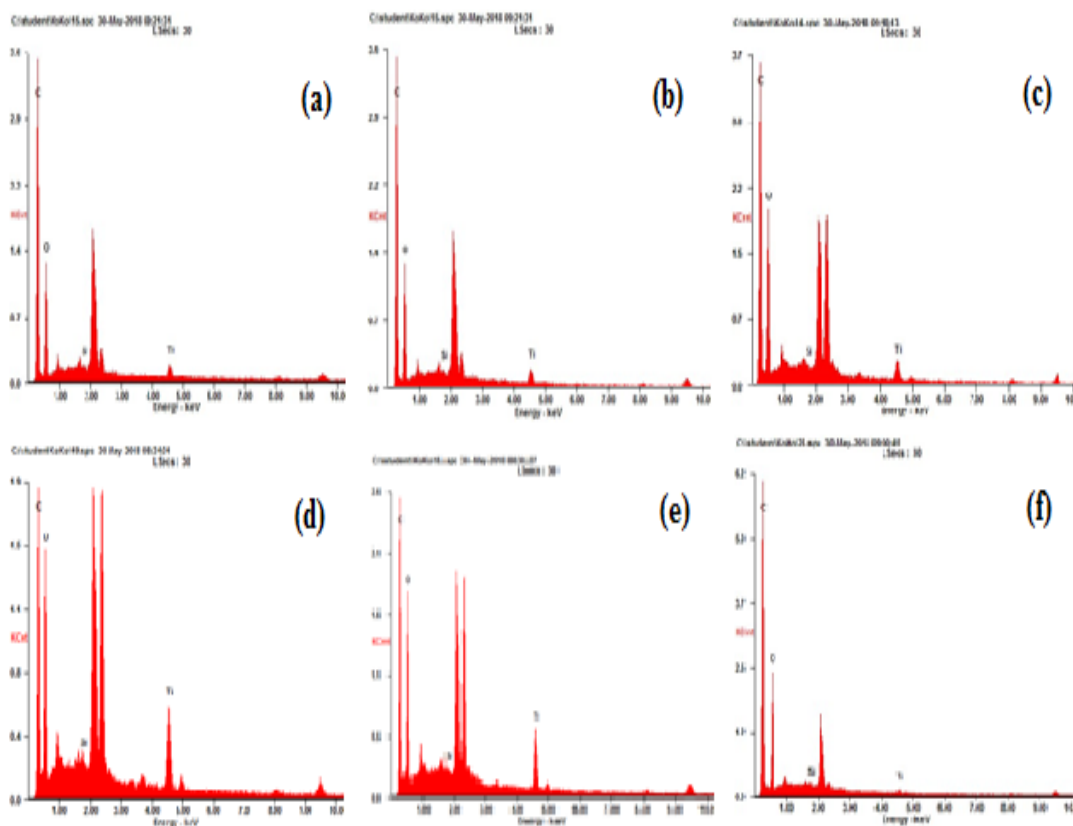


Figure 4- 6 EDX spectra of membrane active surfaces: (a) used AqP (black) (b) used AqP (HCHO-red), (c) used AqP (PVA-blue), (d) used CTA (red), (e) used CTA (HCHO-blue), and (f) used CTA (PVA-black).

The water contact angles of the virgin, used, and TiO<sub>2</sub> modified FO membranes were measured to understand the effects of TiO<sub>2</sub> surface modification on membrane hydrophilicity (Table 4.2). The water contact angles of the virgin CTA and AqP membranes were  $60.67 \pm 1.27^\circ$  and  $41.22 \pm 2.24^\circ$ , respectively. As anticipated, there was a smaller contact angle for the AqP membrane than the CTA membrane, due to the improved surface hydrophilicity via embedding aquaporin molecules into the polyamide active surface. Binding with the MEMO-PMMA-Br monomer chains slightly increased the contact angle of the AqP membrane and decreased that of the CTA membrane. However, the variations on surface hydrophilicity caused by spraying the MEMO-PMMA-Br reagent were insignificant.



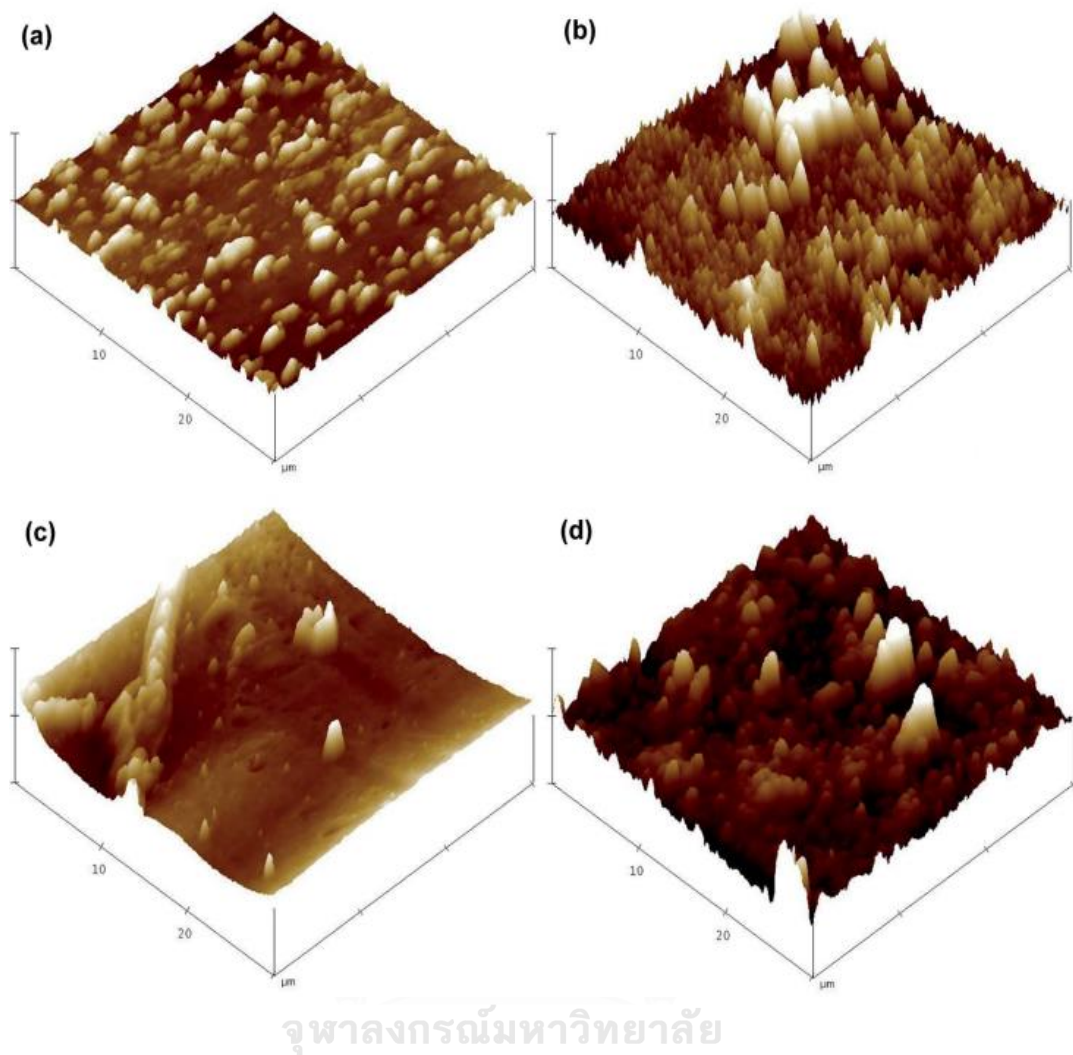
Table 4-1 Surface element coverages on the virgin, used, and modified forward osmosis membranes.

Types of membrane	Surface element coverage, at%			
	Carbon (C)	Oxygen (O)	Silicon (Si)	Titanium (Ti)
Virgin CTA	75.44 ± 1.29	24.05 ± 1.38	0.23 ± 0.06	0.28 ± 0.17
Used CTA	55.65 ± 3.11	36.72 ± 2.95	7.24 ± 1.56	0.39 ± 0.21
TiO <sub>2</sub> modified CTA	16.66 ± 7.60	54.52 ± 1.26	0.53 ± 0.24	28.29 ± 6.33
Virgin AqP	67.77 ± 1.29	31.95 ± 1.33	0.15 ± 0.05	0.13 ± 0.03
Used AqP	62.72 ± 2.69	28.61 ± 3.80	8.48 ± 1.17	0.17 ± 0.09
TiO <sub>2</sub> modified AqP	12.79 ± 4.00	54.80 ± 0.60	0.76 ± 0.19	31.64 ± 3.45
Used TiO <sub>2</sub> modified CTA	23.3 ± 1.02	50.51 ± 1.31	0.31 ± 0.01	25.85 ± 1.10
Used TiO <sub>2</sub> modified AqP	9.96 ± 0.45	50.11 ± 1.24	0.50 ± 0.03	39.43 ± 1.41
Used CTA (red)	45.64 ± 1.28	46.09 ± 1.11	0.54 ± 0.02	07.73 ± 1.01
Used CTA (PVA-black)	61.05 ± 1.32	38.05 ± 1.31	0.12 ± 0.01	0.78 ± 0.02
Used CTA (HCHO-blue)	47.32 ± 1.14	45.47 ± 2.11	0.45 ± 0.03	6.76 ± 1.01
Used modified CTA (HCHO-black)	25.37 ± 1.15	50.38 ± 2.01	0.35 ± 0.01	23.90 ± 1.03
Used AqP (black)	59.36 ± 2.12	38.01 ± 1.12	0.21 ± 0.01	2.44 ± 0.03
Used modified AqP (PVA-black)	23.31 ± 1.23	50.51 ± 1.22	0.34 ± 0.01	25.85 ± 1.23
Used modified CTA (blue)	16.93 ± 1.13	54.60 ± 2.12	0.55 ± 0.03	27.92 ± 1.23
Used AqP (PVA-blue)	58.30 ± 2.11	39.35 ± 1.31	0.21 ± 0.02	2.13 ± 0.11
Used modified AqP (blue)	14.30 ± 1.14	54.20 ± 2.02	0.32 ± 0.01	31.17 ± 1.12
Used modified CTA (PVA-red)	23.30 ± 1.23	50.51 ± 1.52	0.34 ± 0.02	25.85 ± 0.12
Used AqP (HCHO-red)	59.36 ± 2.14	38.00 ± 1.32	0.21 ± 0.01	2.44 ± 0.05
Used modified AqP (HCHO-red)	8.95 ± 0.09	55.48 ± 2.10	0.83 ± 0.02	34.74 ± 1.22

The surface hydrophilicity of the CTA membrane was significantly enhanced by modification with TiO<sub>2</sub> nanoparticles, with the average contact angle decreasing from 60.67° to 39.60°. This conforms to the conclusion reported by (Hu et al., 2012) that all freshly prepared porous TiO<sub>2</sub> thin films using the sol-gel method possessed the surface contact angles of approximately 40°. In contrast, the average contact angle of the AqP membrane increased from 41.22° to 60.59°, indicating an adverse effect on the hydrophilicity via surface modification with TiO<sub>2</sub> nanoparticles. One possible reason may be that the coverage of MEMO-PMMA-Br monomers and TiO<sub>2</sub> nanoparticles reduced the amount of the exposed aquaporin, which consequently weakened the surface hydrophilicity of the AqP membrane.

Table 4- 2 Water contact angles of the virgin, used membrane, and modified forward osmosis membranes

Types of membrane	Water contact angle (Degree)
Virgin CTA membrane	60.67 ± 1.27
Used CTA membrane	52.69 ± 1.69
TiO <sub>2</sub> modified CTA membrane	39.6
Virgin AqP membrane	41.22 ± 2.24
Used AqP membrane	44.35 ± 1.15
TiO <sub>2</sub> modified AqP membrane	60.59
Used CTA (black)	70.45±1.31
Used CTA (PVA-black)	68.12±1.23
Used CTA (HCHO-black)	69.25±0.98
Used modified CTA (black)	61.63±2.41
Used modified CTA (PVA-black)	41.24±1.09
Used modified CTA (HCHO-black)	43.45±2.14
Used AqP (black)	38.21±2.13
Used AqP (PVA-black)	46.67±0.78
Used AqP (HCHO-black)	39.24±1.45
Used modified AqP (black)	29.36±1.23
Used modified AqP (PVA-black)	39.13±0.56
Used modified AqP (HCHO-black)	50.12±1.35
Used CTA (blue)	68.38±2.14
Used CTA (PVA-blue)	75.25±2.45
Used CTA (HCHO-blue)	88.91±0.67
Used modified CTA (blue)	78.12±1.22
Used modified CTA (PVA-blue)	75.35±1.13
Used modified CTA (HCHO-blue)	85.23±1.03
Used AqP (blue)	41.14±2.11
Used AqP (PVA-blue)	38.25±1.08
Used AqP (HCHO-blue)	30.94±2.05
Used modified AqP (blue)	34.15±1.03
Used modified AqP (PVA-blue)	39.43±2.12
Used modified AqP (HCHO-blue)	39.13±0.56
Used CTA (red)	67.35±1.03
Used CTA (PVA-red)	65.21±1.15
Used CTA (HCHO-red)	66.23±1.08
Used modified CTA (red)	89.21±1.42
Used modified CTA (PVA-red)	86.45±1.34
Used modified CTA (HCHO-red)	87.23±1.23
Used AqP (red)	33.24±2.15
Used AqP (PVA-red)	31.29±2.33
Used AqP (HCHO-red)	23.34±1.32
Used modified AqP (red)	46.23±3.32
Used modified AqP (PVA-red)	34.73±1.03
Used modified AqP (HCHO-red)	30.94±2.05



จุฬาลงกรณ์มหาวิทยาลัย

Figure 4- 7 AFM images of membrane active surfaces: (a) virgin CTA membrane, (b) modified CTA membrane, (c) virgin AqP membrane, and (d) modified AqP membrane.

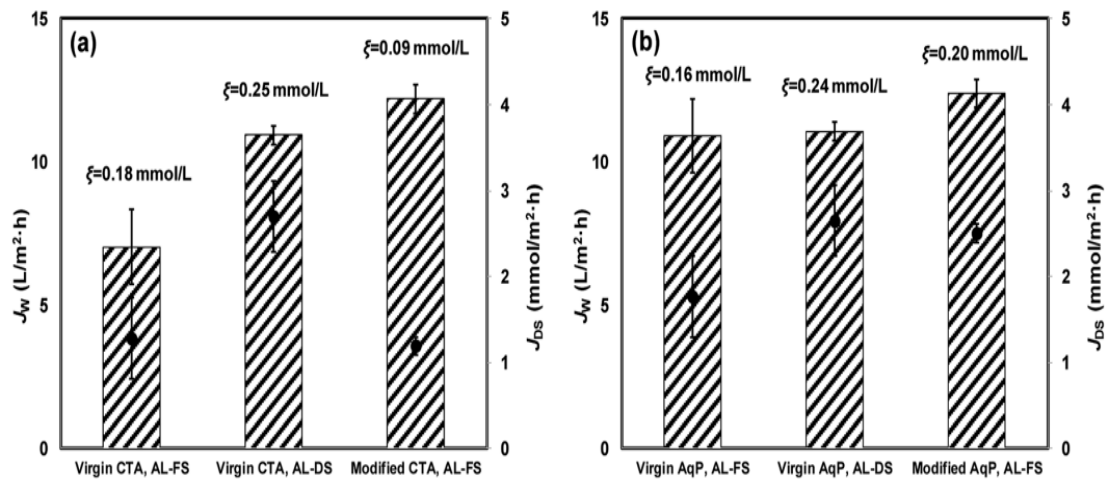


Figure 4- 8 Forward osmosis water flux, reverse solute flux, and specific reverse diffusion rate for (a) CTA membrane and (b) AqP membrane. The columns with error bars show the averages and standard deviations of water flux; the scatters with error bars show the averages and standard deviations of reverse salt flux;  $\xi$  is the specific reverse diffusion rate.

Table 4-1 Zeta potential of the virgin, used, and modified forward osmosis membranes

<b>Types of membrane</b>	<b>Zeta potential (mV)</b>
Virgin CTA membrane	-32.7
Used CTA membrane	-33.0
TiO <sub>2</sub> modified CTA membrane	-35.8
Virgin AqP membrane	-19.8
Used AqP membrane	-20.5
TiO <sub>2</sub> modified AqP membrane	-31.4
Used CTA (black)	-27.2
Used CTA (PVA-black)	-30.4
Used CTA (HCHO-black)	-23.9
Used modified CTA (black)	-29.1
Used modified CTA (PVA-black)	-32.3
Used modified CTA (HCHO-black)	-29.3
Used AqP (black)	-38.3
Used AqP (PVA-black)	-26.1
Used AqP (HCHO-black)	-25.6
Used modified AqP (black)	-33.9
Used modified AqP (PVA-black)	-31.4
Used modified AqP (HCHO-black)	-36.2
Used CTA (blue)	-24.1
Used CTA (PVA-blue)	-27.5
Used CTA (HCHO-blue)	-28.3
Used modified CTA (blue)	-31.6
Used modified CTA (PVA-blue)	-29.5
Used modified CTA (HCHO-blue)	-29.4
Used AqP (blue)	-21.1
Used AqP (PVA-blue)	-27.4
Used AqP (HCHO-blue)	-27.4

Table 4-2 Zeta potential of the virgin, used, and modified forward osmosis membranes (Cont....)

Types of membrane	Zeta potential (mV)
Used modified AqP (blue)	-32.3
Used modified AqP (PVA-blue)	-34.2
Used modified AqP (HCHO-blue)	-34.2
Used CTA (red)	-29.0
Used CTA (PVA-red)	-28.9
Used CTA (HCHO-red)	-28.2
Used modified CTA (red)	-34.2
Used modified CTA (PVA-red)	-30.4
Used modified CTA (HCHO-red)	-32.6
Used AqP (red)	-21.1
Used AqP (PVA-red)	-27.0
Used AqP (HCHO-red)	-29.2
Used modified AqP (red)	-30.9
Used modified AqP (PVA-red)	-31.6
Used modified AqP (HCHO-red)	-34.8

The zeta potential of the membranes was represented in Table 4.3. The results showed that the charge of the thin layers was changed to establish further negative charge. The neat membrane and the membrane composed of 0.005 wt.% TiO<sub>2</sub> showed the zeta potential amounts of about  $-26.1 \pm 1.87$  and  $-34.8 \pm 2.65$  mV, respectively. The increase of the negative charge was expected due to hydrogen bonds and coordination interactions. Hydrogen bonds and coordination interaction led to the space compressing of the C=O groups in the MEMO-PMMA-Br monomers molecules. Hence, the conversion of the remaining and reacted TiO<sub>2</sub> particles to carboxylic acid functional groups resulted in an increase of the negative charge. Consequently, enhancing the negative charge of the membrane surfaces caused an increase in color and ions rejection.

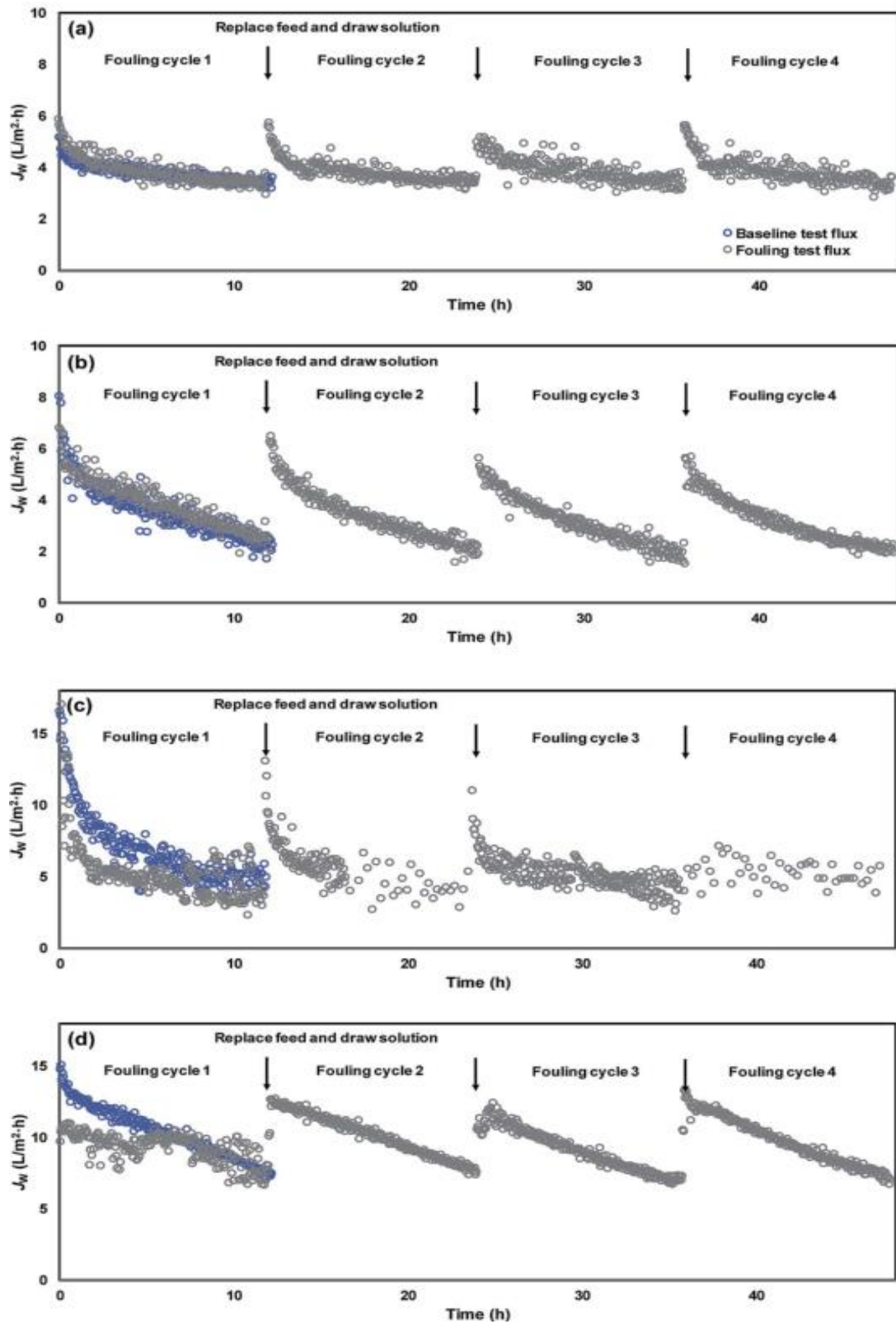


Figure 4- 9 Membrane flux variation during organic fouling tests for (a) virgin CTA membrane, (b) modified CTA membrane, (c) virgin AqP membrane, and (d) modified AqP membrane.

The process of membrane fouling was considered by the way of conducting a series of fouling cycles for each membrane sheet and comparing the variation of Flux patterns during the fouling cycles (Fig. 4.8). A NaCl was using to substitute the model foulants in the feed solution in order to maintain an equivalent initial conductivity, to perform the baseline measurement prior to the fouling cycles. Therefore, comparable water flux was expected between the baseline and the first fouling cycle at the beginning of the filtration test. The flux decline that occurred in the baseline can be attributed to the effect of membrane fouling. It can be seen in Fig. 4.8 (a) and (b) that CTA membrane fouling was not observed in the first fouling cycles for either virgin or modified membranes. To zoom the difference on flux variation caused by membrane fouling, four cycles of fouling tests were continually conducted, with each test lasting for approximately 12 h. The variation of the average water flux for the initial 30 min of the baseline measurement and different fouling cycles is presented in Fig. 4.9.

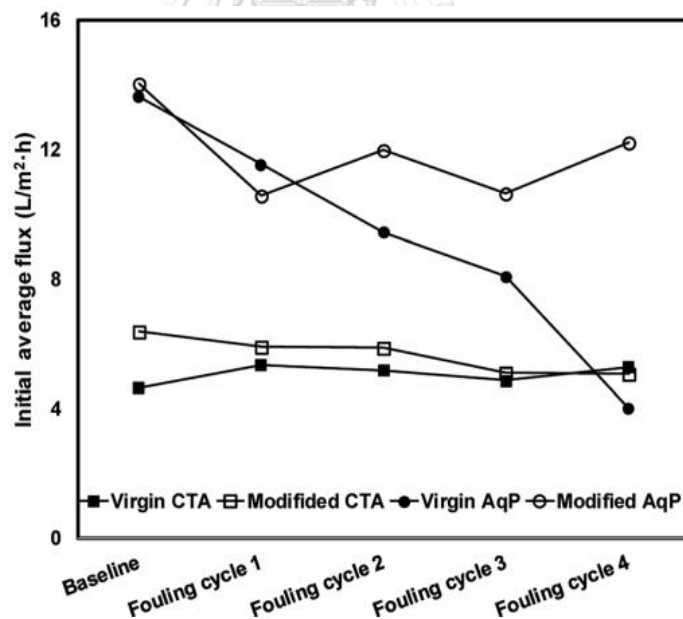


Figure 4- 10 The average water flux in the initial 30 min of the baseline and fouling cycle experiments.



Although the initial flux of the modified membrane was always higher than that of the virgin membrane, there was no apparent decline of the initial water flux in each series observed. The strong antifouling property of the CTA membrane was indicated, which has been verified by several previous studies (Xue et al., 2015), (Rodrigo Valladares Linares et al., 2012), (Li et al., 2012). Nevertheless, since there was no significant membrane fouling observed even for the virgin CTA membrane, it is difficult to conclude whether the surface modification resulted in obvious enhancement of the antifouling performance of the membrane from the current data. Further studies with more fouling cycles may be needed to clarify this issue in the future. In terms of the AqP membrane, slightly higher water flux was observed in the baseline for the modified AqP membrane than that for the virgin membrane. Flux decline caused by membrane fouling was apparently observed in the first fouling cycle for the virgin AqP membrane (Fig. 4.8 (c) and (d)). In addition, the membrane fouling developed dramatically in the following fouling cycles, with the initial water flux dropping from  $13.6 \text{ L m}^{-2} \text{ h}^{-1}$  to  $4.0 \text{ L m}^{-2} \text{ h}^{-1}$  (Fig. 4.9). This rapid fouling development in may be caused by the clogging of the functional water channels in aquaporins. Due to limited available information on the antifouling performance of commercial AqP membranes, this finding may be of great significance for the further improvement of the membrane material design. In contrast, a constant initial water flux at approximately  $12.0 \text{ L m}^{-2} \text{ h}^{-1}$  was well maintained during the four fouling cycles for the modified AqP membrane, indicating the improved antifouling performance by surface modification in this study. It is worth mentioning that the low flux appeared at the beginning of the first fouling cycle may be caused by improper data collection which was rectified later in the experiment. Apart from the photodegradation of organic foulants which was catalyzed by  $\text{TiO}_2$  modified membrane interface, another possible mechanism is that the surface coverage by MEMO-PMMA-Br monomer chains and  $\text{TiO}_2$  nanoparticles partially prevented the approach of organic foulants, obstructing them from blocking the functional water channels.

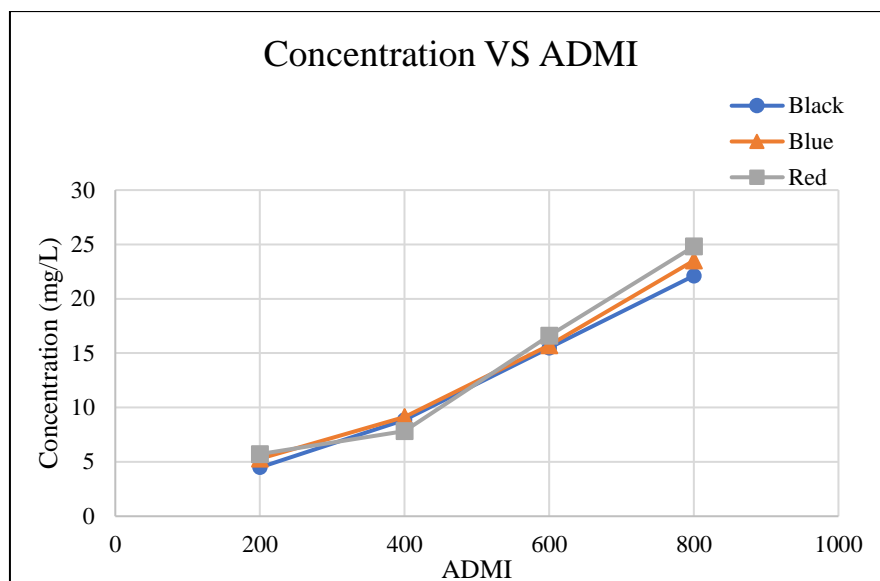


Figure 4- 11 Correlation between ADM I and concentration of reactive dyes

#### 4.2 Effects of Original and TiO<sub>2</sub> coated FO membranes on colour, TOC removal of synthetic textile wastewater

Figure 4-10 illustrates the results of color removal with both original and modified CTA and aquaporin FO membranes. Forward osmosis membranes were operated for treatment of the synthetic textile wastewater with varying the ADM I values 200, 400, 600 and 800 for reactive black, blue and red, respectively. In the present of UV illumination, no detectable dyestuff permeated through the FO membrane, the rejection of dyes and other coloured agents in dye mixture were >99.98% in all experiments as determined by spectrophotometry. According to Figure 4-10, as all the ADM I values for original and modified membrane of both AqP and CTA membrane were less than 10, the color removal efficiencies were 99.61% for reactive black, 99.99% for reactive blue and 99.99% for reactive red removal. It has been reported that in FO mode, a dissolved solid with lower aqueous diffusivity, larger ion/molecule size and higher viscosity will cause more severe dilutive concentration polarization (CP), leading to lower water flux (Zhao and Zou, 2011). This phenomena also attributed to the severe concentrative CP and low water flux in the FO mode in our experiment. Moreover, the dye molecules were hard to adhere to the active layer of membrane which was smoother than the porous layer (Jin et al., 2012).

Table 4- 3 Removal efficiencies for color (ADMI value) after treated with both virgin and modified CTA and aquaporin membranes for reactive black, reactive blue and reactive red with interferences (HCHO and PVA).

Reactive dyes	Removal Efficiencies (%)
Black	99.61
Blue	99.99
Red	99.99
Black (HCHO)	99.99
Blue (HCHO)	99.99
Red (HCHO)	99.99
Black (PVA)	99.99
Blue (PVA)	99.99
Red (PVA)	99.99

Moreover, another analysis of dye removal efficiency, organic matters in terms of TOC values were also analyzed to know TOC removal efficiencies. Indeed, TOC reduction performance is in the same direction as color removal for water and wastewater treatment. Figures from 4-11 to 4-13 show the performances of FO membranes for TOC removal efficiencies.

#### 4.3 Effect of TiO<sub>2</sub> coating on membrane filtration performance

The synthetic textile wastewater flux for original and modified FO membranes was measured using 1 mol L<sup>-1</sup> NaCl as the draw solution and varying the concentration of reactive dye (black, blue and red) in synthetic textile wastewater, the results are illustrated in Fig. 6. The CTA membrane exhibited a water flux of  $7.34 \pm 1.42$  L m<sup>2</sup> h<sup>-1</sup> with original membrane and  $11.15 \pm 1.82$  L m<sup>2</sup> h<sup>-1</sup> with modified one using synthetic waste water with reactive black, obviously lower than that of the AqP membrane of  $10.53 \pm 1.25$  L m<sup>2</sup> h<sup>-1</sup> with original and  $12.57 \pm 1.31$  L m<sup>2</sup> h<sup>-1</sup> with modified one. For synthetic wastewater with reactive black, the CTA membrane exhibited a water flux of  $7.84 \pm 0.92$  L m<sup>2</sup> h<sup>-1</sup> with original membrane and  $11.23 \pm 0.32$  L m<sup>2</sup> h<sup>-1</sup> with modified one, obviously lower than that of the AqP membrane of  $10.11 \pm 1.45$  L m<sup>2</sup> h<sup>-1</sup> with original and  $11.67 \pm 2.71$  L m<sup>2</sup> h<sup>-1</sup> with modified one. Consequently, the CTA membrane exhibited a water flux of  $7.44 \pm 1.92$  L m<sup>2</sup> h<sup>-1</sup>

with original membrane using reactive red and  $11.13 \pm 1.82 \text{ L m}^2 \text{ h}^{-1}$  with modified one, obviously lower than that of the AqP membrane of  $7.21 \pm 1.85 \text{ L m}^2 \text{ h}^{-1}$  with original and  $11.57 \pm 1.81 \text{ L m}^2 \text{ h}^{-1}$  with modified one. The water flux of modified FO membranes were measured with the AL-FS orientation. 68.2% and 12.16% of flux increments were obtained for CTA and AqP membranes after the surface modification, respectively. It is worth noting that the water flux of the CTA membrane was significantly improved by TiO<sub>2</sub> nanoparticle modification, which is consistent with the improved surface hydrophilicity.

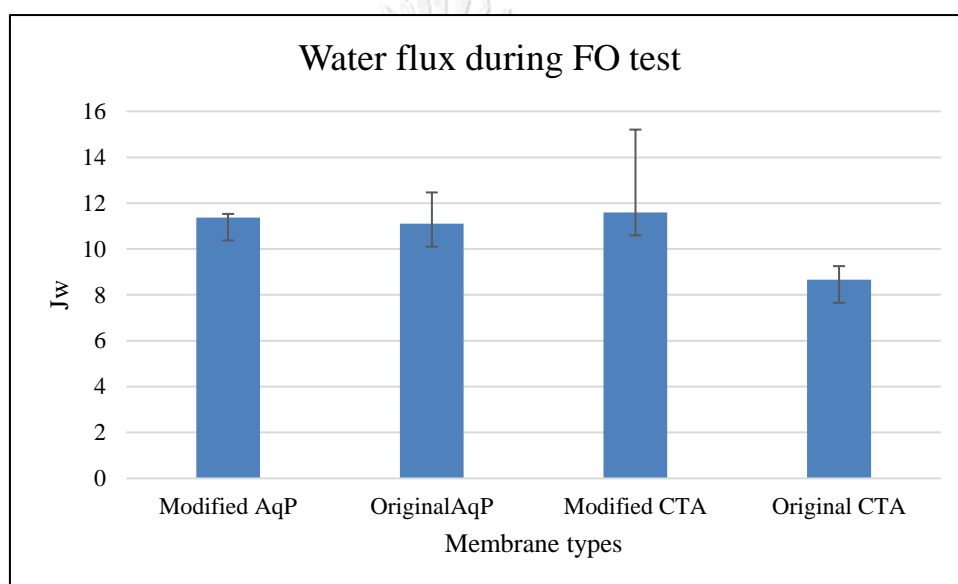


Figure 4- 12 Membrane flux variation during synthetic textile wastewater with different ADMI values (reactive black) tests for modified AqP membrane, original AqP membrane, modified CTA membrane and original CTA membrane.

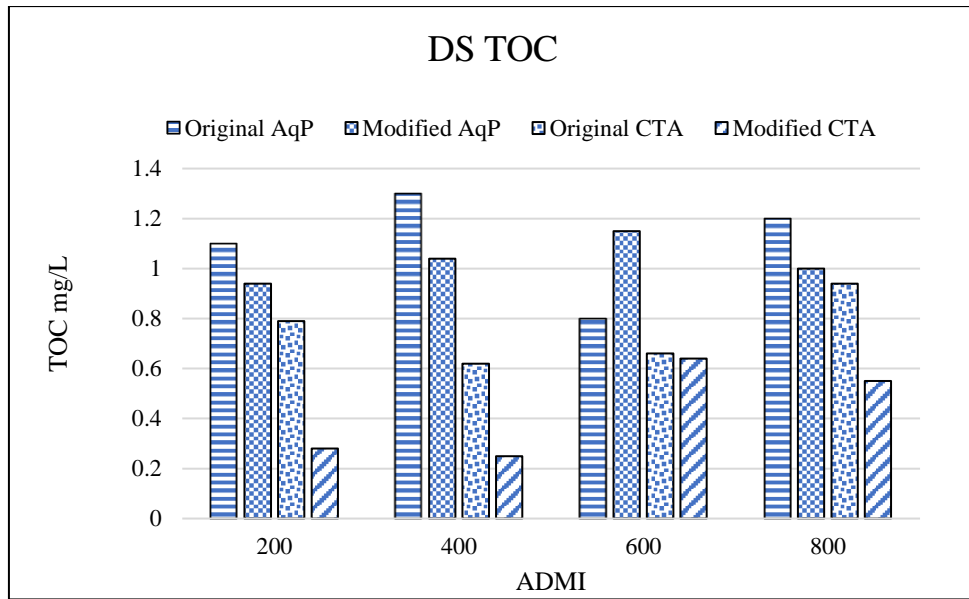


Figure 4- 13 Comparison of effluent TOC values, while varying the initial ADMI values of synthetic textile effluent (reactive black) with original AqP modified AqP , original CTA and modified CTA membrane.

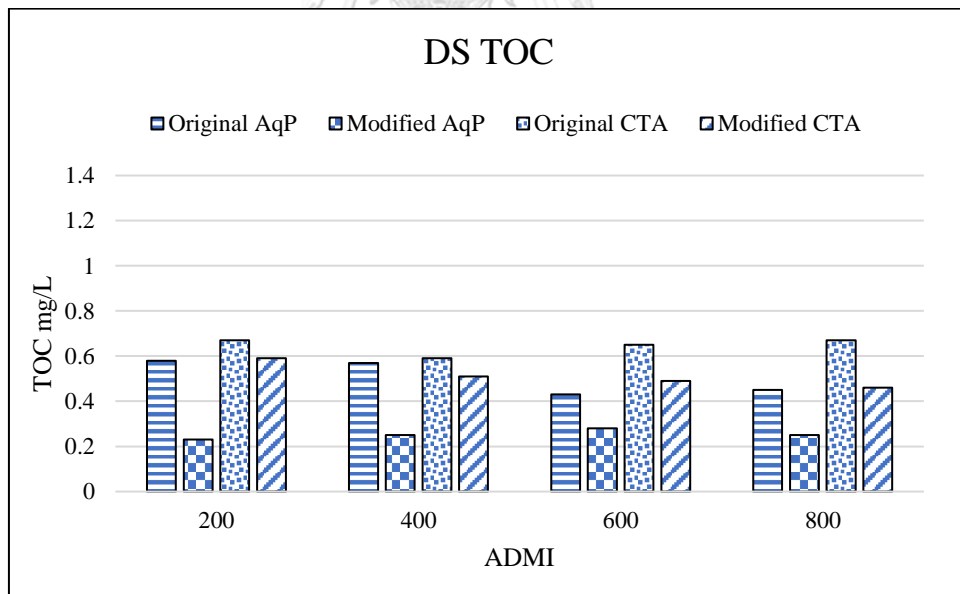


Figure 4- 14 Comparison of draw solution TOC values, while varying the initial ADMI values of synthetic textile effluent (reactive blue) with original AqP, modified AqP original CTA and modified CTA membrane.

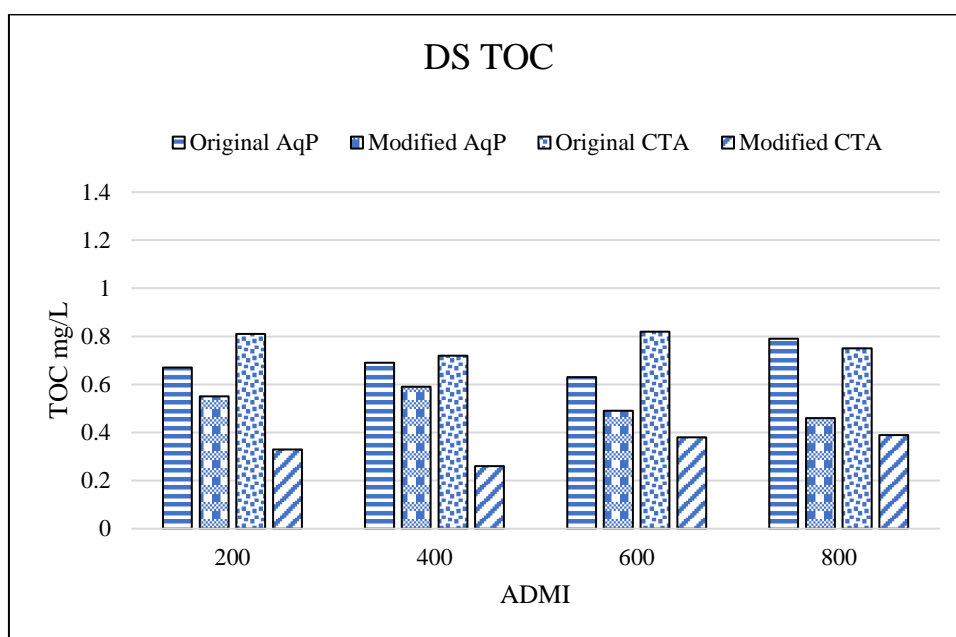


Figure 4- 15 Comparison of draw solution TOC values, while varying the initial ADMI values of synthetic textile effluent (reactive red) with original CTA , modified CTA membrane , original AqP and modified AqP membrane

During this study, raw water TOC value was averagely 4.9 mg/L. From Figures 4-11 to 4-13, the comparison of effluent TOC value from varying ADMI values of synthetic wastewater of three reactive dyes with forward osmosis performance of original and modified CTA and AqP membranes were done . In all cases, our system shows reliable performance of TOC removal efficiencies. Effluent TOC concentration of both original and modified CTA membranes were  $0.72 \pm 0.16$  mg/l and  $0.43 \pm 0.18$  mg/l with reactive black,  $0.68 \pm 0.97$  mg/l and  $0.51 \pm 0.87$  mg/l with reactive blue and  $0.7 \pm 0.88$  mg/l and  $0.5 \pm 0.92$  mg/l with reactive red, respectively. Effluent TOC concentration for original and modified AqP membranes were  $\pm 1.8$  mg/l  $\pm 0.81$  and  $1.4 \pm 0.65$  mg/l for reactive black,  $0.5$  mg/l  $\pm 0.86$  and

$0.25 \pm 0.88$  mg/l for reactive blue and  $0.77 \pm 9.4$  mg/l and  $0.34 \pm 0.87$  mg/l with reactive red, respectively.

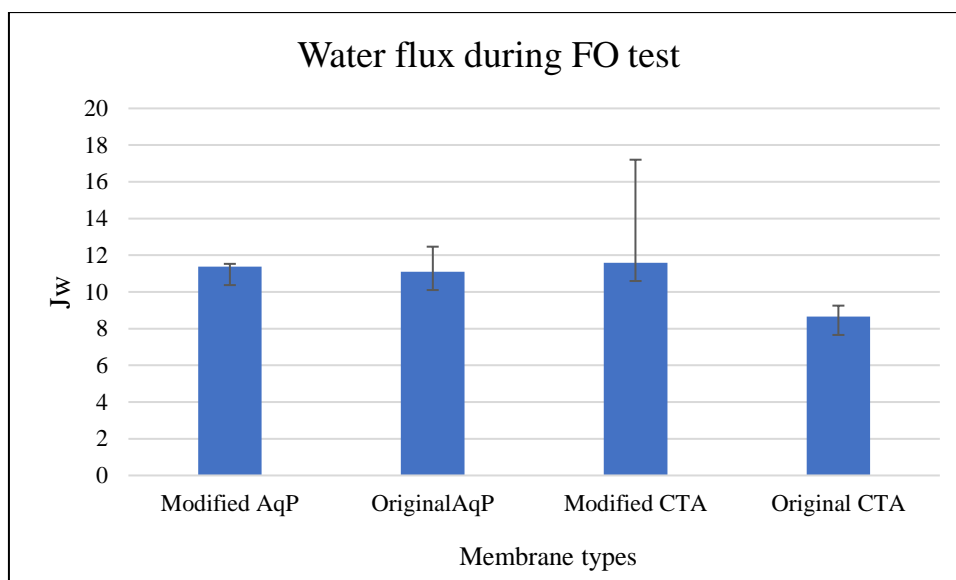


Figure 4- 16 Membrane flux variation during synthetic textile wastewater filtration (reactive black) of modified AqP membrane, original AqP membrane, modified CTA membrane and original CTA membrane.

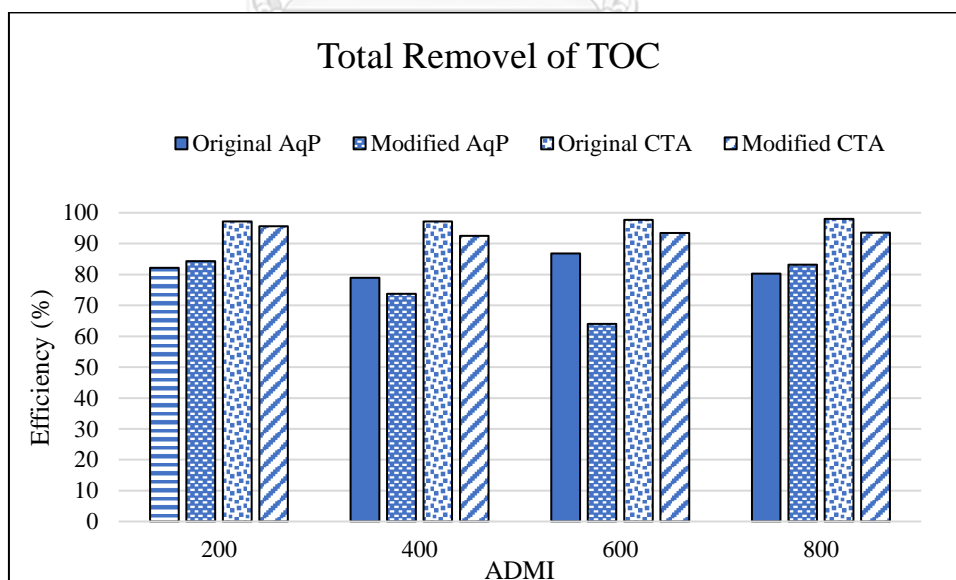


Figure 4- 17 Total removal efficiency of TOC during synthetic textile wastewater filtration with reactive black for modified AqP membrane, original AqP membrane, modified CTA membrane and original CTA membrane.

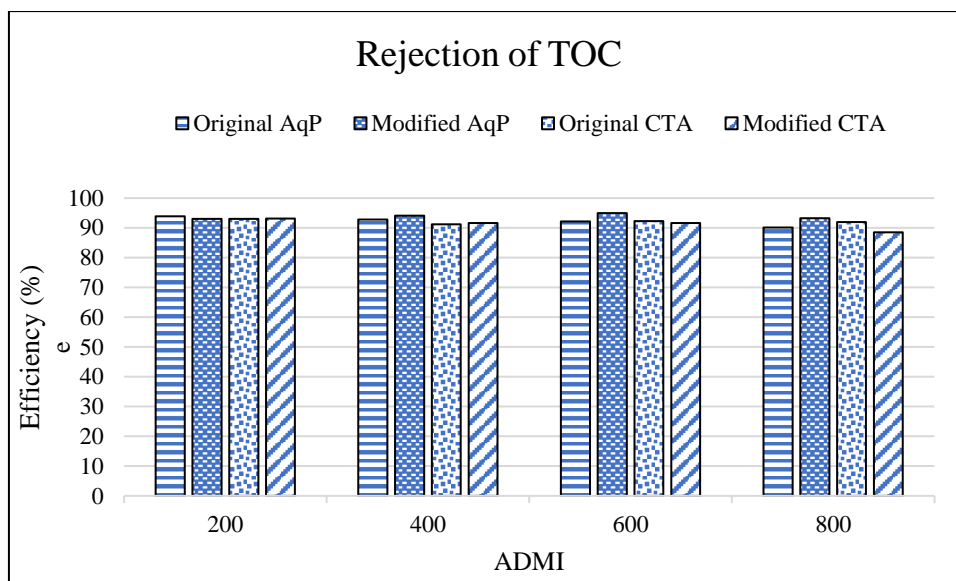


Figure 4- 18 Rejection efficiency for TOC during synthetic textile wastewater filtration reactive black of modified AqP membrane, original AqP membrane, modified CTA membrane and original CTA membrane.

#### 4.4 Effects of Original and TiO<sub>2</sub> coated FO membranes on anion pollutants removal of synthetic textile wastewater with reactive dyes

The ions removal studies were illustrated graphically in (Fig.4.16-25 ) which showed that both sulphate, nitrate and phosphate removals of synthetic textile effluents and also with and without interferences (PVA and HCOH) using original and modified CTA and AqP membranes with reactive black, blue and red. Both original and modified membranes show differences in water permeability, but minor differences in rejection.

Maximum removal percentages of sulphate were found to be 99.16 % and 99.17 % with reactive black, 99.28 % and 99.92% with reactive red and 99.83 % and 99.92% with reactive blue using original and modified CTA membrane. Consequently, the sulphate removal percentages of 99.35 % and 99.31 % with reactive black, 99.15 % and 99.38 % with reactive blue and 99.33 % and 99.39 % with reactive red using original and modified AqP membrane with HCOH as interference. With PVA interference, the maximum removal percent of sulphate was found to be around 99.68% and 99.82 % with reactive black, 99.51% and 99.37 % with reactive blue and 99.69% and 99.84 % with



reactive red using original and modified CTA membrane, similarly, 99.6 % and 99.71 % with reactive black, 99.56% and 99.84 % with reactive blue and 99.69% and 99.84 % with reactive red using original and modified AqP membrane.

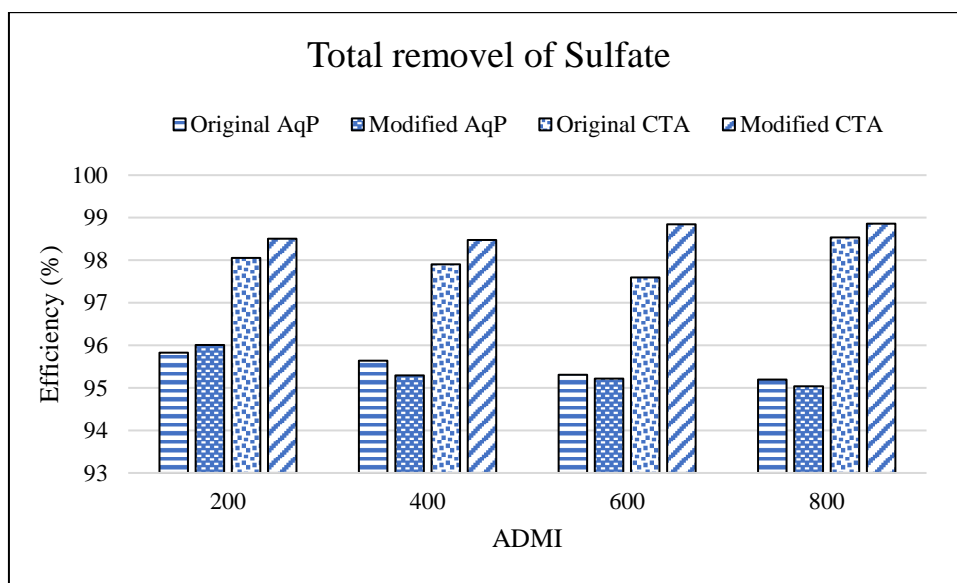


Figure 4- 19 Total removal of sulfate during synthetic textile wastewater filtration reactive black of modified AqP membrane, original AqP membrane, modified CTA membrane and original CTA membrane.

Maximum removal percentage of nitrate was found to be 99.9 % using original and modified both CTA and AqP membrane with three type of reactive dyes, with and without HCOH and PVA as interference. Maximum removal percentages of sulphate and nitrate were found to be around 99.4% and 99.9% with reactive dye and the interferences.

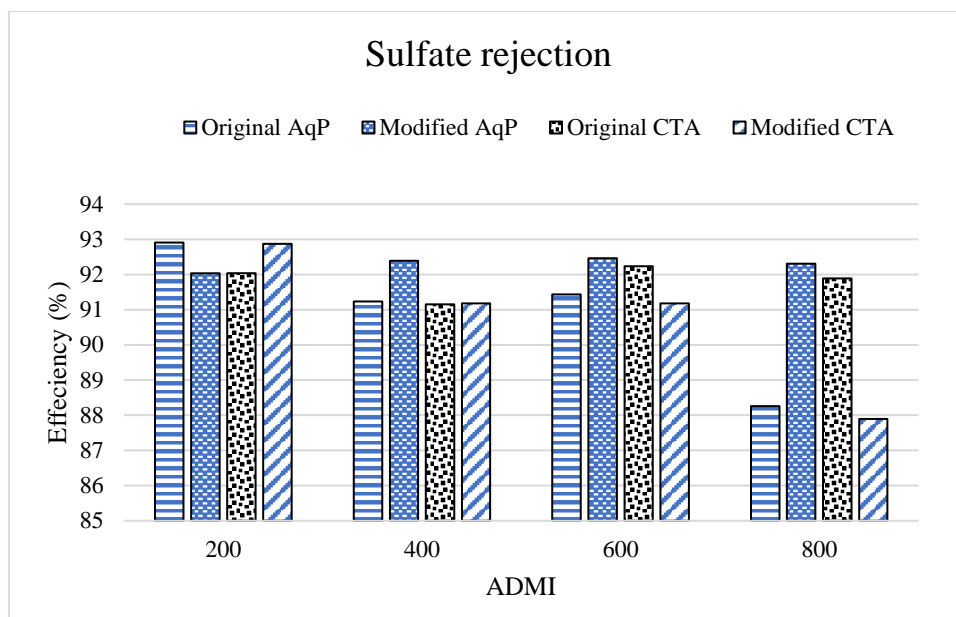


Figure 4- 20 Rejection efficiency of sulfate during synthetic textile wastewater filtration reactive black of modified AqP membrane, original AqP membrane, modified CTA membrane and original CTA membrane.

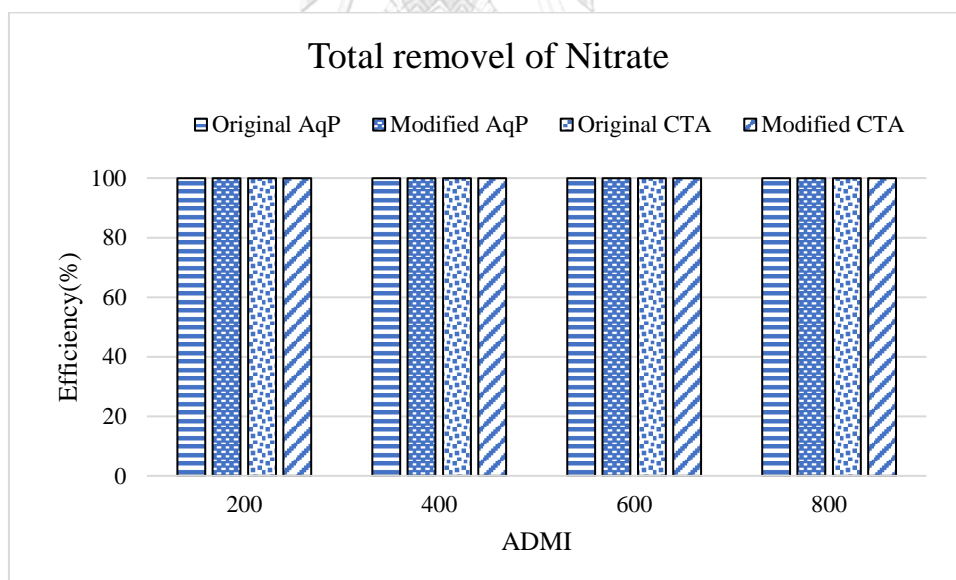


Figure 4- 21 Total removal efficiency of nitrate during synthetic textile wastewater filtration with reactive black of modified AqP membrane, original AqP membrane, modified CTA membrane and original CTA membrane.

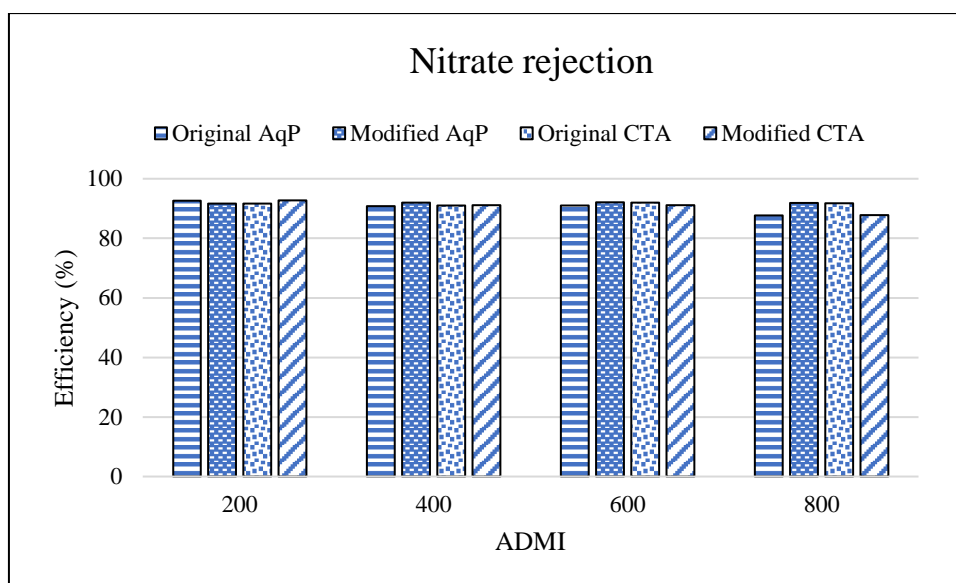


Figure 4- 22 Rejection efficiency of nitrate during synthetic textile wastewater filtration reactive black of modified AqP membrane, original AqP membrane, modified CTA membrane and original CTA membrane.

Phosphate was completely removed within experimental time with all set of experiments that use original and modified FO membrane with and without HCOH and PVA as interferences.

After grafting MEMO-PMMA-BR, the mean effective pore radius of modified membranes decreases implying a greater size exclusion effect. In addition, modified membranes become highly negatively charged and Donnan repulsion starts to play a more important role in the anion removal. On the other hand, the mechanisms that are mainly for solute rejection are molecular sieving and electrostatic repulsion (Alturki et al., 2013; Hancock and Cath, 2009; Phuntsho et al., 2013). The higher molecular weights and hydrated ion diameters for  $\text{NO}_3^-$  (62.01 g/mole and 0.3 nm),  $\text{SO}_4^{2-}$  (96.06 g/mol and 0.52 nm) and  $\text{PO}_4^{2-}$  (94.97 g/mole and 0.4 nm) resulted in higher rejection rates owing to attenuated transfer across the membrane.

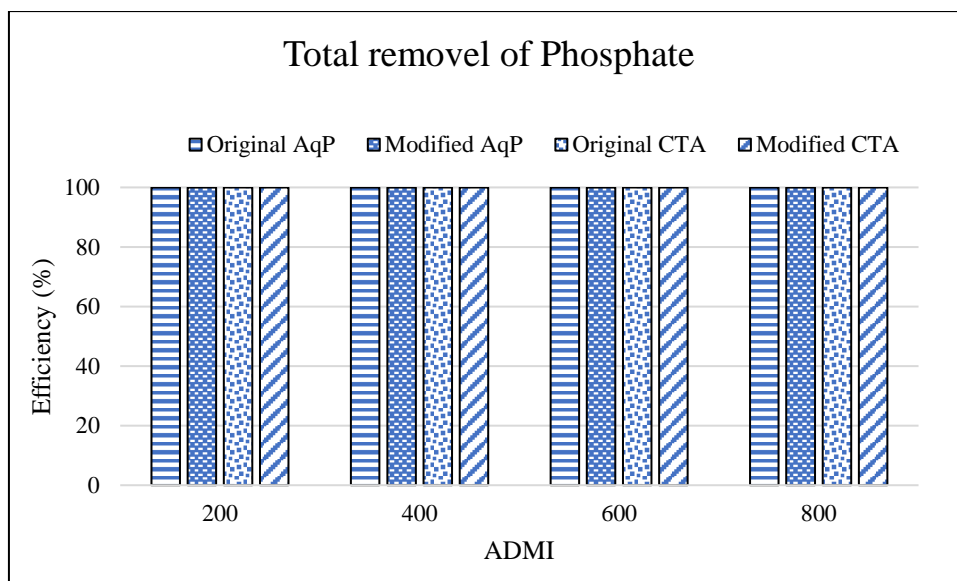


Figure 4- 23 Total removal efficiency of phosphate during synthetic textile wastewater filtration with reactive black of modified AqP membrane, original AqP membrane, modified CTA membrane and original CTA membrane.

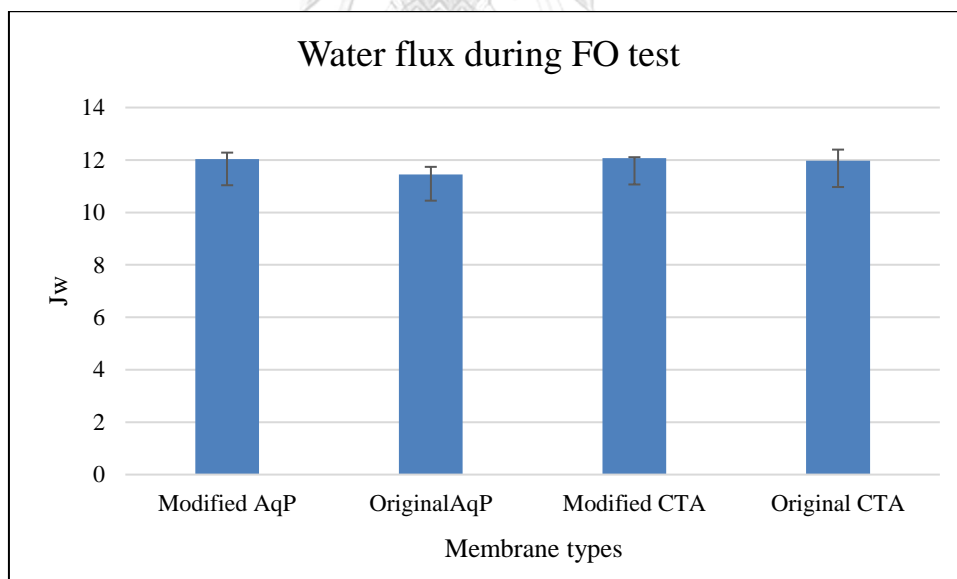


Figure 4- 24 Membrane flux variation during synthetic textile wastewater filtration reactive black with varying HCHO interference for modified AqP membrane, original AqP membrane, modified CTA membrane and original CTA membrane.

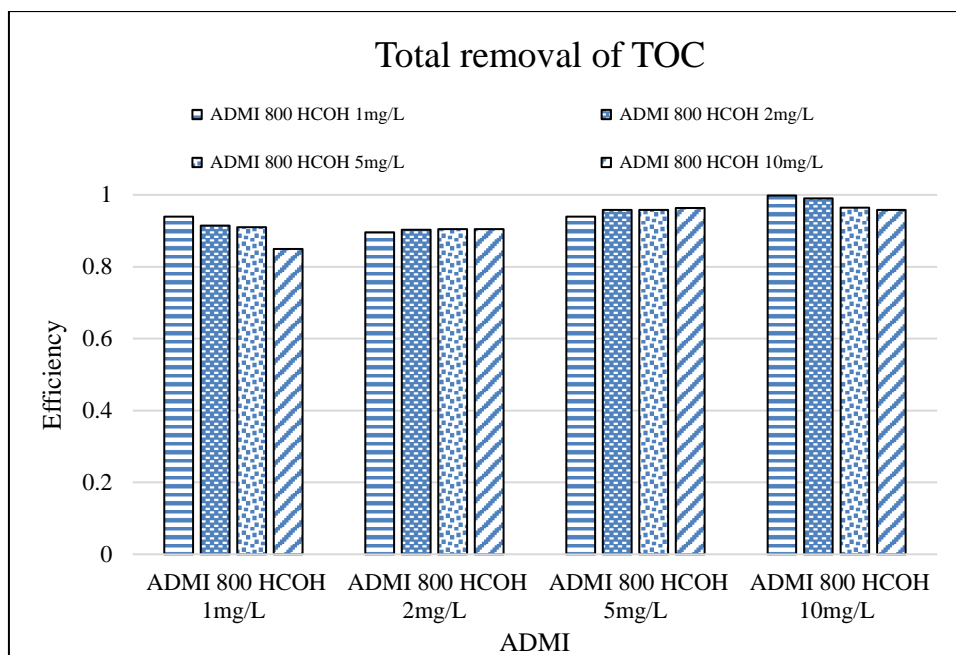


Figure 4- 25 Total removal of TOC value during synthetic textile wastewater filtration (reactive black) with varying HCHO interference for modified AqP membrane, original AqP membrane, modified CTA membrane and original CTA membrane.

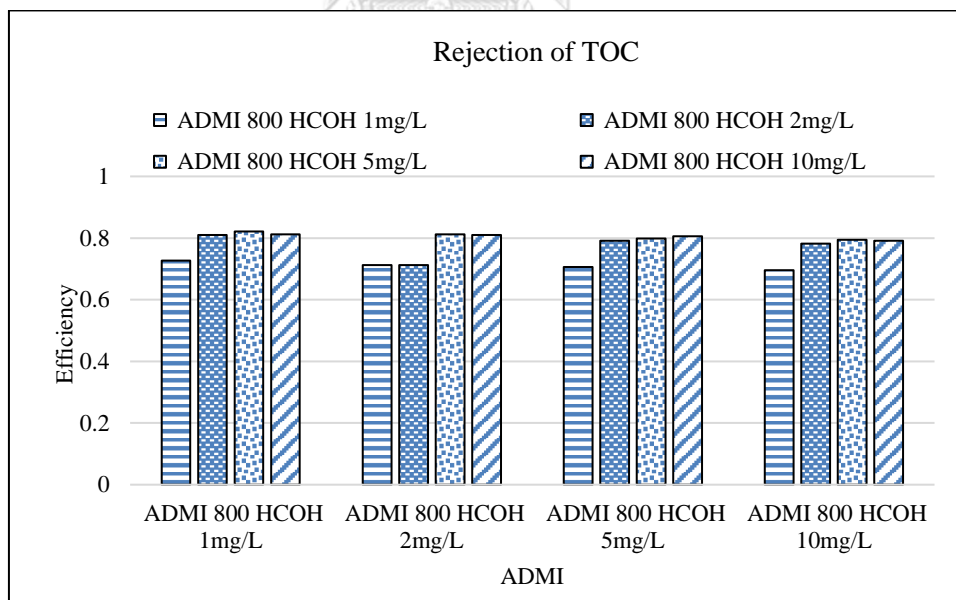


Figure 4- 26 Rejection efficiency of TOC value during synthetic textile wastewater filtration (reactive black) with varying HCHO interference for modified AqP membrane, original AqP membrane, modified CTA membrane and original CTA membrane.

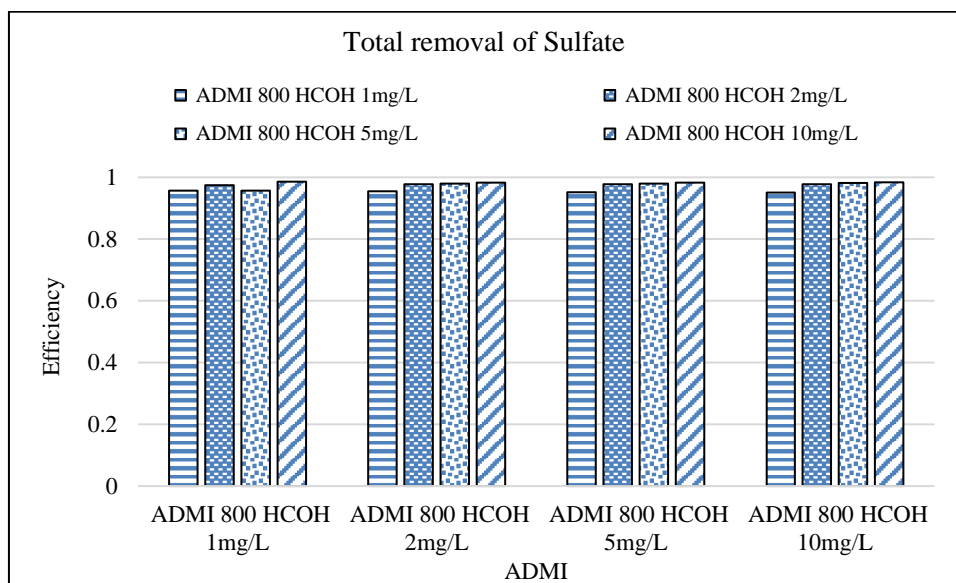


Figure 4- 27 Total retention of sulfate during synthetic textile wastewater filtration (reactive black) with varying HCHO interference for modified AqP membrane, original AqP membrane, modified CTA membrane and original CTA membrane

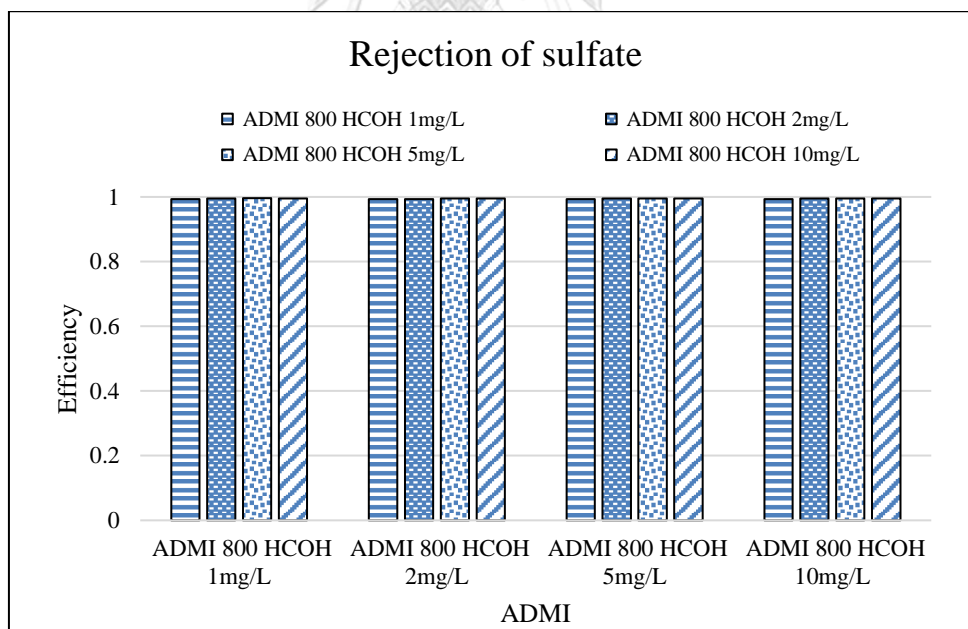


Figure 4- 28 Rejection efficiency of sulfate during synthetic textile wastewater filtration (reactive black) with varying HCHO interference for modified AqP membrane, original AqP membrane, modified CTA membrane and original CTA membrane

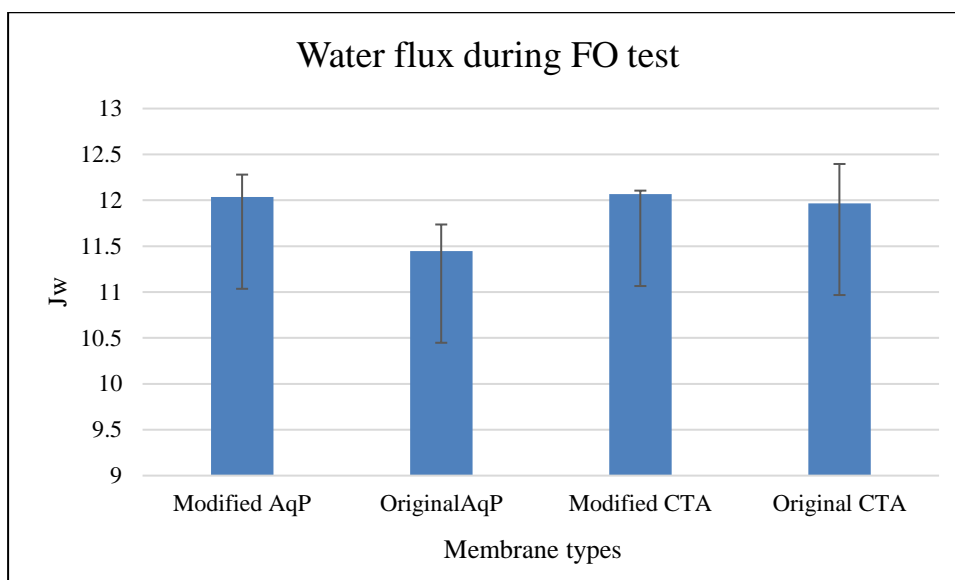


Figure 4- 29 Membrane flux variation during synthetic textile wastewater filtration (reactive blue) with varying HCHO interference of modified AqP membrane, original AqP membrane, modified CTA membrane and original CTA membrane.

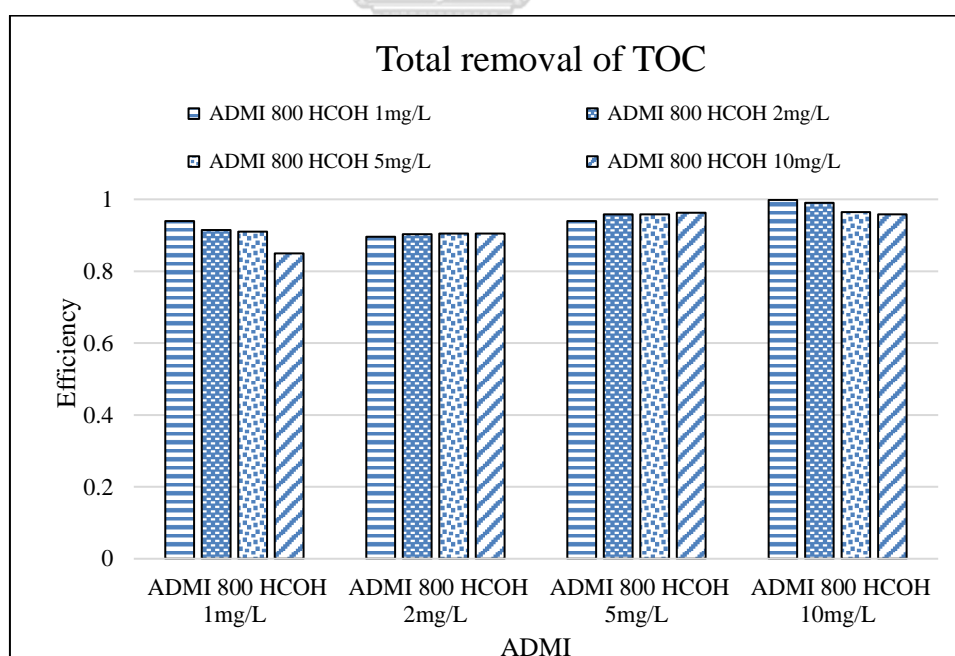


Figure 4- 30 Total removal of TOC during synthetic textile wastewater filtration reactive blue of modified AqP membrane, original AqP membrane, modified CTA membrane and original CTA membrane.

The occurrence of this phenomenon was attributed to the following reasons. There are many hydroxyl groups (-OH) in the molecular structure of PVA, which was easy to be oxidized and generated many small molecule organic acids. Meanwhile, (Jiang, Zhang et al. 2013) also found that many organic acids (e.g., formic acid, oxalic acid, pentadecanoic acid, and hexadecanoic acid) were detected during the degradation process of PVA and desizing wastewater by the supercritical water oxidation. In addition, since the PVA with many hydroxyl groups (i.e., -OH) was easy to be transferred into the small molecule organic acids, which can be easily filtered by membranes and oxidation processes of TiO<sub>2</sub> particles.

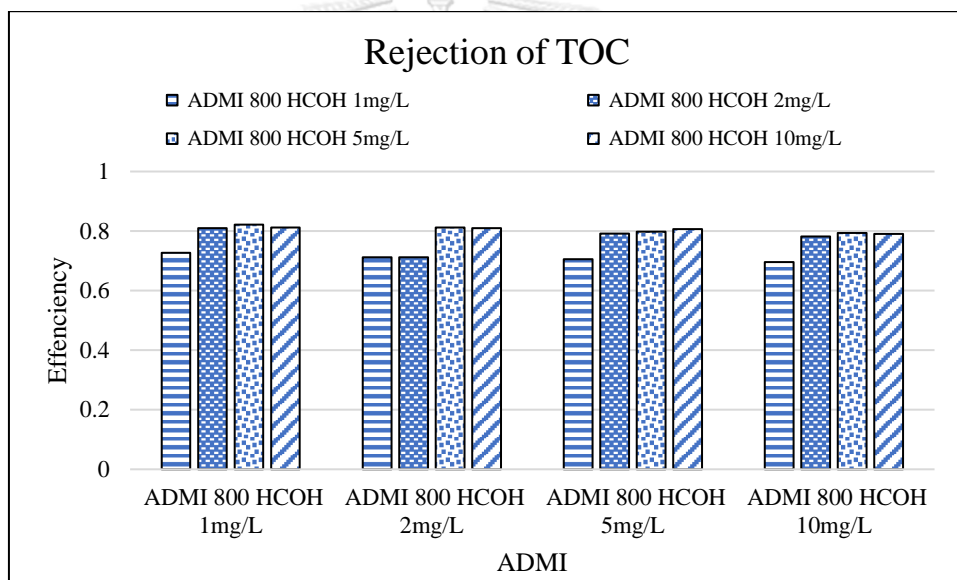


Figure 4- 31 Rejection efficiency of TOC value during synthetic textile wastewater filtration with reactive blue with modified AqP membrane, original AqP membrane, modified CTA membrane and original CTA membrane.



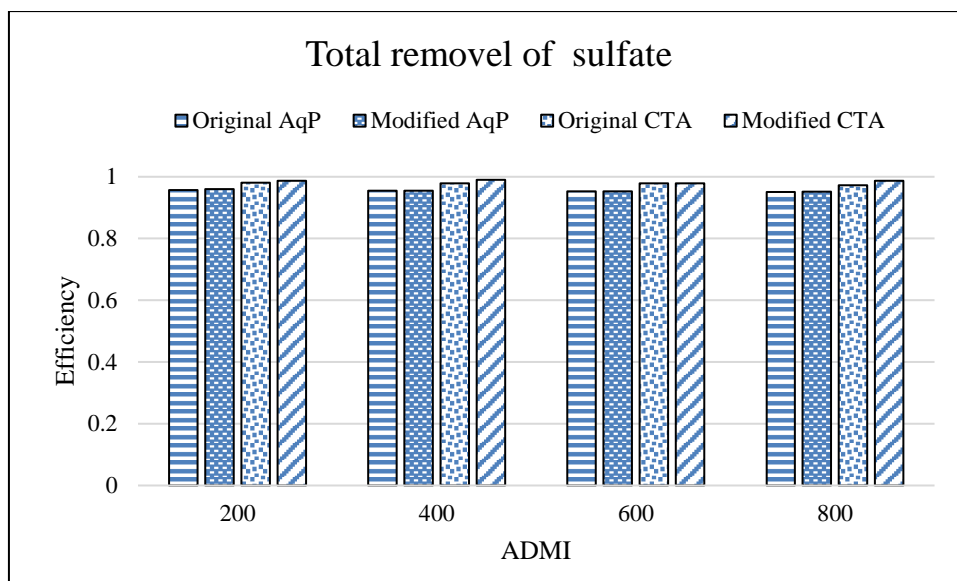


Figure 4- 32 Total retention of sulfate during synthetic textile wastewater filtration (reactive blue) with modified AqP membrane, original AqP membrane, modified CTA membrane and original CTA membrane.

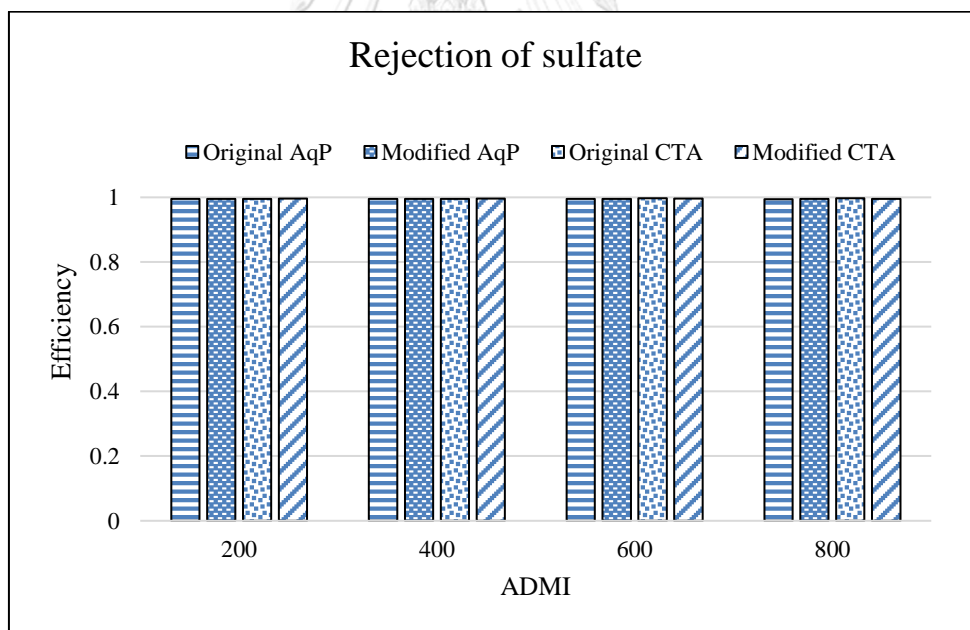


Figure 4- 33 Rejection efficiency of sulfate during synthetic textile wastewater filtration (reactive blue) of modified AqP membrane, original AqP membrane, modified CTA membrane and original CTA membrane.

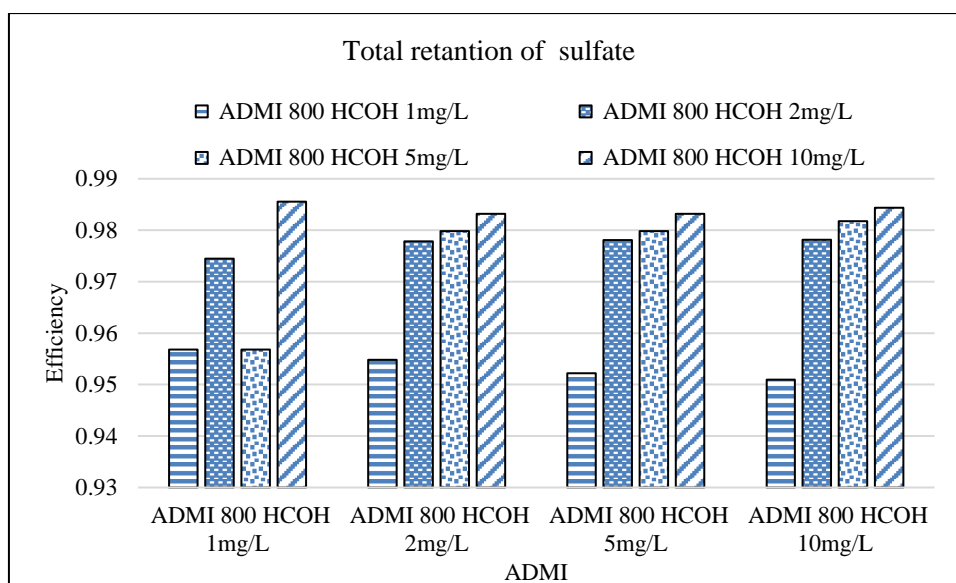


Figure 4- 34 Total retention of sulfate during synthetic textile wastewater filtration (reactive blue) with varying HCHO interference for modified AqP membrane, original AqP membrane, modified CTA membrane and original CTA membrane

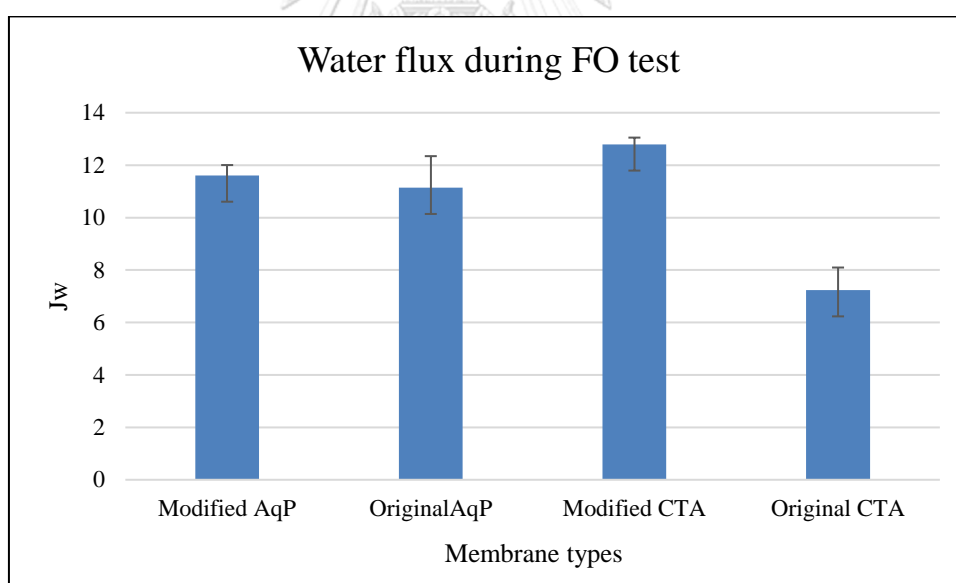


Figure 4- 35 Membrane flux variation during synthetic textile wastewater with different ADMI values (reactive red) tests for modified AqP membrane, original AqP membrane, modified CTA membrane and original CTA membrane.

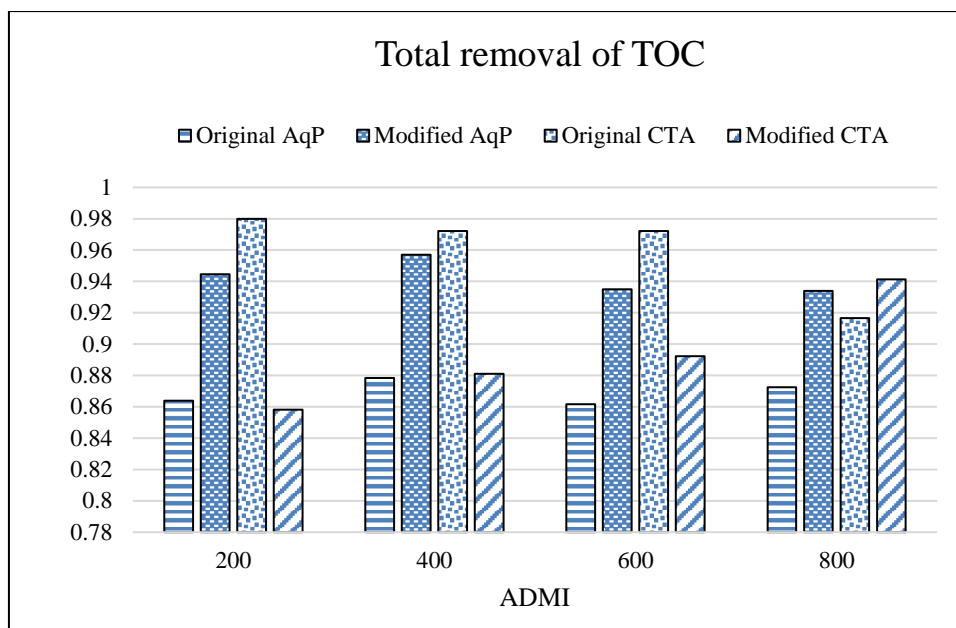


Figure 4- 36 Total retention of TOC value during synthetic textile wastewater filtration with reactive red of modified AqP membrane, original AqP membrane, modified CTA membrane and original CTA membrane.

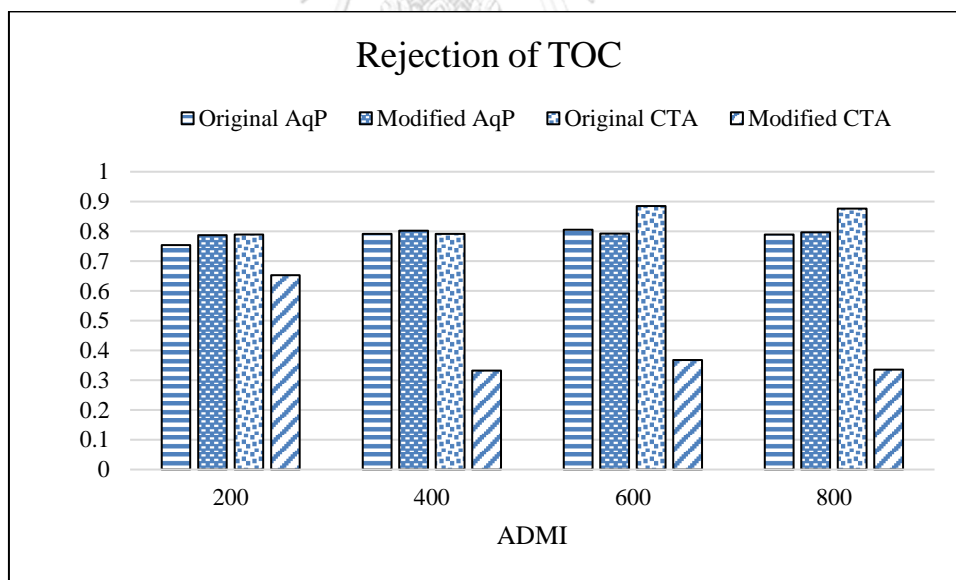


Figure 4- 37 Rejection efficiency of TOC value during synthetic textile wastewater filtration with reactive red with modified AqP membrane, original AqP membrane, modified CTA membrane and original CTA membrane.

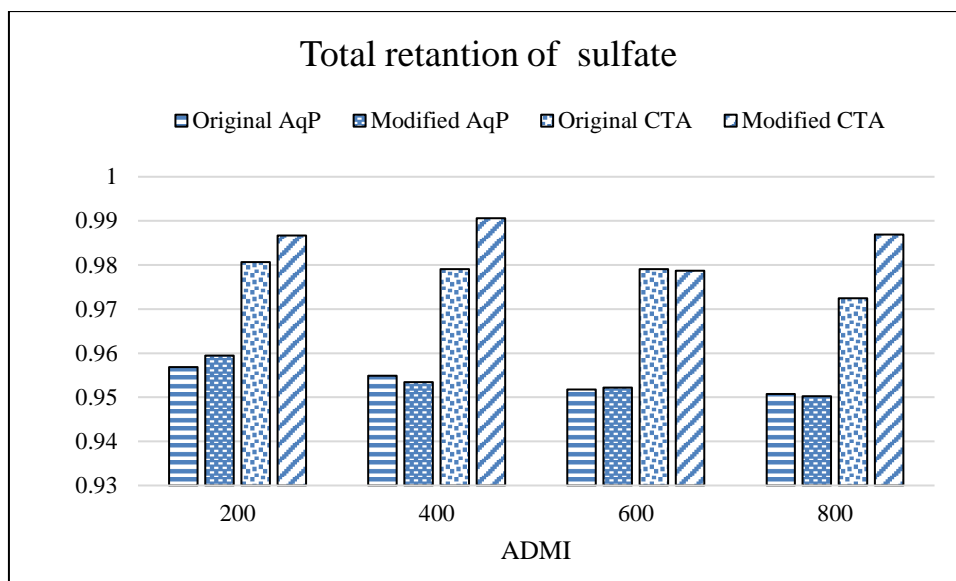


Figure 4- 38 Total retention of sulfate during synthetic textile wastewater filtration (reactive red) with modified AqP membrane, original AqP membrane, modified CTA membrane and original CTA membrane.

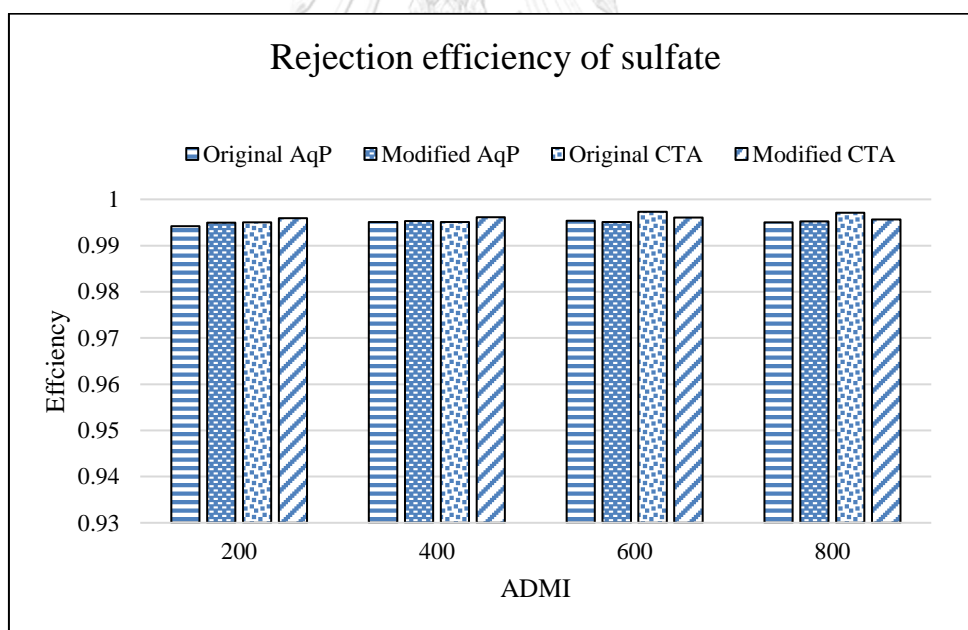


Figure 4- 39 Rejection efficiency of sulfate during synthetic textile wastewater filtration (reactive red) with modified AqP membrane, original AqP membrane, modified CTA membrane and original CTA membrane.

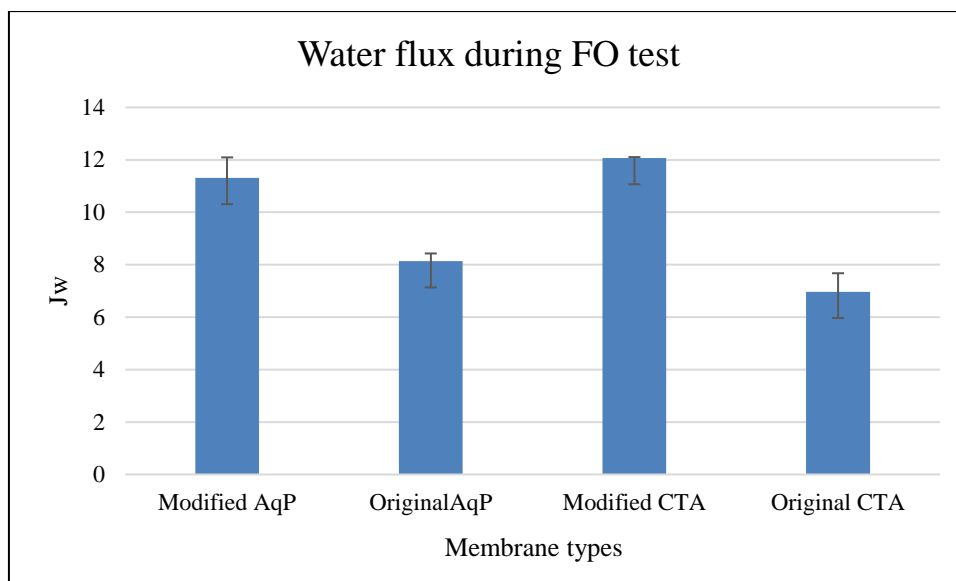


Figure 4- 40 Membrane flux variation during synthetic textile wastewater (reactive red) with varying the concentration of interference (HCHO) tests for modified AqP membrane, original AqP membrane, modified CTA membrane and original CTA membrane.

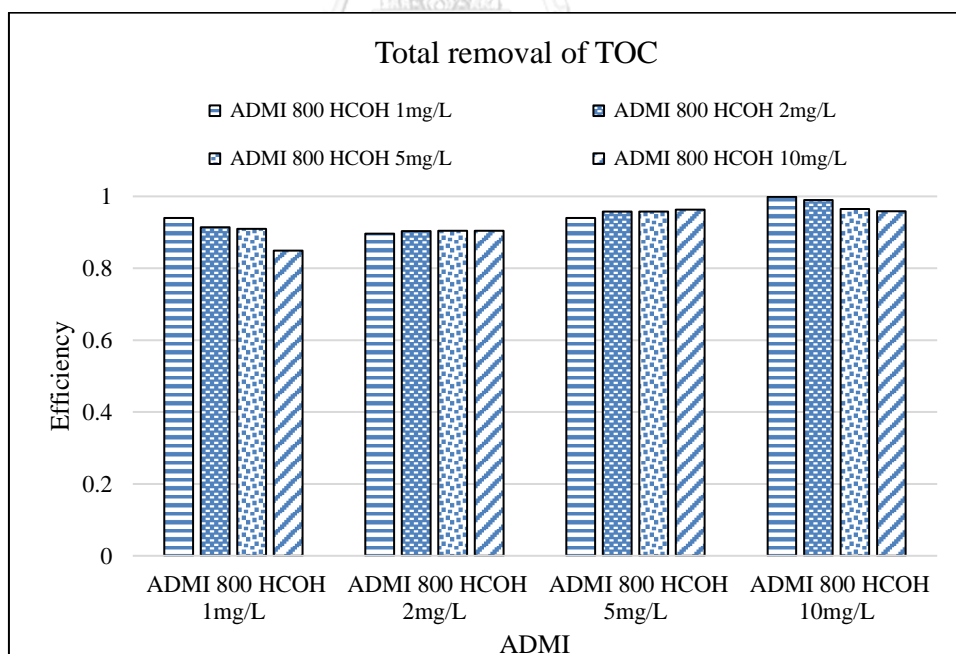


Figure 4- 41 Total retention of TOC value during synthetic textile wastewater filtration (reactive red) with varying HCHO interference for modified AqP membrane, original AqP membrane, modified CTA membrane and original CTA membrane.

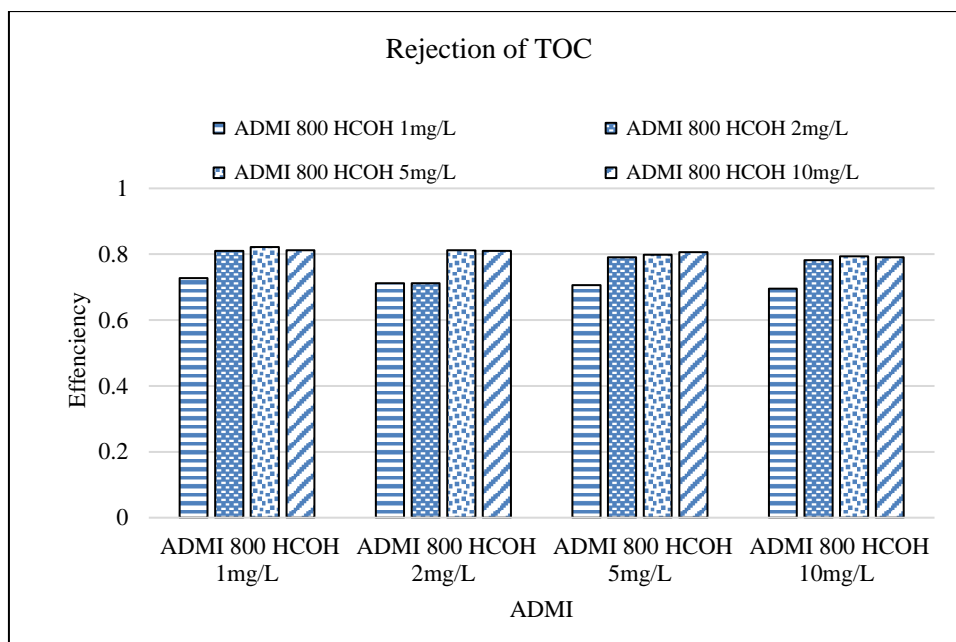


Figure 4- 42 Rejection efficiency of TOC value during synthetic textile wastewater filtration (reactive red) with varying HCHO interference for modified AqP membrane, original AqP membrane, modified CTA membrane and original CTA membrane.

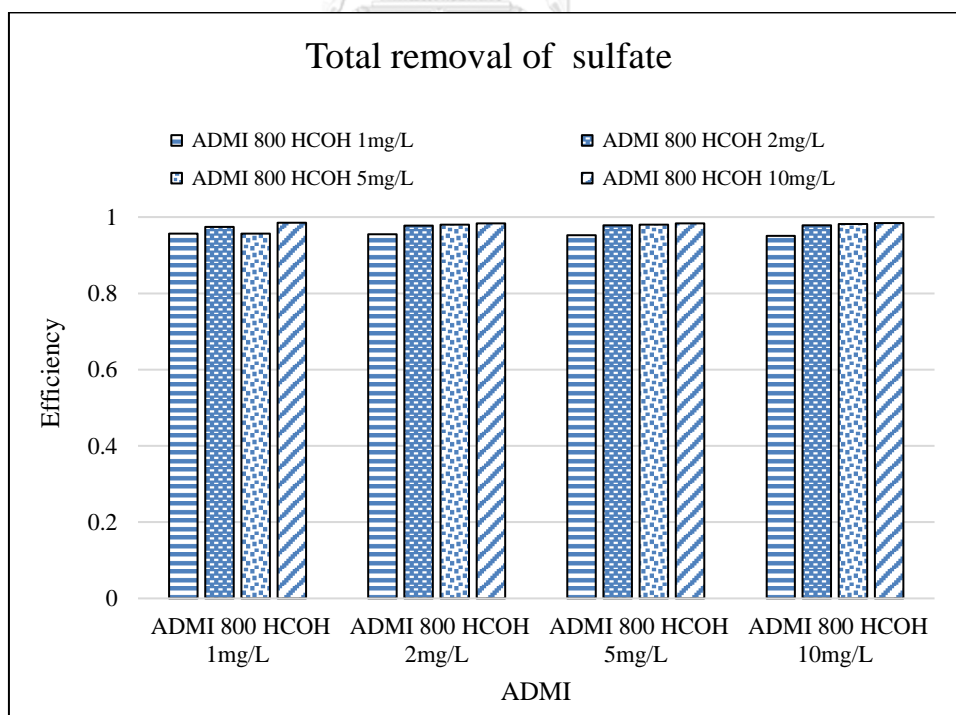


Figure 4- 43 Total retention of sulfate during synthetic textile wastewater filtration (reactive red) with varying HCHO interference for modified AqP membrane, original AqP membrane, modified CTA membrane and original CTA membrane

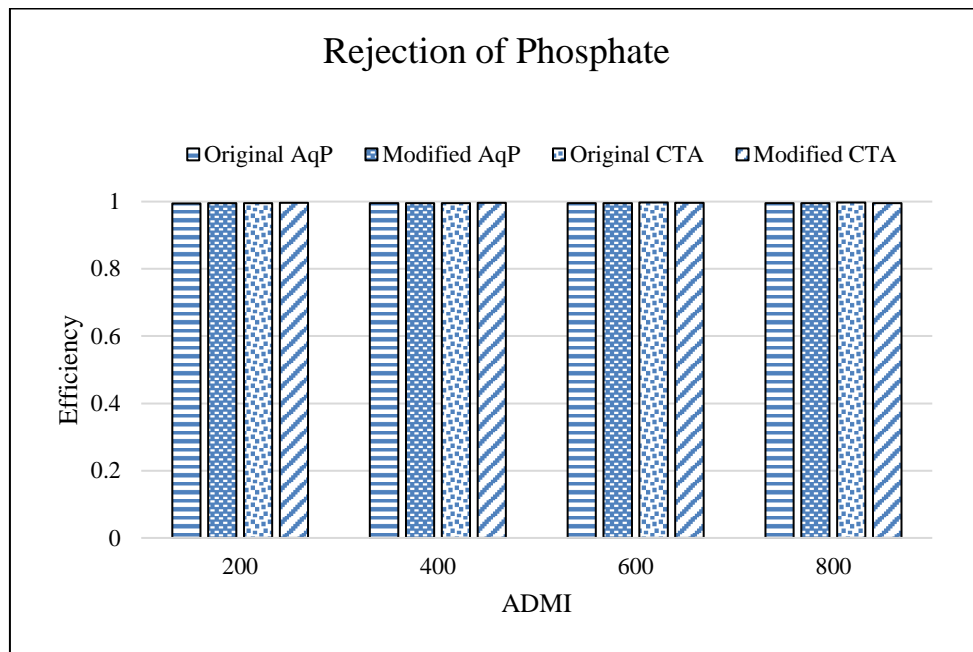


Figure 4- 44 Rejection efficiency of phosphate during synthetic textile wastewater filtration (reactive blue) of modified AqP membrane, original AqP membrane, modified CTA membrane and original CTA membrane.

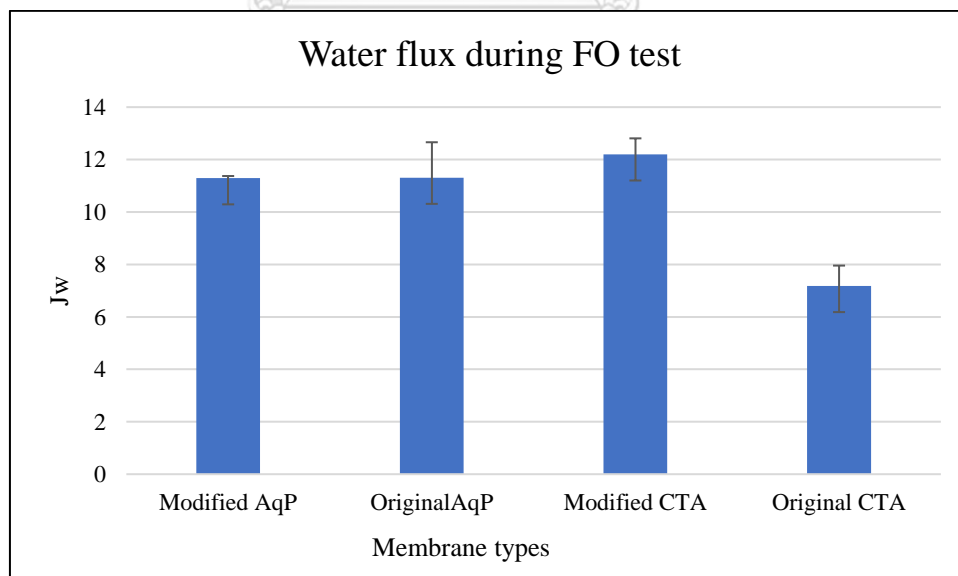


Figure 4- 45 Membrane flux variation during synthetic textile wastewater (blue) with varying the concentration of interference (PVA) tests for modified AqP membrane, original AqP membrane, modified CTA membrane and original CTA membrane.

#### 4.5 The interferences of Polyvinyl alcohol (PVA) on dyes removal using TiO<sub>2</sub> coated membrane

The occurrence of this phenomenon was attributed to the following reasons. There are many hydroxyl groups (-OH) in the molecular structure of PVA, which was easy to be oxidized and generated many small molecule organic acids. Meanwhile, (Jiang, Zhang et al. 2013) also found that many organic acids (e.g., formic acid, oxalic acid, pentadecanoic acid, and hexadecanoic acid) were detected during the degradation process of PVA and desizing wastewater by the supercritical water oxidation. In addition, since the PVA with many hydroxyl groups (i.e., -OH) was easy to be transferred into the small molecule organic acids, which can be easily filtered by membranes and oxidation processes of TiO<sub>2</sub> particles.

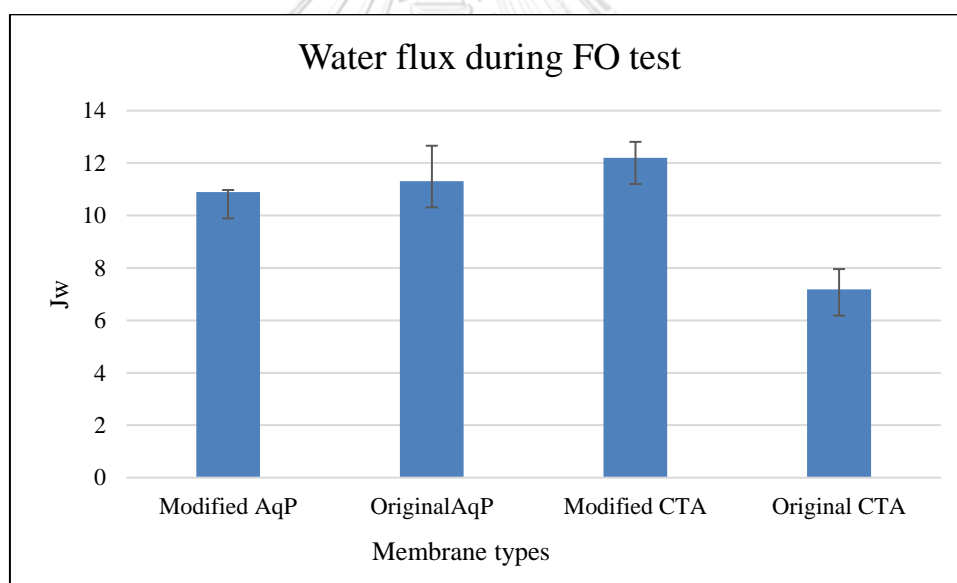


Figure 4- 46 Membrane flux variation during synthetic textile wastewater (red) with varying the concentration of interference (PVA) tests for modified AqP membrane, original AqP membrane, modified CTA membrane and original CTA membrane.



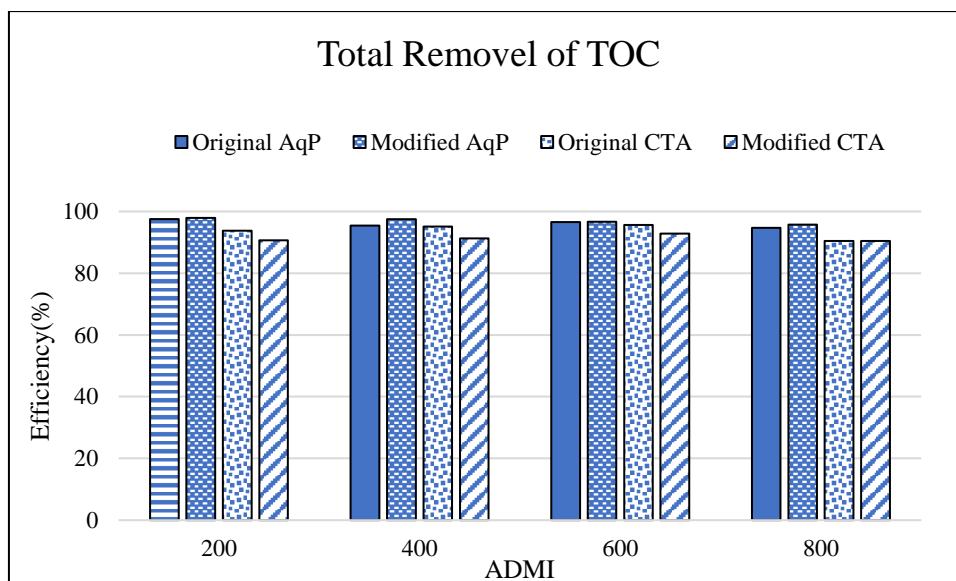


Figure 4- 47 Total retention of TOC value during synthetic textile wastewater filtration (reactive red) with varying HCHO interference for modified AqP membrane, original AqP membrane, modified CTA membrane and original CTA membrane

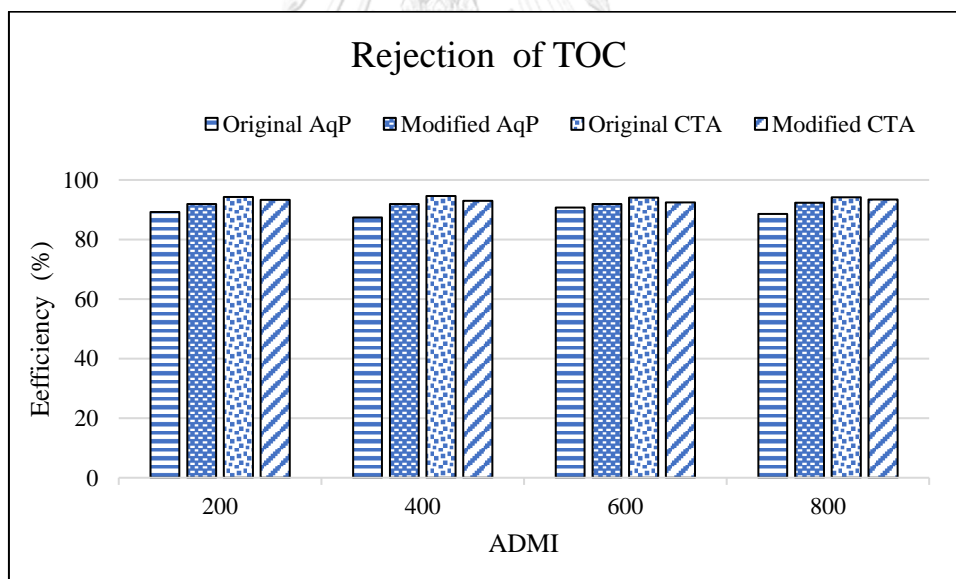


Figure 4- 48 Rejection efficiency of TOC value during synthetic textile wastewater filtration (reactive red) with varying HCHO interference for modified AqP membrane, original AqP membrane, modified CTA membrane and original CTA membrane.

PVA and HCOH rejection increases dramatically as the compound transforms from a neutral to a positively charged species as solution pH exist below its pKa value

(PVA is 10.67 and HCOH is 13.27). Negatively charged membrane surface may absorb these positively charged compounds. Ionic strength screens the molecule and membrane charges and therefore reduces the effectiveness of electrostatic repulsion as a major retention mechanism by the modified membrane than original membrane. Rejection of wastewater pollutants is an important factor when evaluating concentrating efficiency. The TOC rejection was >98% and the rejection of  $\text{PO}_4^{2-}$ ,  $\text{NO}_3^{2-}$  and  $\text{SO}_4^{2-}$  was >99%. A good rejection of macromolecules, and trace organics compounds have been also presented by several studies (Kong et al., 2015) (Sun et al., 2016) (Xie et al., 2018).

The fast moving of ions is hindered by the developed electrical potential and accelerate the slow moving of ions to maintain the electroneutrality condition. The ion distribution is purely due to the diffusion and electro-migration. This leads to the formation of an electrical double layer, so that a charged surface and a neutralizing excess of counter-ions exists in the adjacent solution. Therefore ions rejection can be said as mainly due to molecular sieving by the dense active layer of the FO membrane (Phuntsho et al., 2011).

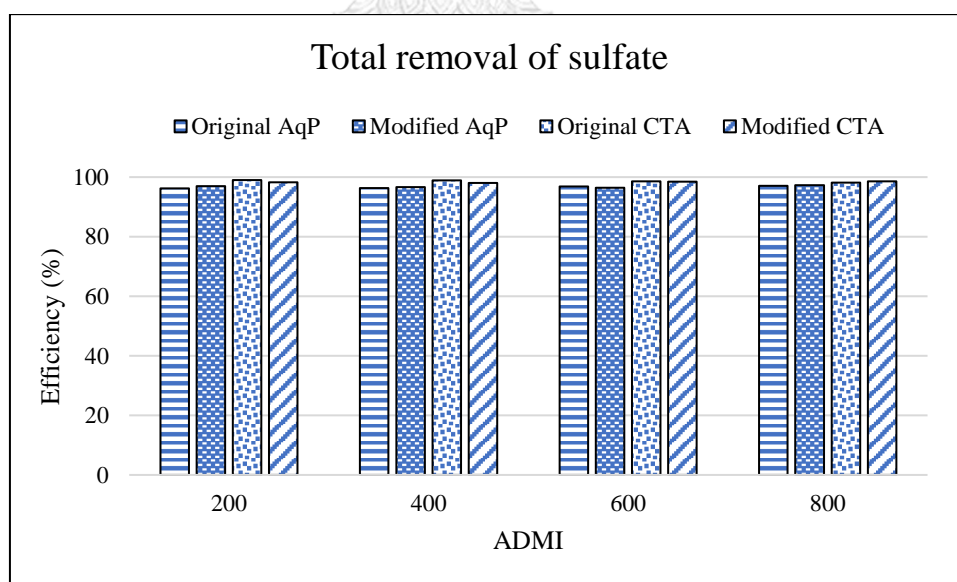


Figure 4- 49 Total removal of sulfate during synthetic textile wastewater filtration (reactive red) with varying HCHO interference for modified AqP membrane, original AqP membrane, modified CTA membrane and original CTA membrane

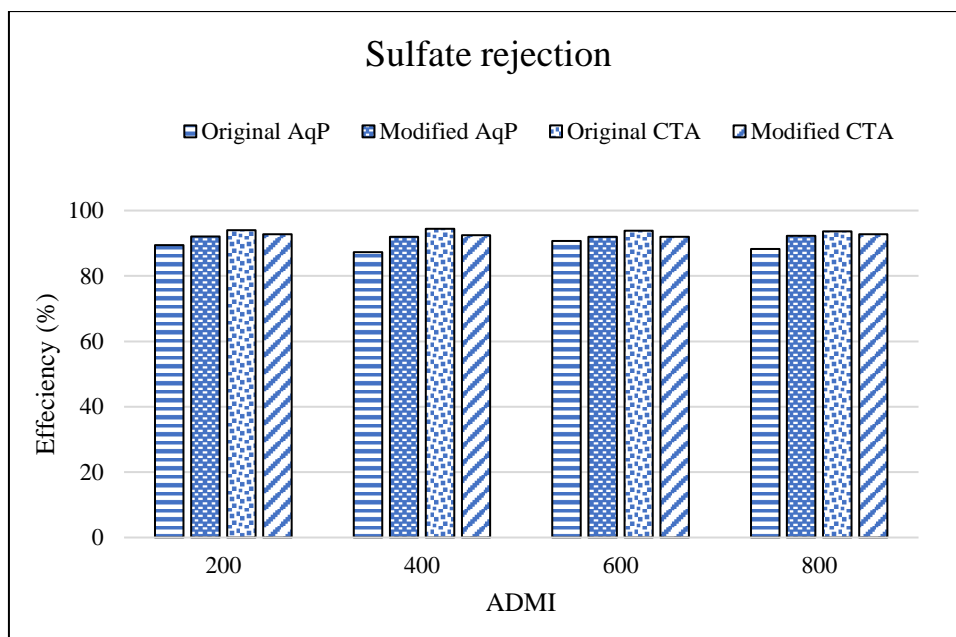


Figure 4- 50 Rejection efficiency of sulfate during synthetic textile wastewater filtration (reactive red) of modified AqP membrane, original AqP membrane, modified CTA membrane and original CTA membrane.

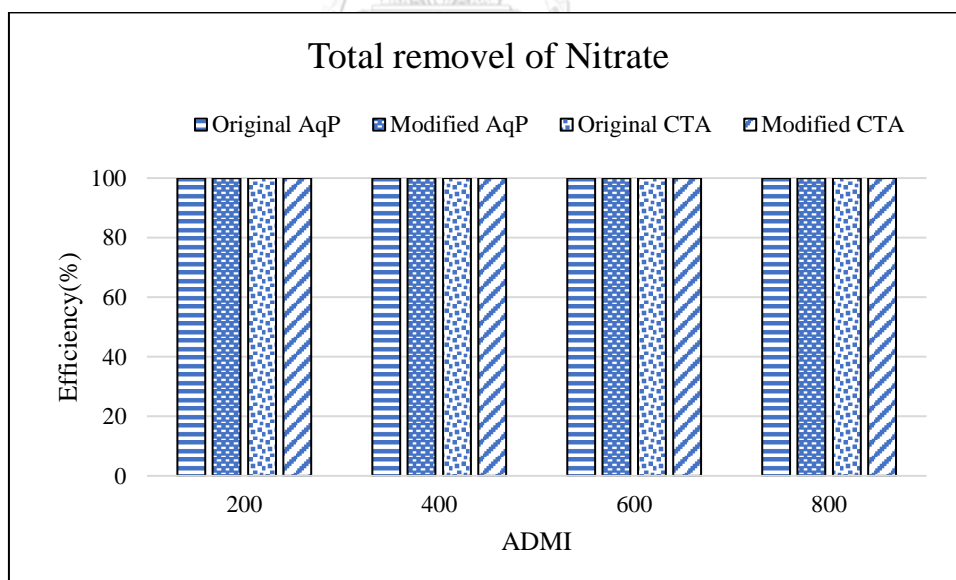


Figure 4- 51 Total removal of nitrate during synthetic textile wastewater filtration (reactive red) with varying HCHO and PVA interference for modified AqP membrane, original AqP membrane, modified CTA membrane and original CTA membrane

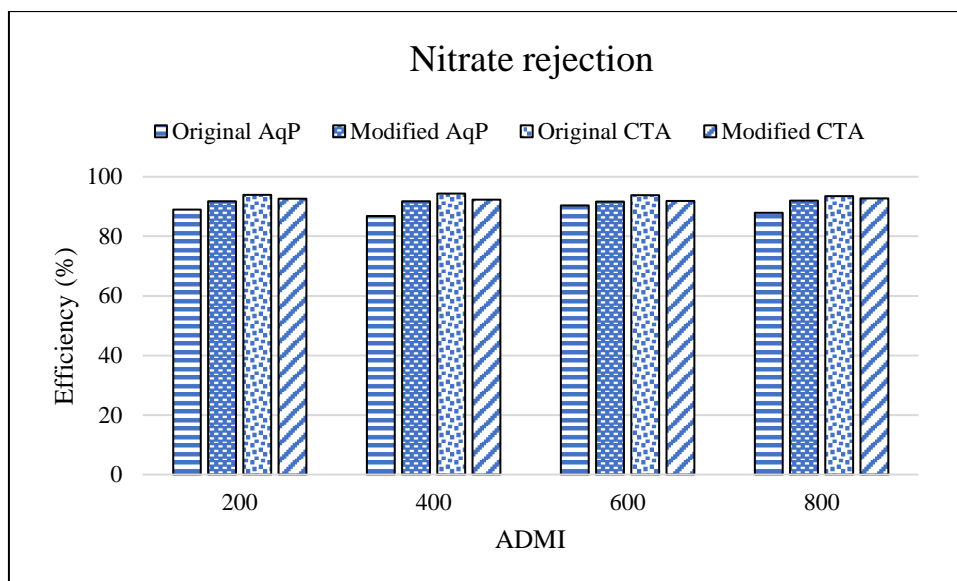


Figure 4- 52 Rejection efficiency of nitrate during synthetic textile wastewater filtration (reactive red) of modified AqP membrane, original AqP membrane, modified CTA membrane and original CTA membrane.

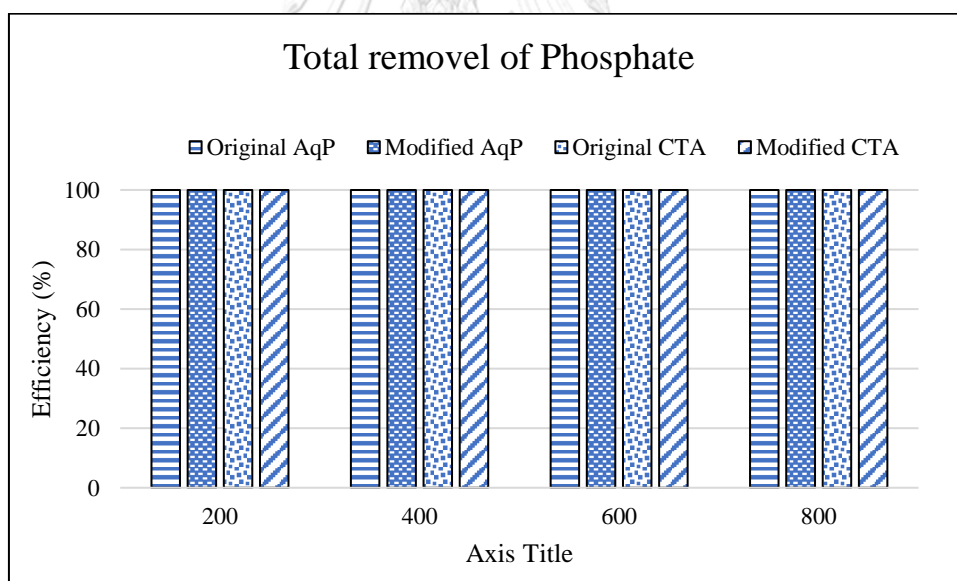


Figure 4- 53 Total removal of phosphate during synthetic textile wastewater filtration (reactive red) with varying HCHO and PVA interference for modified AqP membrane, original AqP membrane, modified CTA membrane and original CTA membrane

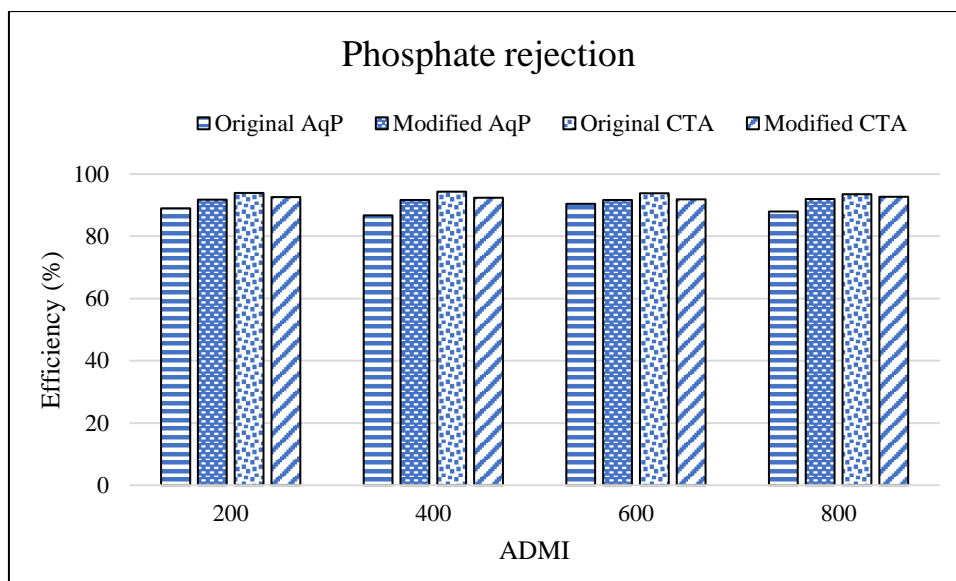


Figure 4- 54 Rejection efficiency of nitrate during synthetic textile wastewater filtration (reactive red) with varying HCHO and PVA interference of modified AqP membrane, original AqP membrane, modified CTA membrane and original CTA membrane.

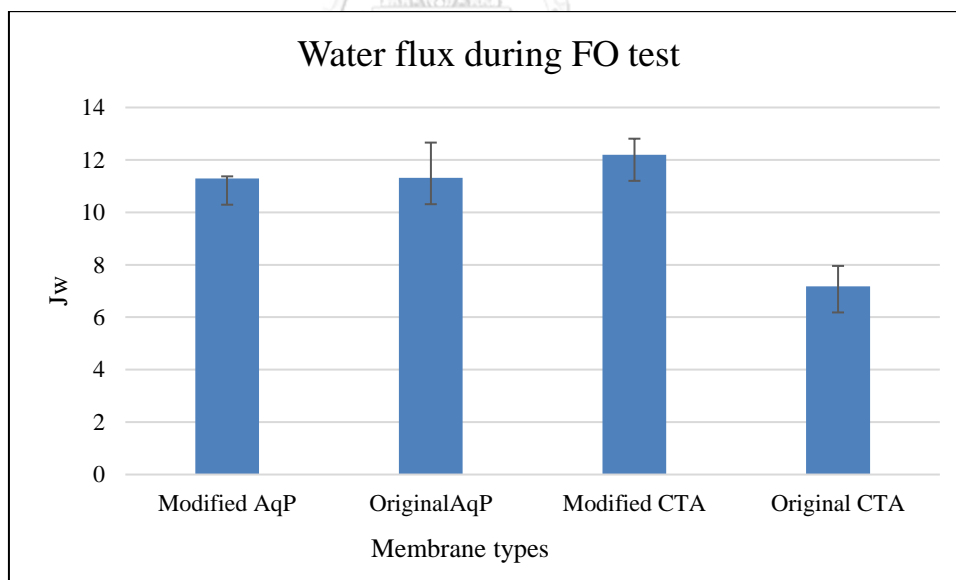


Figure 4- 55 Membrane flux variation during synthetic textile wastewater (red) with varying the concentration of interference (HCHO) tests for modified AqP membrane, original AqP membrane, modified CTA membrane and original CTA membrane.

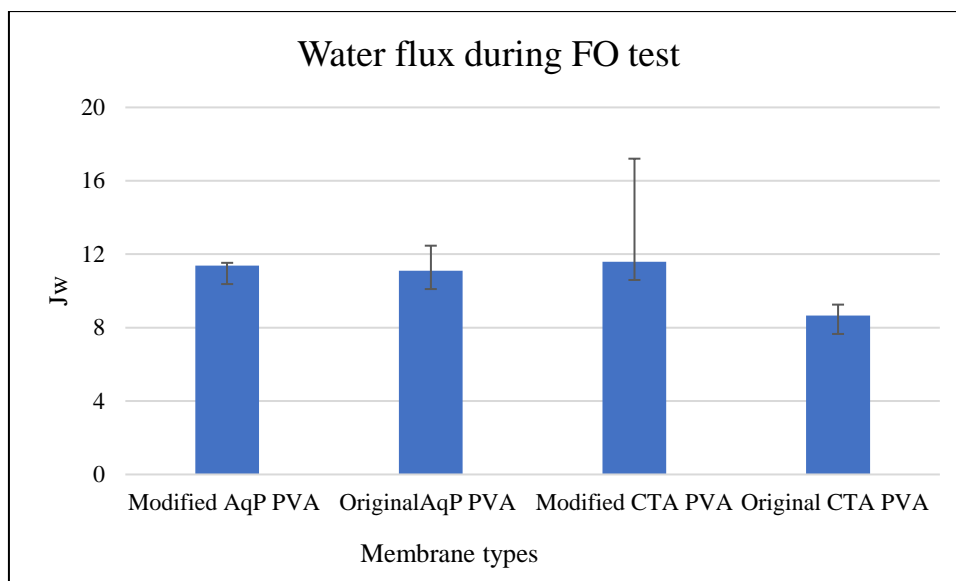


Figure 4- 56 Membrane flux variation during synthetic textile wastewater (black) with varying the concentration of interference (PVA) tests for modified AqP membrane, original AqP membrane, modified CTA membrane and original CTA membrane.

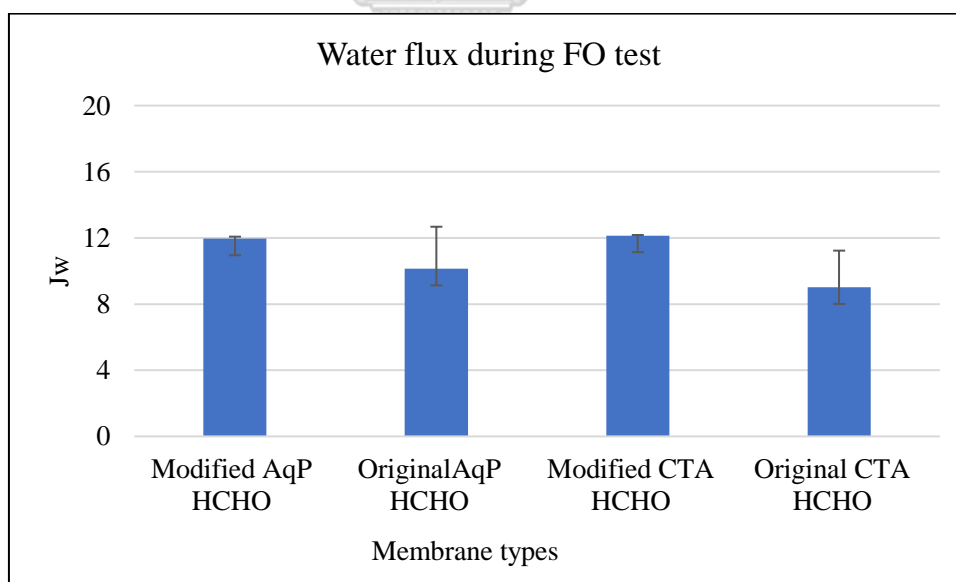


Figure 4- 57 Membrane flux variation during synthetic textile wastewater (blue) with varying the concentration of interference (HCHO) tests for modified AqP membrane, original AqP membrane, modified CTA membrane and original CTA membrane.

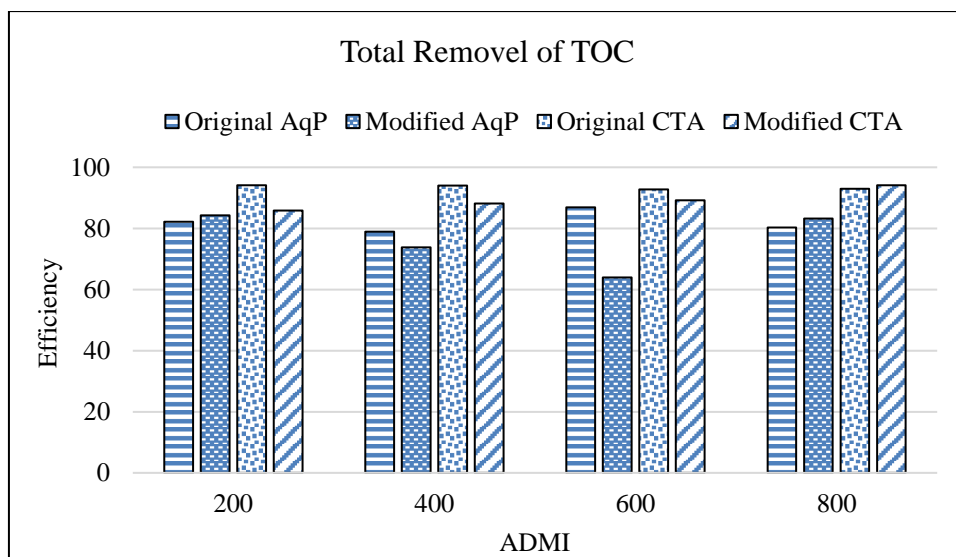


Figure 4- 58 Total removal efficiency of TOC value during synthetic textile wastewater filtration (reactive black) with varying HCHO and PVA interference of modified AqP membrane, original AqP membrane, modified CTA membrane and original CTA membrane.

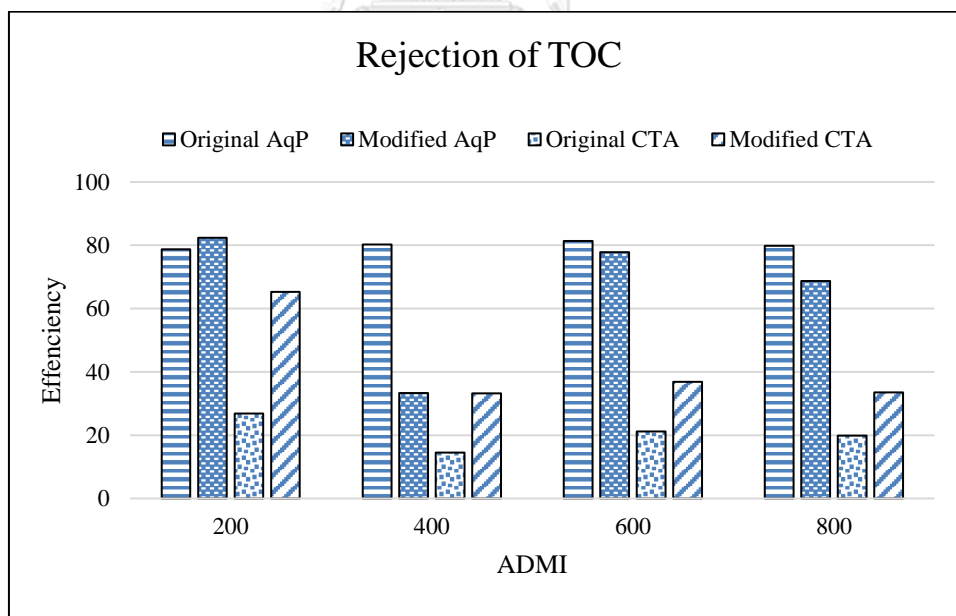


Figure 4- 59 Rejection efficiency for TOC during synthetic textile wastewater filtration (reactive black) with with varying HCHO and PVA interference of modified AqP membrane, original AqP membrane, modified CTA membrane and original CTA membrane.

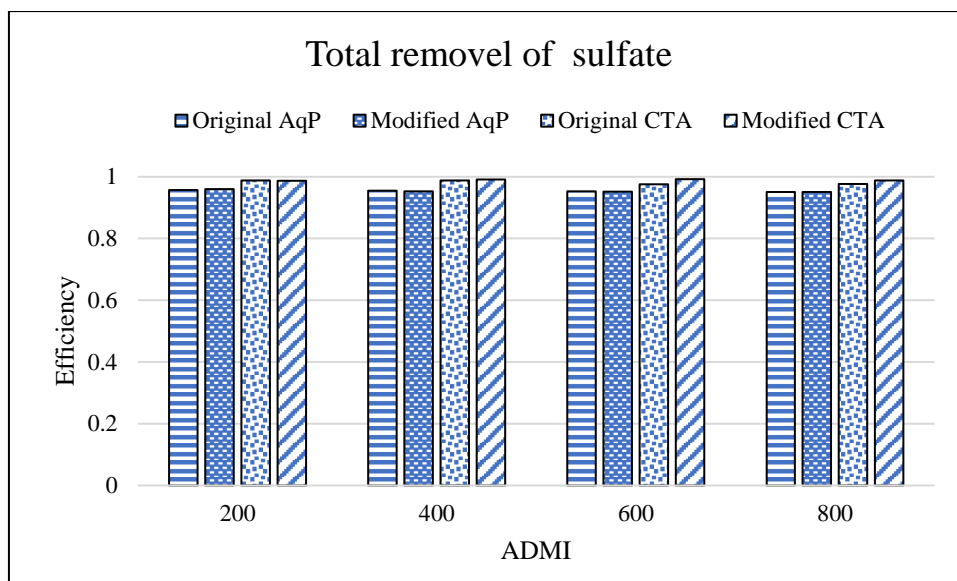


Figure 4- 60 Total removal of sulfate during synthetic textile wastewater filtration (reactive black) of modified AqP membrane, original AqP membrane, modified CTA membrane and original CTA membrane.

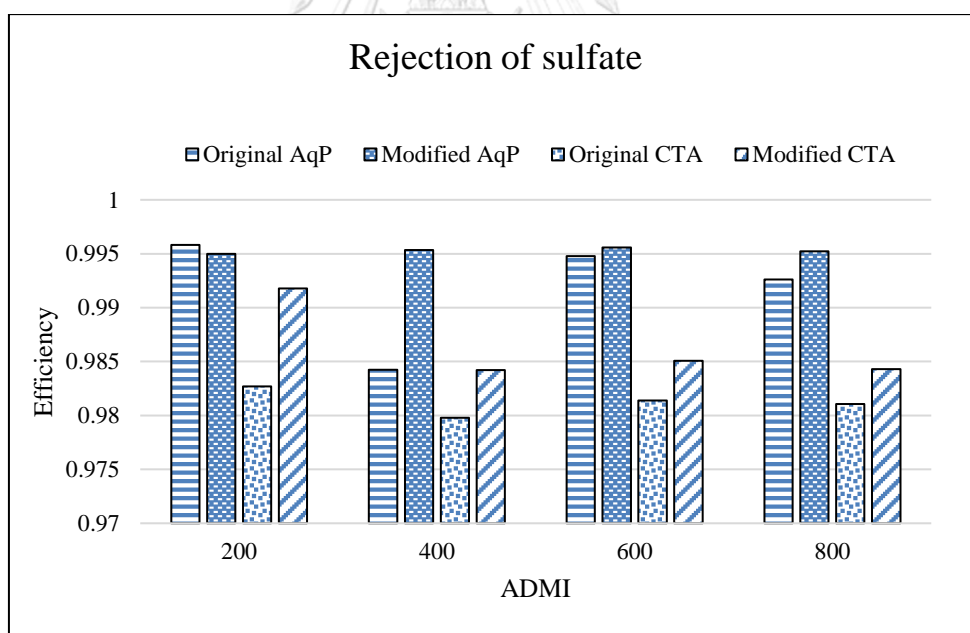


Figure 4- 61 Rejection efficiency of sulfate during synthetic textile wastewater filtration (reactive black) with varying HCHO and PVA interference of modified AqP membrane, original AqP membrane, modified CTA membrane and original CTA membrane.



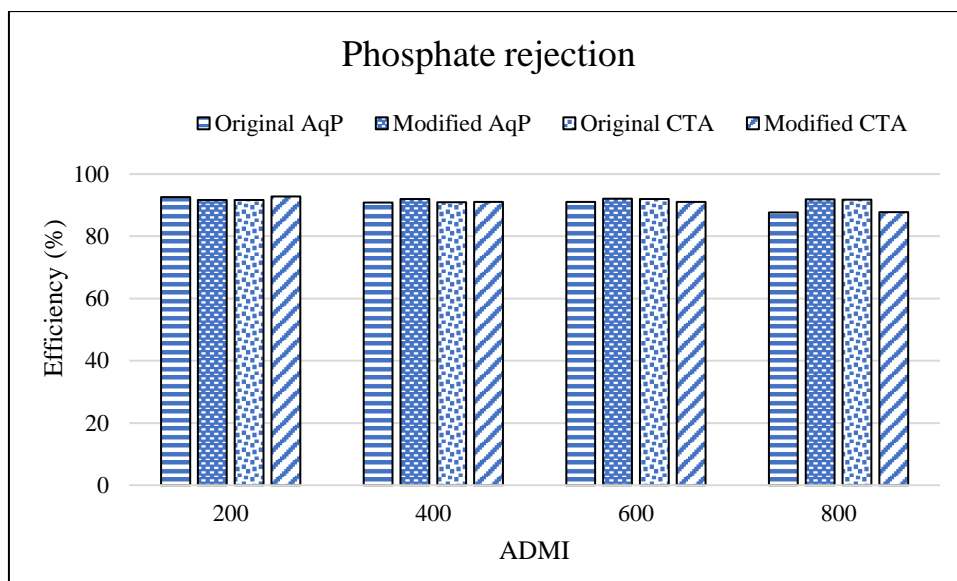


Figure 4- 62 Rejection efficiency of phosphate during synthetic textile wastewater filtration (reactive black) varying HCHO and PVA interference of modified AqP membrane, original AqP membrane, modified CTA membrane and original CTA membrane.

#### **4.6 Feasible application of original and modified both CTA and AqP membranes for water quality improvement of treated textile effluent**

The characteristics of the treated textile effluent is shown in Table 4.5.

Table 4- 4 Characteristic of treated textile wastewater effluent from factory A

Parameter	Unit	Method of Analysis	Results
			Textile Effluent 1
pH		Electrometric method	8.3
COLOUR	ADMI	ADMI weighted-ordinate spectrophotometric method (SM2012:2120 F)	48 (pH 8.3)
COLOUR	ADMI	ADMI weighted-ordinate spectrophotometric method (SM2012:2120 F)	49 (pH 7.0)
NITRATE-NITROGEN	mg/L NO <sub>3</sub> -N	Ion Chromatography method	3.57
CHLORIDE	mg/L Cl <sup>-</sup>	Ion Chromatography method	189
FLUORIDE	mg/L F <sup>-</sup>	Ion Chromatography method	0.84
SULPHATE	mg/L SO <sub>4</sub> <sup>2-</sup>	Ion Chromatography method	467
PHOSPHATE	mg/L PO <sub>4</sub> <sup>3-</sup>	Ion Chromatography method	0.56
PVA	mg/L	Distillation, Colourimetric method	25
FORMALDEHYDE	mg/L	Distillation, Colourimetric method	32
TOTAL ORGANIC CARBON	mg/L F	High-temperature combustion method	8.27
SAMPLE CONDITION (WATER COLOUR/TURBID SEDIMENT)			Almost colourless/ yellowish white

This is the water characteristic of the treated textile water effluent from factory A which is located at Sahapat Industrial Estate, Cholburi Province. According to this table, the ADMI values for the effluent are 46 and 51 at pH 5.9 and pH 7. The chloride content of treated wastewater is 213 mg/L CL<sup>-</sup> for the treated textile water effluent. The amount of nitrate-nitrogen is 8.85 mg/L NO<sub>3</sub>-N, fluoride is 1.21 mg/L F<sup>-</sup>, phosphate is 4,52 mg/L PO<sub>4</sub><sup>3-</sup>, PVA is 43 mg/L and formaldehyde amount of effluents is 41 mg/L. The sulfate contents of treated wastewater are 420 mg/L SO<sub>4</sub><sup>2-</sup> for original aquaporin membrane. The amounts of total organic carbon after the treatment are 8.11 mg/L for the treated textile water effluent.

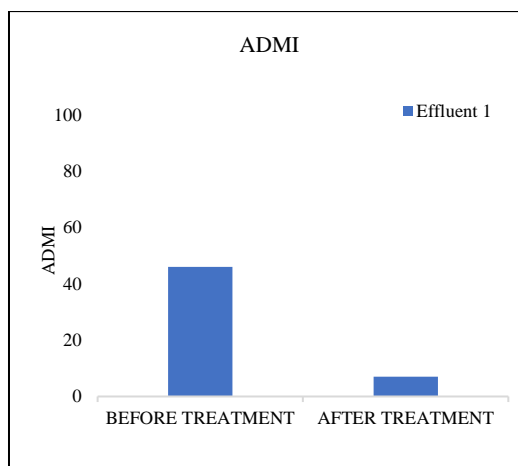


Figure 4- 63 Comparison of ADMI value and after treated with both original and modified FO membranes process

This is the result of the FO treatment for the textile effluent-1 with original and modified both CTA and aquaporin membranes. According to this figure, the ADMI values for the membranes are less than 10 at pH 5.9 and pH7. The amount of nitrate-nitrogen, phosphate and formaldehyde amount of effluents are non-detectable level. The sulfate contents of used wastewater are 0.893 mg/L  $\text{SO}_4^{2-}$  for original aquaporin membrane, 2.03 mg/L  $\text{SO}_4^{2-}$  for modified aquaporin membrane, 0.162 mg/L  $\text{SO}_4^{2-}$  for original CTA membrane and 3.25 mg/L  $\text{SO}_4^{2-}$  for modified aquaporin membrane. The amounts of total organic carbon after the treatment were 1.52 mg/L for original aquaporin membrane, 1.49 mg/L for modified aquaporin membrane, 0.72 mg/L for original CTA membrane and 0.89 mg/L for modified aquaporin membrane.

Table 4- 5 The application of original and modified both CTA and AqP membranes for water quality improvement of treated textile effluent.

Membrane types	Wastewater	Characteristic of water	Total removal Efficiency	Rejection Efficiency
Original AqP	Textile Effluent 1	TOC	0.97	0.98
TiO <sub>2</sub> modified AqP			0.98	0.99
Original CTA			0.97	0.97
TiO <sub>2</sub> modified CTA			0.97	0.98
Original AqP	Textile Effluent 1	Nitrate	0.95	0.99
TiO <sub>2</sub> modified AqP			0.94	0.99
Original CTA			0.97	0.99
TiO <sub>2</sub> modified CTA			0.95	0.99
Original AqP	Textile Effluent 1	Sulfate	0.98	0.98
TiO <sub>2</sub> modified AqP			0.99	0.97
Original CTA			0.98	0.97
TiO <sub>2</sub> modified CTA			0.99	0.99
Original AqP	Textile Effluent 1	Formaldehyde	0.99	0.98
TiO <sub>2</sub> modified AqP			0.99	0.99
Original CTA			0.99	0.97
TiO <sub>2</sub> modified CTA			0.99	0.99
Original AqP	Textile Effluent 1	Phosphate	0.99	0.99
TiO <sub>2</sub> modified AqP			0.99	0.99
Original CTA			0.99	0.99
TiO <sub>2</sub> modified CTA			0.99	0.99
Original AqP	Textile Effluent 1	PVA	0.99	0.99
TiO <sub>2</sub> modified AqP			0.99	0.99
Original CTA			0.99	0.99
TiO <sub>2</sub> modified CTA			0.99	0.99

## Chapter 5

### Conclusion

From overall results, our studies can be summarized as follows;

1) According to the study using synthetic textile wastewater (reactive black, blue and red) with original and modified FO membranes, the effluent colour values in terms of ADMI for original and modified membrane of both AqP and CTA membrane were less than 10 ADMI at pH 7, which is about 99.98% removal. The effluent TOC of both original and modified CTA membranes were  $0.72 \pm 0.96$  mg/l and  $0.48 \pm 0.94$  mg/l, respectively.

2) The CTA membrane exhibited average water flux of  $7.24 \pm 1.52$  L m<sup>2</sup> h<sup>-1</sup> with original membrane and  $11.73 \pm 1.32$  L m<sup>2</sup> h<sup>-1</sup> with modified one, obviously lower than that of the AqP membrane of  $10.21 \pm 1.25$  L m<sup>2</sup> h<sup>-1</sup> with original and  $11.37 \pm 0.31$  L m<sup>2</sup> h<sup>-1</sup> with modified one. The average water flux of modified FO membranes was measured with the synthetic textile wastewater (reactive black, blue and red) 70.43% and 11.24% of flux increments were obtained for CTA and AqP membranes after the surface modification, respectively.

3) Maximum removal percent of sulphate was found to be 99.16 % and 99.17 % using original and modified CTA membrane, consequently, 99.35 % and 99.31 % using original and modified AqP membrane with HCOH as interference. With PVA interference, the maximum removal percent of sulphate was found to be around 99.69% and 99.84 % using original and modified CTA membrane, similarly, 99.6 % and 99.71 % using original and modified AqP membrane.

4) It seems that negatively charged membrane surface may absorb these positively charged compounds. PVA and HCOH rejection increases dramatically as the compound transforms from a neutral to a positively charged species as solution pH exist below its pKa value. The higher molecular weights and hydrated ion diameters

for  $\text{NO}_3^-$ ,  $\text{SO}_4^{2-}$  and  $\text{PO}_4^{2-}$  resulted in higher rejection rates owing to attenuated transfer across the membrane. The negatively charged MEMO–PMMA–BR membrane may have higher rejections to negatively charged ions Phosphate was almost completely removed after experiment. As a result, the rejection of the MEMO–PMMA–BR grafted membrane increases due to the complex feed ions.

5) It is worth noting that the water flux of the CTA membrane was significantly improved by  $\text{TiO}_2$  nanoparticle modification, which is consistent with the improved surface hydrophilicity after coating. And the flux performance of the commercial CTA membrane was much lower than that of the AqP membrane due to the AqP's biomimicry molecular design, the performance of the modified CTA membrane became not better than that of the AqP membrane in this study.

6) The experiment results indicate the successful coating of  $\text{TiO}_2$  nanoparticles onto the surface of a CTA and AqP membranes. The water contact angle measurements demonstrate the significantly improved membrane surface hydrophilicity of the  $\text{TiO}_2$ -coated membranes. The separation properties of these membranes are clearly improved with a much better flux and a great retention for the removal of reactive dye in an aqueous feed solution. The illuminated  $\text{TiO}_2$ -coated TF CPA membranes also demonstrate the significant enhancement of the antifouling property, with the higher maintained flux ratios and the lower irreversible fouling factors compared to the uncoated membranes. Even though, neglecting capital costs, the benefits of treatment reuse system for such high consumer of fresh water will keep increasing, because of environmental pollution and water scarcity. Therefore, FO technology could indeed be a solution for textile wastewater up-cycling/reuse and secure a cleaner (less water consuming) textile production in the future.

## REFERENCES

- Abousnina, R. M. (2012). Oily wastewater treatment: removal of dissolved organic components by forward osmosis.
- Achilli, A., Cath, T. Y. and Childress, A. E. (2010). Selection of inorganic-based draw solutions for forward osmosis applications. *Journal of Membrane Science*, 364(1-2), 233-241.
- Al-Amoudi, A., Williams, P., Al-Hobaib, A. and Lovitt, R. W. (2008). Cleaning results of new and fouled nanofiltration membrane characterized by contact angle, updated DSPM, flux and salts rejection. *Applied Surface Science*, 254(13), 3983-3992.
- Ali, S. and Nadeem, R. (2006). Analyses and treatment of textile effluents. *Int J Agric Biol*, 8, 641-644.
- Alsvik, I. L. and Hägg, M.-B. (2013). Pressure retarded osmosis and forward osmosis membranes: materials and methods. *Polymers*, 5(1), 303-327.
- Altin, A. (2008). An alternative type of photoelectro-Fenton process for the treatment of landfill leachate. *Separation and Purification Technology*, 61(3), 391-397.
- Alturki, A. A., McDonald, J. A., Khan, S. J., Price, W. E., Nghiem, L. D. and Elimelech, M. (2013). Removal of trace organic contaminants by the forward osmosis process. *Separation and Purification Technology*, 103, 258-266.
- Apha, A. (1998). Wpcf. *Standard methods for the examination of water and wastewater*, 20.
- Batchelder, G. W. (1965). Process for the demineralization of water: Google Patents.
- Batchelor, S. N., Bird, J. M. and Lloyd, J. (2006). Laundry treatment compositions: Google Patents.
- Bechtold, T., Burtscher, E. and Hung, Y.-T. (2004). Treatment of textile wastes. *Handbook of Industrial and hazardous waste treatment*, Marcel Dekker, 379-413.
- Ben-Sasson, M., Lu, X., Bar-Zeev, E., Zodrow, K. R., Nejati, S., Qi, G., . . . Elimelech, M. (2014). In situ formation of silver nanoparticles on thin-film composite reverse osmosis membranes for biofouling mitigation. *Water Research*, 62, 260-270.

- Bisschops, I. and Spanjers, H. (2003). Literature review on textile wastewater characterisation. *Environmental technology*, 24(11), 1399-1411.
- Blomqvist, A. (1996). Food and Fashion: Water Management and Collective Action among Irrigation Farmers and Textile Industrialists in South India PDF.
- Bodnar, J., Hajba, L. and Guttman, A. (2016). A fully automated linear polyacrylamide coating and regeneration method for capillary electrophoresis of proteins. *Electrophoresis*, 37(23-24), 3154-3159.
- Cath, T. Y., Childress, A. E. and Elimelech, M. (2006). Forward osmosis: principles, applications, and recent developments. *Journal of Membrane Science*, 281(1), 70-87.
- Chekli, L., Shon, H., Phuntsho, S., Kim, J. and Cho, J. (2015). Draw Solutes in Forward Osmosis Processes. *Forward Osmosis: Fundamentals and Applications*.
- Chen, L., Reddy, N. and Yang, Y. (2013a). Remediation of environmental pollution by substituting poly (vinyl alcohol) with biodegradable warp size from wheat gluten. *Environmental science & technology*, 47(9), 4505-4511.
- Chen, L., Reddy, N. and Yang, Y. (2013b). Soy proteins as environmentally friendly sizing agents to replace poly (vinyl alcohol). *Environmental Science and Pollution Research*, 20(9), 6085-6095.
- Cornelissen, E., Harmsen, D., Beerendonk, E., Qin, J., Oo, H., De Korte, K. and Kappelhof, J. (2011). The innovative osmotic membrane bioreactor (OMBR) for reuse of wastewater. *Water Science and Technology*, 63(8), 1557-1565.
- Cui, W., Cui, Z., Zhang, N., Ma, Q., Liu, L. and Zhang, X. (2016). A new efficient technology for refractory phenol-formaldehyde resin wastewater treatment. *RSC Advances*, 6(23), 19078-19088.
- Duong, P. H. and Chung, T.-S. (2014). Application of thin film composite membranes with forward osmosis technology for the separation of emulsified oil–water. *Journal of Membrane Science*, 452, 117-126.
- Eiroa, M., Kennes, C. and Veiga, M. C. (2004). Formaldehyde and urea removal in a denitrifying granular sludge blanket reactor. *Water Research*, 38(16), 3495-3502.
- Emadzadeh, D., Lau, W. and Ismail, A. (2013). Synthesis of thin film nanocomposite



- forward osmosis membrane with enhancement in water flux without sacrificing salt rejection. *Desalination*, 330, 90-99.
- Emadzadeh, D., Lau, W. J., Matsuura, T., Rahbari-Sisakht, M. and Ismail, A. (2014). A novel thin film composite forward osmosis membrane prepared from PSf-TiO<sub>2</sub> nanocomposite substrate for water desalination. *Chemical Engineering Journal*, 237, 70-80.
- Eswaramoorthi, S., Dhanapal, K. and Chauhan, D. (2008). Advanced in textile waste water treatment: the case for UV-ozonation and membrane bioreactor for common effluent treatment plants in Tirupur, Tamil Nadu, India. *Environment with People's Involvement & Co-ordination in India. Coimbatore, India.*
- Geise, G. M., Cassady, H. J., Paul, D. R., Logan, B. E. and Hickner, M. A. (2014). Specific ion effects on membrane potential and the permselectivity of ion exchange membranes. *Physical Chemistry Chemical Physics*, 16(39), 21673-21681.
- Ghaly, A., Ananthashankar, R., Alhattab, M. and Ramakrishnan, V. (2014). Production, characterization and treatment of textile effluents: a critical review. *J Chem Eng Process Technol*, 5(1), 1-18.
- Grafstrom, R. C., Curren, R. D., Yang, L. L. and Harris, C. C. (1985). Genotoxicity of formaldehyde in cultured human bronchial fibroblasts. *Science*, 228, 89-92.
- Growther, L. and Meenakshi, M. (2011). Biotechnological approaches to combat textile effluents. *ChemInform*, 42(29).
- Gupta, K. K. (2009). *Polyvinyl alcohol size recovery and reuse via vacuum flash evaporation*: Georgia Institute of Technology.
- Halmann, M., Hunt, A. and Spath, D. (1992). Photodegradation of dichloromethane, tetrachloroethylene and 1, 2-dibromo-3-chloropropane in aqueous suspensions of TiO<sub>2</sub> with natural, concentrated and simulated sunlight. *Solar energy materials and solar cells*, 26(1-2), 1-16.
- Hancock, N. T. and Cath, T. Y. (2009). Solute coupled diffusion in osmotically driven membrane processes. *Environmental science & technology*, 43(17), 6769-6775.
- Hao, J. and Zhao, Q. (1994). The development of membrane technology for wastewater treatment in the textile industry in China. *Desalination*, 98(1-3), 353-360.

- He, Y., Wang, X., Xu, J., Yan, J., Ge, Q., Gu, X. and Jian, L. (2013). Application of integrated ozone biological aerated filters and membrane filtration in water reuse of textile effluents. *Bioresource technology*, 133, 150-157.
- Helfferich, F. G. (1995). *Ion exchange*: Courier Corporation.
- Holloway, R. W., Childress, A. E., Dennett, K. E. and Cath, T. Y. (2007). Forward osmosis for concentration of anaerobic digester centrate. *Water Research*, 41(17), 4005-4014.
- Hu, Y., Huang, S., Liu, S. and Pan, W. (2012). A corrosion-resistance superhydrophobic TiO<sub>2</sub> film. *Applied Surface Science*, 258(19), 7460-7464.
- Huang, L. and McCutcheon, J. R. (2015). Impact of support layer pore size on performance of thin film composite membranes for forward osmosis. *Journal of Membrane Science*, 483, 25-33.
- Imtiazuddin, S., Mumtaz, M. and Mallick, K. A. (2012). Pollutants of wastewater characteristics in textile industries. *Journal of Basic & Applied Sciences*, 8, 554-556.
- Jadav, G. L. and Singh, P. S. (2009). Synthesis of novel silica-polyamide nanocomposite membrane with enhanced properties. *Journal of Membrane Science*, 328(1), 257-267.
- Jeong, B.-H., Hoek, E. M., Yan, Y., Subramani, A., Huang, X., Hurwitz, G., . . . Jawor, A. (2007). Interfacial polymerization of thin film nanocomposites: a new concept for reverse osmosis membranes. *Journal of Membrane Science*, 294(1), 1-7.
- Kajitvichyanukul, P., Lu, M.-C., Liao, C.-H., Wirojanagud, W. and Koottatep, T. (2006). Degradation and detoxification of formaline wastewater by advanced oxidation processes. *Journal of hazardous materials*, 135(1), 337-343.
- Kazner, C., Jamil, S. and Phuntsho, S. (2014). Forward osmosis for the treatment of reverse osmosis concentrate from water reclamation: process performance and fouling control. *Water Science and Technology*, 69(12), 2431-2437.
- Klaysri, R., Wichaidit, S., Piticharoenphun, S., Mekasuwandumrong, O. and Praserttham, P. (2016). Synthesis of TiO<sub>2</sub>-grafted onto PMMA film via ATRP: Using monomer as a coupling agent and reusability in photocatalytic application.

*Materials Research Bulletin*, 83, 640-648.

- Kong, F.-x., Yang, H.-w., Wu, Y.-q., Wang, X.-m. and Xie, Y. F. (2015). Rejection of pharmaceuticals during forward osmosis and prediction by using the solution–diffusion model. *Journal of Membrane Science*, 476, 410-420.
- Kumar, A. and Choudhary, P. (2011). A comparative study on the treatment methods of textile dye effluents. *Global J Environ Res*, 5(1), 46-52.
- Lafond, R. (2008). A compact and efficient technology for upgrade of canadian municipal aerated lagoons. *VP Business Development and Marketing*.
- Laxman, M. (2009). Pollution and its control in textile industry. *Dyes and Chemicals*.
- Lee and Baker, R. (1981). Membranes for power generation by pressure-retarded osmosis. *Journal of Membrane Science*, 8(2), 141-171.
- Lee, Haam, S., Kwak, J., Jang, J. and Lee, Y. (1999). Ultrafiltration of desizing wastewater containing PVA in bench scale test. *Environmental technology*, 20(3), 277-283.
- Lee, Im, S. J., Kim, J. H., Kim, H. J., Kim, J. P. and Min, B. R. (2008). Polyamide thin-film nanofiltration membranes containing TiO<sub>2</sub> nanoparticles. *Desalination*, 219(1-3), 48-56.
- Li, Z.-Y., Yangali-Quintanilla, V., Valladares-Linares, R., Li, Q., Zhan, T. and Amy, G. (2012). Flux patterns and membrane fouling propensity during desalination of seawater by forward osmosis. *Water Research*, 46(1), 195-204.
- Linares, R. V., Li, Z., Sarp, S., Bucs, S. S., Amy, G. and Vrouwenvelder, J. S. (2014). Forward osmosis niches in seawater desalination and wastewater reuse. *Water Research*, 66, 122-139.
- Linares, R. V., Yangali-Quintanilla, V., Li, Z. and Amy, G. (2012). NOM and TEP fouling of a forward osmosis (FO) membrane: foulant identification and cleaning. *Journal of Membrane Science*, 421, 217-224.
- Liu, Z., Zhang, X., Nishimoto, S., Jin, M., Tryk, D. A., Murakami, T. and Fujishima, A. (2008). Highly ordered TiO<sub>2</sub> nanotube arrays with controllable length for photoelectrocatalytic degradation of phenol. *The Journal of Physical Chemistry C*, 112(1), 253-259.
- Lutchmiah, K., Verliefde, A., Roest, K., Rietveld, L. C. and Cornelissen, E. R. (2014).

- Forward osmosis for application in wastewater treatment: a review. *Water Research*, 58, 179-197.
- Ma, N., Wei, J., Liao, R. and Tang, C. Y. (2012). Zeolite-polyamide thin film nanocomposite membranes: towards enhanced performance for forward osmosis. *Journal of Membrane Science*, 405, 149-157.
- Magdum, S. S., Minde, G. P. and Kalyanraman, V. (2013). Rapid determination of indirect cod and polyvinyl alcohol from textile desizing wastewater.
- Masupha, T. M. (2008). *Water management at a textile industry: a case study in Lesotho*.
- Matsumura, S., Kurita, H. and Shimokobe, H. (1993). Anaerobic biodegradability of polyvinyl alcohol. *Biotechnology letters*, 15(7), 749-754.
- McCutcheon, J. R. and Elimelech, M. (2006). Influence of concentrative and dilutive internal concentration polarization on flux behavior in forward osmosis. *Journal of Membrane Science*, 284(1), 237-247.
- McGinnis, R. L., Hancock, N. T., Nowosielski-Slepowron, M. S. and McGurgan, G. D. (2013). Pilot demonstration of the NH<sub>3</sub>/CO<sub>2</sub> forward osmosis desalination process on high salinity brines. *Desalination*, 312, 67-74.
- Mo, J. H., Lee, Y. H., Kim, J., Jeong, J. Y. and Jegal, J. (2008). Treatment of dye aqueous solutions using nanofiltration polyamide composite membranes for the dye wastewater reuse. *Dyes and Pigments*, 76(2), 429-434.
- Morikawa, Y., Shiomi, K., Ishihara, Y. and Matsuura, N. (1997). Triple primary cancers involving kidney, urinary bladder, and liver in a dye worker. *American journal of industrial medicine*, 31(1), 44-49.
- Nash, T. (1953). The colorimetric estimation of formaldehyde by means of the Hantzsch reaction. *Biochemical Journal*, 55(3), 416.
- Nightingale Jr, E. (1959). Phenomenological theory of ion solvation. Effective radii of hydrated ions. *The Journal of Physical Chemistry*, 63(9), 1381-1387.
- Oh, S.-Y., Kim, H.-W., Park, J.-M., Park, H.-S. and Yoon, C. (2009). Oxidation of polyvinyl alcohol by persulfate activated with heat, Fe<sup>2+</sup>, and zero-valent iron. *Journal of hazardous materials*, 168(1), 346-351.
- Peternel, I. T., Koprivanac, N., Božić, A. M. L. and Kušić, H. M. (2007). Comparative

- study of UV/TiO<sub>2</sub>, UV/ZnO and photo-Fenton processes for the organic reactive dye degradation in aqueous solution. *Journal of hazardous materials*, 148(1), 477-484.
- Phuntsho, S., Hong, S., Elimelech, M. and Shon, H. K. (2013). Forward osmosis desalination of brackish groundwater: Meeting water quality requirements for fertigation by integrating nanofiltration. *Journal of Membrane Science*, 436, 1-15.
- Phuntsho, S., Shon, H. K., Hong, S., Lee, S. and Vigneswaran, S. (2011). A novel low energy fertilizer driven forward osmosis desalination for direct fertigation: evaluating the performance of fertilizer draw solutions. *Journal of Membrane Science*, 375(1-2), 172-181.
- Porter, J. J. (1998). Recovery of polyvinyl alcohol and hot water from the textile wastewater using thermally stable membranes. *Journal of Membrane Science*, 151(1), 45-53.
- Qu, D., Qiang, Z., Xiao, S., Liu, Q., Lei, Y. and Zhou, T. (2014). Degradation of Reactive Black 5 in a submerged photocatalytic membrane distillation reactor with microwave electrodeless lamps as light source. *Separation and Purification Technology*, 122, 54-59.
- Rahman, F. (2016). The treatment of industrial effluents for the discharge of textile dyes using by techniques and adsorbents. *Journal of Textile Science & Engineering*, 6, 242.
- Rassoul, G., Al-Alawy, A. F. and Khudair, W. N. (2012). Reduction of Concentrating Poisonous Metallic Radicals from Industrial Wastewater by Forward and Reverse Osmosis. *Journal of Engineering*, 18(7).
- Richardson, S. D., Plewa, M. J., Wagner, E. D., Schoeny, R. and DeMarini, D. M. (2007). Occurrence, genotoxicity, and carcinogenicity of regulated and emerging disinfection by-products in drinking water: a review and roadmap for research. *Mutation Research/Reviews in Mutation Research*, 636(1), 178-242.
- Soroush, A. and Ma, W. (2015). Surface modification of thin film composite forward osmosis membrane by silver-decorated graphene-oxide nanosheets. *Environmental Science: Nano*, 2(4), 395-405.

- Standard, A. (1998). *Methods for the Examination of Water and Wastewater*: American Public Health Association.
- Sun, Y., Tian, J., Zhao, Z., Shi, W., Liu, D. and Cui, F. (2016). Membrane fouling of forward osmosis (FO) membrane for municipal wastewater treatment: A comparison between direct FO and OMBR. *Water Research*, 104, 330-339.
- Tan, C. H. and Ng, H. Y. (2008). Modified models to predict flux behavior in forward osmosis in consideration of external and internal concentration polarizations. *Journal of Membrane Science*, 324(1), 209-219.
- Tang, X., Bai, Y., Duong, A., Smith, M. T., Li, L. and Zhang, L. (2009). Formaldehyde in China: Production, consumption, exposure levels, and health effects. *Environment international*, 35(8), 1210-1224.
- Tüfekci, N. and Sivri, N. (2007). Pollutants of textile industry wastewater and assessment of its discharge limits by water quality standards. *Turkish Journal of Fisheries and Aquatic Sciences*, 7(2).
- Uilson de Souza, A., Petrus, J., Santos, F., Brandao, H., Souza, G. U. and Juliano, L. (2009). Color reduction in textile effluents by membranes. *Latin American applied research*, 39(1), 47-52.
- Wu, Y., Lian, Y., Liu, J. and Zhu, H. (2008). Sonochemical degradation of polyvinyl alcohol in aqueous solutions. *Technology of Water Treatment*, 34(2), 32-34.
- Xie, M., Luo, W., Guo, H., Nghiem, L. D., Tang, C. Y. and Gray, S. R. (2018). Trace organic contaminant rejection by aquaporin forward osmosis membrane: Transport mechanisms and membrane stability. *Water Research*, 132, 90-98.
- Xue, W., Sint, K. K. K., Ratanatamskul, C., Praserttham, P. and Yamamoto, K. (2018). Binding TiO<sub>2</sub> nanoparticles to forward osmosis membranes via MEMO-PMMA-Br monomer chains for enhanced filtration and antifouling performance. *RSC Advances*, 8(34), 19024-19033.
- Xue, W., Tobino, T., Nakajima, F. and Yamamoto, K. (2015). Seawater-driven forward osmosis for enriching nitrogen and phosphorous in treated municipal wastewater: effect of membrane properties and feed solution chemistry. *Water Research*, 69, 120-130.
- Yan, J. G. Z. Z. L. and Meixia, D. (2008). Degradation of polyvinyl alcohol with

ozonation and other synergic oxidation [J]. *Chinese Journal of Environmental Engineering*, 12, 002.

Zhang, H.-Z., Liu, B.-L. and Luo, R. (2005). Recent Advances in the Biodegradability of PVA and its Derivatives Materials. *Journal of the Graduate School of the Chinese Academy of Science*, 22, 657-666.



## APPENDIX

Table A-1 Membrane flux variation during synthetic textile wastewater test with different ADMI values (reactive black) for original AqP membrane.

Time (min)	Data (g)	delta W (g)	delta W(a)	FS weight	Temperat	ρ(kg/m <sup>3</sup> )	delta V (L)	FS V (L)	EC (mS/m)	Jw (LMH)	JDS (mmo)
0	0			1000.29	30.1	995.6153		1.004695	142.94		
3	-56.85	56.85456	0.64	999.65		987.5861	0.000648	1.012215		6.48	
6	-57.62	0.76	0.76	998.8859		979.557	0.00078	1.019732		7.80	
9	-58.34	0.72	0.72	998.1634		971.5278	0.000744	1.027416		7.44	
12	-59.12	0.78	0.78	997.387		963.4987	0.000806	1.035172		8.06	
15	-59.87	0.76	0.76	996.6309		955.4695	0.000791	1.04308		7.91	
18	-60.64	0.77	0.77	995.8608		947.4404	0.000813	1.051107		8.13	
21	-61.39	0.75	0.75	995.113		939.4112	0.000796	1.059294		7.96	
24	-62.14	0.75	0.75	994.3618		931.3821	0.000807	1.06762		8.07	
27	-62.92	0.78	0.78	993.5796		923.3529	0.000847	1.076056		8.47	
30	-63.67	0.75	0.75	992.832		915.3237	0.000817	1.084679	145.399	8.17	6.89
33	-64.43	0.75	0.75	992.0781		907.2946	0.000831	1.093447		8.31	
36	-65.24	0.81	0.81	991.2651		899.2654	0.000904	1.102305		9.04	
39	-65.97	0.73	0.73	990.5319		891.2363	0.000823	1.111413		8.23	
42	-66.76	0.79	0.79	989.7407		883.2071	0.000896	1.120621		8.96	
45	-67.51	0.75	0.75	988.9896		875.178	0.000858	1.130044		8.58	
48	-68.24	0.72	0.72	988.2692		867.1488	0.000831	1.139677		8.31	
51	-69.03	0.80	0.80	987.4702		859.1197	0.00093	1.149398		9.30	
54	-69.80	0.76	0.76	986.7067		851.0905	0.000897	1.159344		8.97	
57	-70.56	0.76	0.76	985.9481		843.0613	0.0009	1.169486		9.00	
60	-71.31	0.76	0.76	985.1912		835.0322	0.000906	1.179824	147.737	9.06	8.11
63	-72.06	0.74	0.74	984.4476		827.003	0.000899	1.19038		8.99	
66	-72.85	0.79	0.79	983.6551		818.9739	0.000968	1.201082		9.68	
69	-73.58	0.73	0.73	982.923		810.9447	0.000903	1.212072		9.03	
72	-74.35	0.77	0.77	982.1532		802.9156	0.000959	1.223233		9.59	
75	-75.14	0.79	0.79	981.3626		794.8864	0.000995	1.234595		9.95	
78	-75.90	0.76	0.76	980.6025		786.8573	0.000966	1.246227		9.66	
81	-76.64	0.74	0.74	979.8654		778.8281	0.000946	1.258128		9.46	
84	-77.40	0.76	0.76	979.1081		770.7989	0.000983	1.270251		9.83	
87	-78.17	0.78	0.78	978.3301		762.7698	0.00102	1.282602		10.20	
90	-78.95	0.78	0.78	977.5515		754.7406	0.001032	1.295215	150.961	10.32	10.38
93	-79.72	0.76	0.76	976.7896		746.7115	0.00102	1.308122		10.20	
96	-80.46	0.74	0.74	976.045		738.6823	0.001008	1.321333		10.08	
99	-81.21	0.75	0.75	975.2973		730.6532	0.001023	1.334829		10.23	
102	-82.00	0.79	0.79	974.5066		722.624	0.001094	1.348567		10.94	
105	-82.74	0.74	0.74	973.7672		714.5949	0.001035	1.362684		10.35	
108	-83.52	0.79	0.79	972.9798		706.5657	0.001114	1.377055		11.14	
111	-84.24	0.71	0.71	972.2657		698.5365	0.001022	1.391861		10.22	
114	-85.03	0.79	0.79	971.4763		690.5074	0.001143	1.406902		11.43	
117	-85.80	0.77	0.77	970.7042		682.4782	0.001131	1.422323		11.31	
120	-86.53	0.73	0.73	969.9717		674.4491	0.001086	1.438169	169.141	10.86	23.33
123	-87.30	0.77	0.77	969.201		666.4199	0.001156	1.45434		11.56	
126	-88.06	0.75	0.75	968.4472		658.3908	0.001145	1.470931		11.45	
129	-88.83	0.77	0.77	967.6779		650.3616	0.001183	1.487907		11.83	
132	-89.59	0.77	0.77	966.9113		642.3325	0.001193	1.505313		11.93	
135	-90.36	0.77	0.77	966.1414		634.3033	0.001214	1.523154		12.14	
138	-91.10	0.73	0.73	965.4069		626.2741	0.001173	1.541508		11.73	
141	-91.89	0.79	0.79	964.6172		618.245	0.001277	1.560251		12.77	
144	-92.63	0.75	0.75	963.8704		610.2158	0.001224	1.579557		12.24	
147	-93.39	0.76	0.76	963.1103		602.1867	0.001262	1.599355		12.62	
150	-94.16	0.76	0.76	962.3482		594.1575	0.001283	1.619685	174.903	12.83	19.57
153	-94.91	0.76	0.76	961.5911		586.1284	0.001292	1.640581		12.92	
156	-104.53	9.62	9.62	951.9734		578.0992	0.016637	1.64673		166.37	
159	-105.18	0.65	0.65	951.3264		570.0701	0.001135	1.668789		11.35	
162	-105.76	0.58	0.58	950.7435		562.0409	0.001037	1.691591		10.37	
165	-106.39	0.63	0.63	950.1164		554.0117	0.001132	1.714975		11.32	
168	-107.02	0.63	0.63	949.4865		545.9826	0.001154	1.739042		11.54	
171	-107.60	0.58	0.58	948.9058		537.9534	0.00108	1.763918		10.80	
174	-108.22	0.62	0.62	948.2813		529.9243	0.001178	1.789466		11.78	
177	-108.84	0.61	0.61	947.6679		521.8951	0.001175	1.815821		11.75	
180	-109.43	0.59	0.59	947.0758		513.866	0.001152	1.84304	183.553	11.52	26.89
		109.4288	53.21424				0.076053				
										12.68	12.68



Table A-2 Effluent TOC, sulfate, nitrate and phosphate values and total removal and total rejection efficiency while varying the initial ADMI values of synthetic textile effluent(reactive black) with original AqP membrane.

FS													
Time (h)	Weight (g)	delta W (g)	Temperat (°C)	p (kg/m <sup>3</sup> )	V (L)	delta V (L)	Jw' (LMH)	EC (mS/m)	pH	TOC conc: (mg/L)	Sulfate co (mg/L)	Nitrate co (mg/L)	Phosphate (mg/L)
0	1007.94		30.1	995.6153	1.012379			142.94	7.04	7.09	300	250	300
2	861.05	-146.89	27.9	996.26	0.864282	-0.1481	12.34138	198.52	6.55				
									Js/Jw	0.430843	21.26024	18.48798	22.1856
									μ0	7.177767	303.7137	253.0947	303.7137
	2013.64								μ	1.279686	12.66889	0.001163	0.001163
	2159.74								Total rem	82.17153	95.82867	99.99954	99.99962
	1000.74								Rejection	-0.78781	0.957748	0.949298	0.957748
DS													
Time (h)	Weight (g)	delta W (g)	Temperat (°C)	EC (S/m)	pH	V (L)				TOC conc: (mg/L)	Sulfate co (mg/L)	Nitrate co (mg/L)	Phosphate (mg/L)
0	1012.9		29.5	8.41	6.11	0				0	0	0	0
2	1159	146.1	24.9	7.94	6.83	1.163351				1.1	10.89	0.001	0.001
									Rejection	93.92323	92.91325	92.60481	92.6048

Table A-3 Effluent TOC, sulfate, nitrate and phosphate values and total removal and total rejection efficiency while varying the initial ADMI values of synthetic textile effluent(reactive black) with modified AqP membrane.

	1516.98												
	1341.15												
	533.24												
FS													
Time (h)	Weight (g)	delta W (g)	Temperat (°C)	p (kg/m <sup>3</sup> )	V (L)	delta V (L)	Jw' (LMH)	EC (mS/m)	pH	TOC conc: (mg/L)	Sulfate co (mg/L)	Nitrate co (mg/L)	Phosphate (mg/L)
0	983.74		30.1	995.6153	0.988072			143.41	7.04	7.09	300	250	300
3	807.91	-175.83	27.9	996.26	0.810943	-0.17713	14.76079	184.19	6.55				
									Js/Jw	0.417886	22.83706	19.97092	23.96512
									μ0	7.005433	296.4217	247.0181	296.4217
	2013.95								μ	1.836666	13.95389	0.001193	0.001193
	2188.92								Total rem	73.78226	95.29255	99.99952	99.9996
	1000.74								Rejection	-0.61532	0.961825	0.95419	0.961825
									Js	4.785895	261.5443	228.7194	274.4635
DS													
Time (h)	Weight (g)	delta W (g)	Temperat (°C)	EC (S/m)	pH	V (L)				TOC conc: (mg/L)	Sulfate co (mg/L)	Nitrate co (mg/L)	Phosphate (mg/L)
0	1013.21		29.5	8.41	6.11	0				0	0	0	0
3	1188.18	174.97	24.9	7.94	6.83	1.19264				1.54	11.7	0.001	0.001
									Rejection	94.10597	92.38765	92.01163	92.01163

Table A-4 Membrane flux variation during synthetic textile wastewater test with different ADMI values (reactive black) for modified AqP membrane.

Time (min)	Data (g)	delta W (g)	delta W(a)	FS weight	Temperat	p(kg/m3)	delta V (L)	FS V (L)	EC (mS/m)	Jw (LMH)	JDS (mmol)
0	0			1000.29	30.1	995.6153		1.004695	147.54		
3	-56.3781	56.37814	0.856	999.434		987.5861	0.000867	1.011997		8.67	
6	-57.1981	0.81999	0.81999	998.614		979.557	0.000837	1.019455		8.37	
9	-58.0452	0.84703	0.84703	997.767		971.5278	0.000872	1.027008		8.72	
12	-58.8381	0.792892	0.792892	996.9741		963.4987	0.000823	1.034744		8.23	
15	-59.6811	0.843062	0.843062	996.131		955.4695	0.000882	1.042557		8.82	
18	-60.5012	0.82012	0.82012	995.3109		947.4404	0.000866	1.050526		8.66	
21	-61.3279	0.826622	0.826622	994.4843		939.4112	0.00088	1.058625		8.80	
24	-62.1428	0.814949	0.814949	993.6693		931.3821	0.000875	1.066876		8.75	
27	-62.9957	0.852855	0.852855	992.8165		923.3529	0.000924	1.07523		9.24	
30	-63.8046	0.808889	0.808889	992.0076		915.3237	0.000884	1.083778	149.999	8.84	7.01
33	-64.6235	0.818987	0.818987	991.1886		907.2946	0.000903	1.092466		9.03	
36	-65.441	0.817499	0.817499	990.3711		899.2654	0.000909	1.101311		9.09	
39	-66.2826	0.841562	0.841562	989.5295		891.2363	0.000944	1.110289		9.44	
42	-67.1233	0.840697	0.840697	988.6888		883.2071	0.000952	1.11943		9.52	
45	-67.9669	0.843605	0.843605	987.8452		875.178	0.000964	1.128736		9.64	
48	-68.7473	0.780424	0.780424	987.0648		867.1488	0.0009	1.138288		9.00	
51	-69.6208	0.873436	0.873436	986.1914		859.1197	0.001017	1.147909		10.17	
54	-70.4042	0.783444	0.783444	985.4079		851.0905	0.000921	1.157818		9.21	
57	-71.2689	0.864652	0.864652	984.5433		843.0613	0.001026	1.167819		10.26	
60	-72.093	0.824171	0.824171	983.7191		835.0322	0.000987	1.178061	152.337	9.87	8.26
63	-72.9255	0.832458	0.832458	982.8867		827.003	0.001007	1.188492		10.07	
66	-73.7086	0.783068	0.783068	982.1036		818.9739	0.000956	1.199188		9.56	
69	-74.5548	0.846209	0.846209	981.2574		810.9447	0.001043	1.210018		10.43	
72	-75.3753	0.820512	0.820512	980.4369		802.9156	0.001022	1.221096		10.22	
75	-76.1885	0.813274	0.813274	979.6236		794.8864	0.001023	1.232407		10.23	
78	-77.0366	0.848089	0.848089	978.7755		786.8573	0.001078	1.243905		10.78	
81	-77.8643	0.827707	0.827707	977.9478		778.8281	0.001063	1.255666		10.63	
84	-78.6688	0.804453	0.804453	977.1433		770.7989	0.001044	1.267702		10.44	
87	-79.5116	0.842802	0.842802	976.3005		762.7698	0.001105	1.279941		11.05	
90	-80.3634	0.851809	0.851809	975.4487		754.7406	0.001129	1.292429	155.561	11.29	10.55
93	-81.1619	0.79854	0.79854	974.6502		746.7115	0.001069	1.305257		10.69	
96	-81.9992	0.837273	0.837273	973.8129		738.6823	0.001133	1.318311		11.33	
99	-82.8096	0.81041	0.81041	973.0025		730.6532	0.001109	1.331689		11.09	
102	-83.6149	0.805285	0.805285	972.1972		722.624	0.001114	1.345371		11.14	
105	-84.4551	0.840193	0.840193	971.357		714.5949	0.001176	1.359312		11.76	
108	-85.3091	0.853974	0.853974	970.5031		706.5657	0.001209	1.37355		12.09	
111	-86.1101	0.800978	0.800978	969.7021		698.5365	0.001147	1.388191		11.47	
114	-86.9216	0.811525	0.811525	968.8906		690.5074	0.001175	1.403157		11.75	
117	-87.7711	0.849528	0.849528	968.041		682.4782	0.001245	1.41842		12.45	
120	-88.5892	0.818065	0.818065	967.223		674.4491	0.001213	1.434093	173.741	12.13	23.52
123	-89.4357	0.846496	0.846496	966.3765		666.4199	0.00127	1.450101		12.70	
126	-90.2499	0.814189	0.814189	965.5623		658.3908	0.001237	1.466549		12.37	
129	-91.0912	0.841388	0.841388	964.7209		650.3616	0.001294	1.483361		12.94	
132	-91.9179	0.826681	0.826681	963.8942		642.3325	0.001287	1.500616		12.87	
135	-92.7094	0.791491	0.791491	963.1027		634.3033	0.001248	1.518363		12.48	
138	-93.5318	0.822382	0.822382	962.2803		626.2741	0.001313	1.536516		13.13	
141	-94.3962	0.864352	0.864352	961.416		618.245	0.001398	1.555073		13.98	
144	-95.2121	0.81593	0.81593	960.6001		610.2158	0.001337	1.574197		13.37	
147	-96.0039	0.791802	0.791802	959.8083		602.1867	0.001315	1.593872		13.15	
150	-96.8783	0.874391	0.874391	958.9339		594.1575	0.001472	1.613939	179.503	14.72	19.82
153	-97.6833	0.805068	0.805068	958.1288		586.1284	0.001374	1.634674		13.74	
156	-98.5109	0.827603	0.827603	957.3012		578.0992	0.001432	1.655946		14.32	
159	-99.3404	0.829406	0.829406	956.4718		570.0701	0.001455	1.677814		14.55	
162	-100.175	0.83447	0.83447	955.6373		562.0409	0.001485	1.700299		14.85	
165	-101.006	0.83122	0.83122	954.8061		554.0117	0.0015	1.72344		15.00	
168	-101.806	0.800014	0.800014	954.0061		545.9826	0.001465	1.74732		14.65	
171	-102.616	0.809598	0.809598	953.1965		537.9534	0.001505	1.771894		15.05	
174	-103.477	0.861707	0.861707	952.3348		529.9243	0.001626	1.797115		16.26	
177	-104.281	0.803896	0.803896	951.4609		521.8951	0.001674	1.823088		16.74	
180	-105.135	0.853927	0.853927	950.567		513.866	0.00174	1.849834	188.153	17.40	28.52
	-105.935										
		105.1352	49.72304				0.068716				





Table A-8 Membrane flux variation during synthetic textile wastewater test with different ADMI values (reactive black) for modified CTA membrane.

Time (min)	Data (g)	delta W (g)	delta W(a)	FS weight	Temperat	p(kg/m3)	delta V (L)	FS V (L)	EC (mS/m)	Jw (LMH)	JDS (mmol/m2H)
0	0			1000.29	30.1	995.6153		1.004695	143.91		
3	-56.757	56.75696	0.846	999.444		987.5861	0.000857	1.012007		8.57	
6	-57.5573	0.800333	0.800333	998.6437		979.557	0.000817	1.019485		8.17	
9	-58.3684	0.811061	0.811061	997.8326		971.5278	0.000835	1.027076		8.35	
12	-59.1968	0.828409	0.828409	997.0042		963.4987	0.00086	1.034775		8.60	
15	-59.9996	0.802877	0.802877	996.2013		955.4695	0.00084	1.04263		8.40	
18	-60.8034	0.803782	0.803782	995.3975		947.4404	0.000848	1.050618		8.48	
21	-61.6351	0.831715	0.831715	994.5658		939.4112	0.000885	1.058712		8.85	
24	-62.3993	0.76414	0.76414	993.8017		931.3821	0.00082	1.067018		8.20	
27	-63.2238	0.824499	0.824499	992.9772		923.3529	0.000893	1.075404		8.93	
30	-64.0763	0.852488	0.852488	992.1247		915.3237	0.000931	1.083906	146.369	9.31	6.88
33	-64.8775	0.801204	0.801204	991.3235		907.2946	0.000883	1.092615		8.83	
36	-65.6741	0.796673	0.796673	990.5268		899.2654	0.000886	1.101484		8.86	
39	-66.4984	0.824305	0.824305	989.7025		891.2363	0.000925	1.110483		9.25	
42	-67.2969	0.798482	0.798482	988.904		883.2071	0.000904	1.119674		9.04	
45	-68.1079	0.810977	0.810977	988.0931		875.178	0.000927	1.12902		9.27	
48	-68.9117	0.803822	0.803822	987.2892		867.1488	0.000927	1.138546		9.27	
51	-69.7341	0.822332	0.822332	986.4669		859.1197	0.000957	1.14823		9.57	
54	-70.5276	0.79357	0.79357	985.6733		851.0905	0.000932	1.15813		9.32	
57	-71.365	0.837346	0.837346	984.836		843.0613	0.000993	1.168166		9.93	
60	-72.1703	0.805358	0.805358	984.0306		835.0322	0.000964	1.178434	148.707	9.64	8.11
63	-73.0187	0.848336	0.848336	983.1823		827.0003	0.001026	1.18885		10.26	
66	-73.8085	0.789878	0.789878	982.3924		818.9739	0.000964	1.199541		9.64	
69	-74.6375	0.828997	0.828997	981.5634		810.9447	0.001022	1.210395		10.22	
72	-75.4264	0.788897	0.788897	980.7745		802.9156	0.000983	1.221516		9.83	
75	-76.2424	0.815968	0.815968	979.9586		794.8864	0.001027	1.232828		10.27	
78	-77.0754	0.833036	0.833036	979.1255		786.8573	0.001059	1.24435		10.59	
81	-77.8975	0.822069	0.822069	978.3034		778.8281	0.001056	1.256122		10.56	
84	-78.6848	0.787301	0.787301	977.5161		770.7989	0.001021	1.268186		10.21	
87	-79.5199	0.835082	0.835082	976.6811		762.7698	0.001095	1.28044		10.95	
90	-80.3226	0.802747	0.802747	975.8783		754.7406	0.001064	1.292998	151.931	10.64	10.37
93	-81.1262	0.803562	0.803562	975.0748		746.7115	0.001076	1.305825		10.76	
96	-81.9613	0.835074	0.835074	974.2397		738.6823	0.00113	1.318889		11.30	
99	-82.7663	0.805065	0.805065	973.4346		730.6532	0.001102	1.33228		11.02	
102	-83.5868	0.820431	0.820431	972.6142		722.624	0.001135	1.345948		11.35	
105	-84.3825	0.795771	0.795771	971.8184		714.5949	0.001114	1.359957		11.14	
108	-85.1809	0.798328	0.798328	971.0201		706.5657	0.00113	1.374281		11.30	
111	-85.9992	0.818335	0.818335	970.2018		698.5365	0.001171	1.388906		11.71	
114	-86.8362	0.836942	0.836942	969.3648		690.5074	0.001212	1.403844		12.12	
117	-87.5998	0.763663	0.763663	968.6011		682.4782	0.001119	1.419241		11.19	
120	-88.4206	0.820801	0.820801	967.7803		674.4491	0.001217	1.43492	170.111	12.17	23.30
123	-89.2509	0.830318	0.830318	966.95		666.4199	0.001246	1.450962		12.46	
126	-90.0679	0.816928	0.816928	966.1331		658.3908	0.001241	1.467416		12.41	
129	-90.8543	0.786418	0.786418	965.3467		650.3616	0.001209	1.484323		12.09	
132	-91.7002	0.845909	0.845909	964.5008		642.3325	0.001317	1.50156		13.17	
135	-92.5259	0.825738	0.825738	963.675		634.3033	0.001302	1.519265		13.02	
138	-93.296	0.7701	0.7701	962.9049		626.2741	0.00123	1.537513		12.30	
141	-94.1271	0.831048	0.831048	962.0739		618.245	0.001344	1.556137		13.44	
144	-94.9314	0.804335	0.804335	961.2696		610.2158	0.001318	1.575294		13.18	
147	-95.7832	0.851776	0.851776	960.4178		602.1867	0.001414	1.594884		14.14	
150	-96.5755	0.792293	0.792293	959.6255		594.1575	0.001333	1.615103	175.873	13.33	19.53
153	-97.369	0.793474	0.793474	958.832		586.1284	0.001354	1.635874		13.54	
156	-98.1753	0.806338	0.806338	958.0257		578.0992	0.001395	1.657199		13.95	
159	-99.011	0.835681	0.835681	957.19		570.0701	0.001466	1.679074		14.66	
162	-99.8395	0.828554	0.828554	956.3614		562.0409	0.001474	1.701587		14.74	
165	-100.653	0.813506	0.813506	955.5479		554.0117	0.001468	1.724779		14.68	
168	-101.466	0.812799	0.812799	954.7351		545.9826	0.001489	1.748655		14.89	
171	-102.244	0.77837	0.77837	953.9568		537.9534	0.001447	1.773307		14.47	
174	-103.076	0.831739	0.831739	953.125		529.9243	0.00157	1.798606		15.70	
177	-103.907	0.831179	0.831179	952.2938		521.8951	0.001593	1.824684		15.93	
180	-104.679	0.771533	0.771533	951.5223		513.866	0.001501	1.851694	184.523	15.01	28.17
	-105.532										
		104.6787	48.76769				0.067319				Js/Jw

**VITA**

<b>NAME</b>	Mr. Kaung Ko Ko Sint
<b>DATE OF BIRTH</b>	2 July 1990
<b>PLACE OF BIRTH</b>	Pathein
<b>INSTITUTIONS ATTENDED</b>	University of Yangon
<b>HOME ADDRESS</b>	No (326), Rajtevee Apartment, Soi (18) Petchaburi Road, Bangkok, 10400.
<b>PUBLICATION</b>	Sint, K. K. K., Ratanatamskul, C., (2018). TiO <sub>2</sub> -nanoparticles Coated Forward Osmosis Membranes for Enhanced Filtration of Textile Effluent. The proceedings of international Conference on Environmental, Industrial and Energy Engineering (EI2E), Novotel Hotel, Bangkok, 19-21 November 2018.